Flanders
State of
the Art

12_155_1
FHR reports

Sediment Budget for the Belgian Coast

Final report

DEPARTMENT
MOBILITY &
PUBLIC
WORKS

www.flandershydraulicsresearch.be

Sediment Budget for the Belgian Coast

Final report

Vandebroek, E.; Dan S.; Vanlede, J.; Verwaest, T.; Mostaert, F.

anteagroup

Flanders Hydraulics Research

Flanders State of the Art

Cover figure © The Government of Flanders, Department of Mobility and Public Works, Flanders Hydraulics Research

Legal notice

Copyright and citation

This publication should be cited as follows:

Vandebroek, E.; Dan S.; Vanlede, J.; Verwaest, T.; Mostaert, F. (2017). Sediment Budget for the Belgian Coast: Final report. Version 2.0. FHR Reports, 12_155_1. Flanders Hydraulics Research: Antwerp & Antea Group.

Document identification

Customer:	Agentschap Maritieme Dienstverlening en Kust - Afdeling Kust (Agency for Maritime Services and Coast)	Ref.:	WL2017R12_155_1
Keywords (3-5):	Sediment budget, uncertainty, Belgian coast, sediment transport, closure depth		
Text (p.):	57	Appendices (p.):	35
Confidentiality:	☒ No	☒ Available online	

Author(s):	Vandebroek, E.; Dan S.

Control

	Name	Signature
Reviser(s):	Vanlede, J.	
Project leader:	Dan, S.	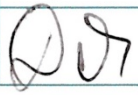

Approval

Coordinator research group:	Verwaest, T.	
Head of Division:	Mostaert, F.	

Abstract

In the framework of the Vlaamse Baaien project, Flanders Hydraulics Research developed a sediment budget for the nearshore Belgian coast. The study describes the sediment volumes available in the coastal system and their circulation patterns. The sediment budget equation takes into account all the sources and sinks of sediment for each of 9 longshore coastal cells, delimited based on the gradient or disruption of sediment transport. The onshore limit is usually delineated by the coastal defense structures, while the offshore limit is either the closure depth or the offshore limit of data availability. A custom tool was developed to solve the sediment budget equation for each cell. This study also estimates the uncertainties in the data and methods used. The final budget spans a ten year period, between 2000 and 2009. Most inputs to the sediment budget, such as human interventions and bathymetric and topographic data, were developed in previous studies. Other inputs, such as the closure depth, volume changes, and uncertainty of the data and methods were computed in the present study. Longshore sediment transport was calculated empirically and compared to numerical modeling results from previous studies. The latter was ultimately used in the sediment budget. The loss of sediment at the onshore boundary by aeolian transport was assumed to be very small compared to the sediment exchange at the offshore boundary. A sediment budget was built based on the change between the survey at the beginning and at the end of the considered period (2000 – 2009) considering all volume measurements, corrected and uncorrected for human interventions. However, a second sediment budget based on the linear trend was made in order to check the sensitivity of different method of calculation for the volume differences. The Belgian coast is generally balanced in terms of loss and gain of sand, with relatively little exchange to the offshore areas. The exception is in the vicinity of Zeebrugge Harbour, where large volumes of sand are exchanged with deeper offshore areas. Finally, recommendations are made about how to increase accuracy of the sediment budget in the future, including quantifying aeolian sediment transport, measuring closure depth, and extending the sediment budget to the entire Belgian shelf.

Contents

List of tables

List of figures

1 Background and literature review

1.1 Introduction

The Belgian coast, stretching 67 km between the borders with France and the Netherlands, was historically characterized by sandy beaches and wide sand dunes, backed by mudflats and tidal marshes. Over the last 1200 years, the marshes and mudflats were diked, drained, and developed for agriculture, tourism and economic activities. Today the developed coast faces increasing challenges as a result of coastal erosion, flooding, and sea level rise. The Masterplan Kustveiligheid (Integrated Coastal Safety Plan), which was approved by the Flemish government in 2011, describes existing and future coastal hazards and a plan to mitigate them.

Coherent management of the coastal zone requires a global view of the sediment volumes available in the coastal system and their circulation patterns. A sediment budget of the Belgian coast is needed in order to understand and quantify the global processes controlling the dynamics of the coast. Coastal engineers and planners around the world use sediment budgets to make informed decisions about coastal management. Sediment budgets identify the key sediment sources, sinks, and transport paths along a defined stretch of coast. The Vlaamse Baaien Kust work group has repeatedly identified the need for such a budget. While a sediment budget is in development for finer sediments across the Belgian Continental Plate (Fettweis et al 2002, Fettweis et al 2008), none exists yet for sand along the Belgian coast, primarily due to a lack of research (Fettweis 1999).

Since the 1970s, the Belgian government has been monitoring the Belgian coast by regularly (~annually) surveying 266 cross-shore bathymetric profiles and collecting LiDAR data (IMDC 2010, Houthuys 2012). Previous studies (Van Lancker et al., 2009 and Houthuys et al. 2012) describe the morphodynamic state of the coast (erosion/accretion), and this information serves as starting point for building a sediment budget. In the current study, a sediment budget is developed for the Belgian coast by applying methods described in recent literature to this extensive monitoring dataset.

This report introduces the concepts behind sediment budgets, describes existing knowledge about sediment transport along the coastline, and presents a sediment budget for the Belgian coast.

1.2 Objectives

The following objectives were outlined in the project plan for the current project:

1. Define relevant time limits for the sediment budget.
2. Define budget boundaries and develop selection criteria for dividing the coast into cells .
3. Estimate longshore transport rates for individual cells.
4. Assess the dependency between analysis cells.
5. Identify transport pathways and their corresponding magnitudes.
6. Assess uncertainty associated with assumptions made.

1.3 The sediment budget equation

The goal of a sediment budget is to understand the sediment sources, sinks, and volume changes along the coast (Figure 1). The following equation governs the sediment budget in each cell (Rosati 2005):

$$Residual = \sum Q_{source} - \sum Q_{sink} - \Delta V + P - R \quad (1)$$

The Q-terms represent the sources and sinks, or the sediment that moves into or out of the cell, respectively. In the case of the Belgian coast (Figure 2), the main sources of sediment are dune erosion, wind-blown transport, input from rivers, and longshore transport into the cell[1]. The main sinks are dune accretion, wind-blown transport, relative sea level rise, losses to offshore areas, and longshore transport out of the cell[2]. The P- and R-terms represent the sediment that is placed into or removed from the cell by beach nourishment or dredging/mining, respectively. ΔV is the change in volume in the cell. The residual is an indicator of how balanced the cell is. If the residual is zero, then the cell is perfectly balanced, and all inputs, outputs, and volumetric changes are accounted for. If the residual is not zero, then not all processes have been accounted for, likely due to lack or accuracy of data. These residuals should be documented to identify where a lack of data exists (e.g. Rosati et al 2015). All terms in the equation must be consistent in units, most commonly as volume (m^3) or volumetric rate of change (m^3/year). All terms should be estimated or derived on the basis of the same temporal and spatial scale (see section 1.3).

Figure 1 – Sediment budget parameters, see Equation (1) (Source: Rosati and Kraus, 1999).

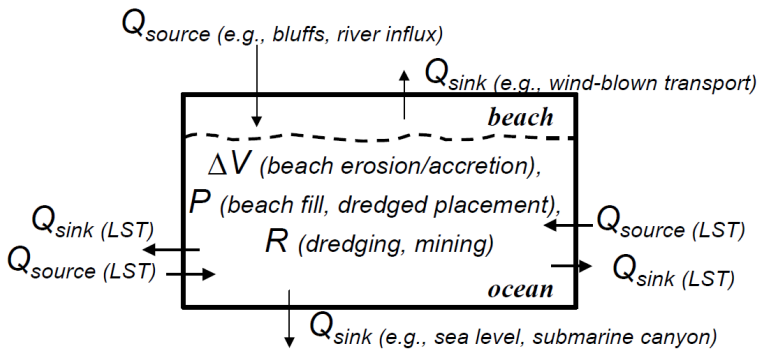

Often, one or more components of the sediment budget are unknown or highly uncertain (e.g. aeolian transport from the beach to the dunes). In these cases, the sediment budget can be used to estimate these unknowns when the transport at the other borders are better known (and when the residual is set to zero).

Sediment budgets are often used to test future management scenarios (e.g. Cooper et al 2001). This can be done by changing the inputs and seeing how the change affects other terms in the equation. For example, one could test the impacts of a groin at the down drift end of the cell by reducing the rate of longshore sediment transport out of the cell. This, in turn, would result in sand building up in the cell, increasing ΔV.

1.3.1 Temporal scale

Sediment budgets are always defined based on a chosen temporal scale. Rosati and Kraus (1999) identify four temporal scales commonly used in sediment budgets. The most common is the existing conditions budget, which represents the present coast, and is used to understand the current natural state and/or the effects of management actions. This is the type of sediment budget developed in the current study, since the objective is to understand the Belgian coast at the present state, and how to best manage it in the future. Sediment budgets can also be used to research historical (pre-engineering) conditions to assess how the budget has changed over time, often with introduction of engineered structures. Moreover, it is possible to forecast a future sediment budget by adjusting an

[1] In other locations, bluff/cliff erosion and relative sea level fall can also be important sources of sediment.
[2] In other locations, losses to a submarine canyon can also be and important sink of sediment.

existing conditions budget to reflect anticipated changes to the inputs (e.g. effects of climate change). Finally, it is possible to use a sediment budget to evaluate any intermediate condition between these three types. The current project uses data between 2000 and 2009 to represent existing conditions along the Belgian coast. A ten year period of time is considered sufficient to reflect these conditions, and it was selected mainly based on data availability. Additional reasons for selecting this time period was to ensure the homogeneity and synchronisation of the data, meaning that the data was gathered using consistent methods and available for all parameters (hydrodynamics and morphology) over the same time period.

1.3.2 Spatial scale

The next step in developing a sediment budget is to identify the geographic area of interest. This requires defining the landward, seaward, and alongshore limits of study. In the present study, the upcoast and downcoast limits of the study area are the French and Dutch borders, respectively. This study focuses on the Belgian coast west of Zeebrugge Harbour, as sediment transport east of the harbour is complicated significantly by the Westerschelde estuary, just east of the border with the Netherlands.

Figure 2 – Study area (from the Kustatlas).

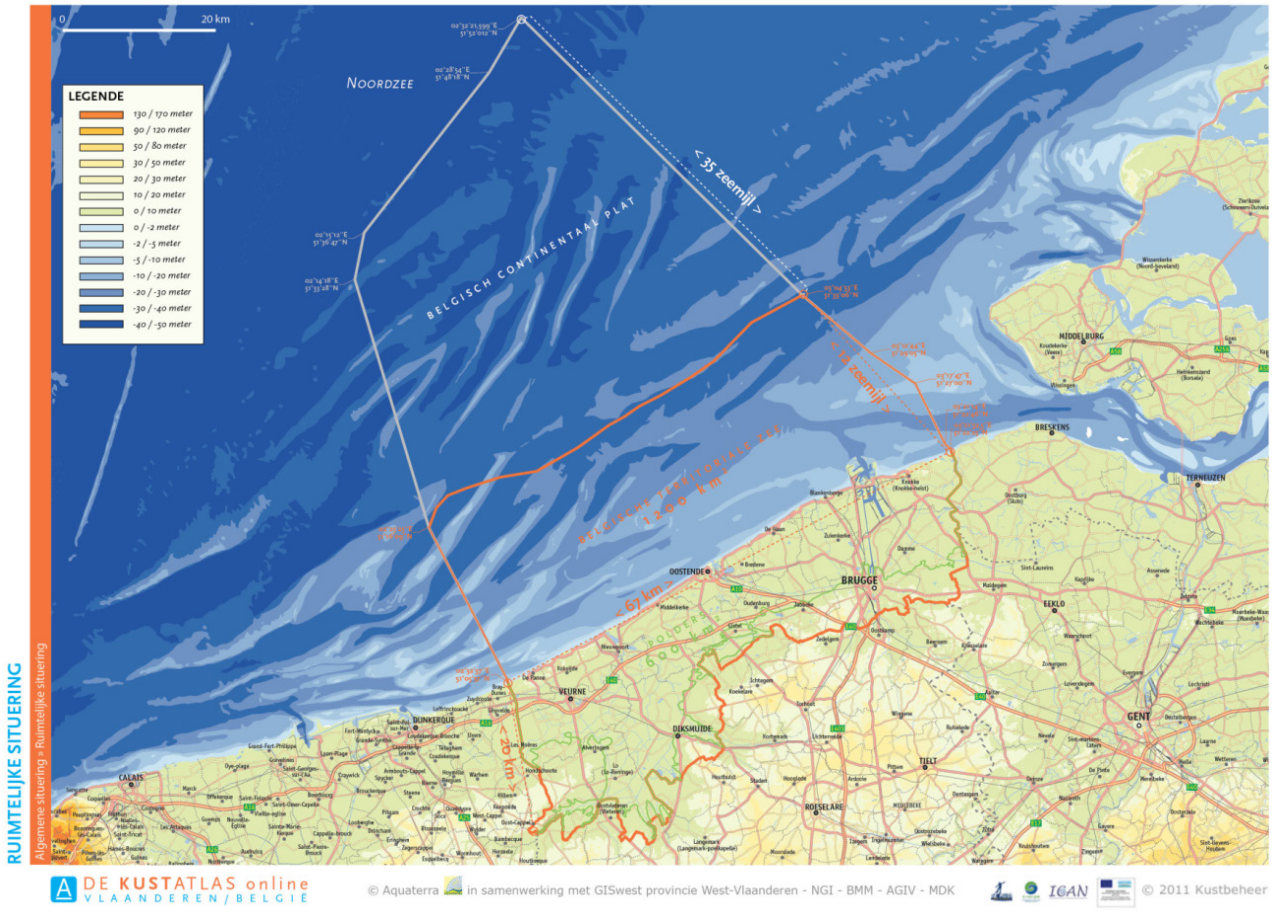

In most cases, including in this study, the study area is further subdivided into smaller cells to allow for a higher-resolution sediment budget of the coast. Cells can be delimitated in any direction (e.g. alongshore or cross-shore) (e.g. van Rijn 1997, van Vessem and Stolk 1990). However, smaller cells require higher resolution input data and increased confidence in the methods used to estimate alongshore transport rates.

Whenever possible, the selection of cell boundaries should be based on discontinuities in rate or direction of sediment transport (Bray et al 1995). Bray et al 1995 presents an approach to defining sediment budget cells based on the stability and permeability of natural or artificial discontinuities. A boundary is *fixed* if it has been stable over a long period of time (e.g. headlands or harbours), while a *transient* boundary tends to evolve over time. A boundary is *absolute* if it blocks all littoral drift, while it is *partial* when some sediment can bypass (e.g. intermittent transport or a valve). Another approach is to select boundaries at locations where the sediment transport rate is known with some confidence (e.g. Bowen and Inman 1966).

Researchers have already developed a system of beach "**sections**" (*secties* in Dutch) along the Belgian coast, which are implemented in this study. In total, there are 277 sections, each approximately 250 meters in width. However, section 1 and sections 256-277 are located in France and the Netherlands, respectively. Therefore, this study will focus on sections 2 through 255 (). Annual beach and shoreface monitoring surveys are conducted based on this system of sections. Previous studies on the Belgian Coast have aggregated the sections into groups of 2 to 10 called "**stretches**" (*stroken* in Dutch), based on their similar morphological trends. There are 51 coastal stretches along the Belgian coast ().

Figure 3 – Coastal sections and stretches along the Belgian coast.

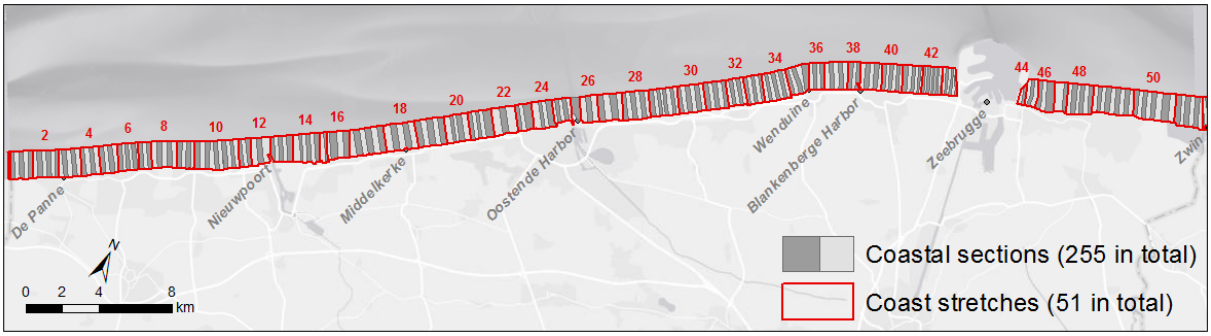

Previous studies have also divided the coast into cross-shore "**zones**" (Figure 4), IMDC 2010, Houthuys 2012). These five zones were defined in the 1980s on the basis of elevation bands: dune (above +6.89 m TAW), dry beach (between +4.39 and +6.89 m TAW), intertidal beach (between +1.39 and +4.39 m TAW), shoreface (between -4.11m and +1.39 m TAW), and sea bottom (below -4.11 m TAW). These elevations were originally defined relative to MOW vertical datum (-4, 1.5, 4.5, and 7 m MOW) and later converted to TAW by subtracting 0.11 m. The elevations are approximate boundaries and not defined on the basis of tidal datums (Rik Houthuys, personal communication, January 6, 2016). The approach of using elevations to identify the sediment budget cells is limited by the offshore extent of the bathymetric surveys, which generally extend to 1500 m offshore of the dune toe or seawall. Just east and west of Zeebrugge harbour, for instance, the lower limit of the shoreface zone usually occurs more than 1500 m offshore, and is therefore not captured in the survey data.

This project uses the aforementioned section-zone framework as a basis from which to build aggregated cells for the sediment budget analysis (see section 2.3 for elaboration).

Figure 4 – Elevation band convention defined in the 1980s. Source: Houthuys 2012.

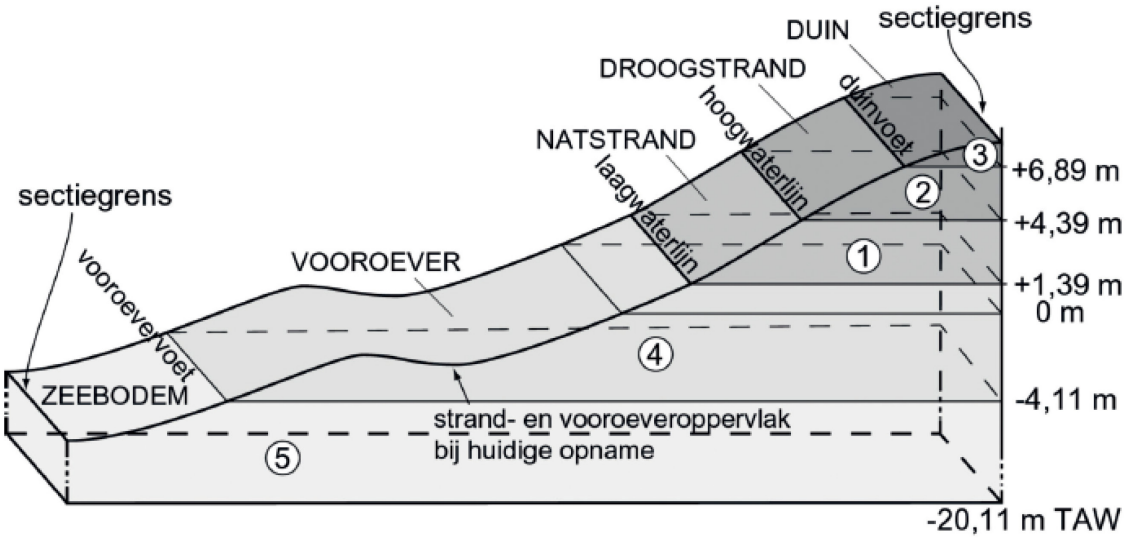

1.4 Implementing the sediment budget equation

While the governing equation for sediment budgets, equation (1), is simple, each component must be estimated based on existing data and literature. This section walks though each of the terms, summarizing existing studies and outlining ways to estimate the terms if no data is available in the literature. Section 2, Methods, follows a similar structure and details which datasets and assumptions were ultimately implemented in the present sediment budget.

1.4.1 Sediment sources and sinks (L, T)

As summarized in the previous section, the relevant sediment sources and sinks for the Belgian coast are longshore transport (either into or out of the cell), cross-shore transport (to/from the offshore and landwards areas), and losses due to sea level rise.

1.4.1.1 Longshore sediment transport rates (L)

1.4.1.1.1. Existing studies

It is well understood that the direction of net littoral drift on the Belgian coast is from southwest to northeast, from the border with France to the border with the Netherlands (Deronde et al 2006, Verwaest et al 2010, Houthuys 2011). Houthuys (2011) observed longshore sediment transport (LST) rates on the order of 10^5 m^3/year along the Belgian Coast.

Most quantitative studies have focused on the areas around Zeebrugge Harbour. Zeebrugge Harbour was extended to a total length of 3 km in 1986, resulting in rapid accumulation of sand against the western breakwater. Verwaest et al (2010) analysed survey data between 1999 and 2008 (years differing slightly depending on the location along the beach profile), with corrections to account for beach nourishments and mining, and found an impoundment rate of $4*10^5$ m^3/year ($\pm 3.5*10^4$ m^3/year). Modeling work using Litdrift (Teurlincx et al 2009) suggests that this was a result of wave transport in the littoral drift zone (85,000 m^3/year), aeolian transport on the dry beach (16,000 m^3/year), and sedimentation on the shoreface, beyond the littoral drift zone (290,000 m^3/year).

Houthuys et al (2014) updated Teurlincx et al 2009 to establish a sediment budget for beach and nearshore area between Blankenberge to the harbour of Zeebrugge. That study considers 14 surveys spanning the years from 1997 to 2011. It assessed volume changes in 12 cells between Blankenberge and Zeebruge (far more detailed than the present study) and provides a detailed list of dredging and filling that occurred at that location.

Velocity and sediment concentration measurements (1990 – 1993) near Knokke and the Zwin (Eurosense 1991a, b and c, 1994 a, b), combined with a hydrological numerical model (Yu 1993), were analysed to develop a sediment budget and extrapolate transport rates for a typical year (Trouw et al 2015). They found a net input of 340,000 m^3/year into the area just east of Zeebrugge. Similar measurements were conducted in front of Het Zwin, where extrapolation of measured data found that about 280,000 m^3/year moves to the east and 160,000 m^3/year moves to the west (net transport of 120,000 m^3/year to the east). However, much of this transport consists of cohesive material.

While few field datasets exist to quantify longshore transport rates along the Belgian coast, numerical modelling studies have been conducted at various locations. One study used Delft3D and XBeach models to investigate sedimentation in Blankenberge Harbour (Wang et al 2012). It found that tide, wind, and waves all significantly affect the total sediment transport, but that in the nearshore (1500m) wave-driven transport dominates. Net longshore transport around Blankenberge was estimated at 360,000 m^3/year in the west to east direction. Modelling by the Management Unit of North Sea Mathematical Models (MUMM) showed that, just east of Zeebrugge, net transport is toward east, except for around Appelzak, where net movement is west (Van Lancker et al 2007). The same study showed that the (low) residual sand transport inside Baai van Heist is to the west. More recently, a 2D numerical model was developed to estimate longshore sediment transport rates in the surf zone for most of the Belgian coast (Wang et al 2015), from Nieuwpoort to the Zwin.

A significant number of studies are available quantifying sand transport rates in the offshore bank areas (Belgium, Middelkerke Bank: Vincent et al 1998, France, Bassure de Baas Bank: Dewez et al 1989), however, the seaward limit of the present sediment budget does not extend this far offshore. Many other studies have looked at fine cohesive sediments (e.g. Fettweis et al 2002, Mercier and Delhez 2007, Fettweis et al 2008), but the focus of this sediment budget is on coarse, beach-sized sediments.

While relatively few, and mostly site-specific, studies exist in Belgium, more research has been done along the north coast of France and the west coast of the Netherlands. Along the French coast, near the Belgian border, the residual transport is still towards the northeast (Dewez et al 1989, Beck et al 1991, Hequette et al 2008). Hequette et al (2008) found that in the vicinity of Dunkirk and Calais, sediment in the mid-upper shoreface is transported primarily by shore-parallel tidal currents (rather than waves). Flood current speeds exceed those of the ebb (Hequette et al 2008), resulting in a net transport towards the northeast (Anthony 2000). They also observed that very limited cross-shore transport occurred, primarily as a result of the macrotidal tides. The French coast near the Belgian border consists of a well-developed coastal dune system. The dunes closest to the Belgian coast have been stable (not eroding) since 1977, partly due to dune rehabilitation projects in the 1990s (Ruz et al 2005).

Multiple sediment budgets have been developed for various parts of the Dutch coastline (Stive 1989, Ruig and Louisse 1991, van Rijn 1997, van de Rest 2004). Net LST rates along the Holland coast were reported between 1 and $6*10^5$ m^3/year in the northward direction (van Rijn 1997, Stive 1989, van de Rest 2004), consistent with the Belgian values. De Ronde (2008) suggested that the import at the Belgian coast roughly matches the export at the north end of the Dutch coast.

van Rijn (1997) developed a sediment budget for the Dutch coast from Hoek van Holland to Den Helder (118 km). The model was calibrated using beach profile data and dredging volumes between 1964 and 1992. Three cross-shore zones were modelled, with boundaries at the 3, -3, -8, and -20 m

NAP contours. Yearly-averaged sand transport rates were estimated using the UNIBEST model (DELTARES), which includes a wave propagation module, a vertical flow structure module, and a sand transport module (van Rijn 1997). Net LST was between 2.5 and $6*10^5$ m^3/year in the northward direction, with the higher rates observed in the north and south parts of the study area (van Rijn 1997). These rates are similar to the estimates along the Belgian coast, though wave-induced longshore currents were found to dominate (over tidal currents).

A second sediment budget was done for the same stretch of coast (Hoek van Holland to Den Helder) by de Ruig and Louisse (1991). In this case, the coast was split into 1km along-shore sections and 3 shore-perpendicular zones (split at MSL and -6 m). This study found that the sand volume in the study area was constant over time, but when relative sea level rise (5 cm between 1963 and 1986) is factored in, $7*10^5$ m^3/year disappeared from the system (de Ruig and Louisse 1991). However, the paper does not describe how this estimate was made.

A third sand balance was done by van Vessem and Stolk (1990) for the entire Dutch coast, including the Delta and the Wadden Sea. The coast was split into 13 shore-parallel sections. The cross-shore extent was from the deepest point in the measured profiles (between 3 and 10 m depth) to the maximum height of each profile. The overall sand balance (taking into account beach nourishments) found annual losses along the entire Dutch coast to be $5.1*10^5$ m^3/year between 1966 and 1986. This disagrees with the assumption in De Ronde (2008) that inputs and outputs to the Dutch coast are roughly equal.

1.4.1.1.2. Estimating longshore sediment transport (L)

LST rates have been studied extensively around the world. Rates can be estimated using numerical models or bulk transport formulas. Numerical models require extensive data and calibration, which is not within the scope of this project. Bulk transport formulas can be used to estimate the average *potential* rate of sediment transport along the coast. The *potential* rate is the rate that sand is transported when sand is abundant along the coast. If the beach is in an eroded state and/or there is a seawall limiting sand released onto the beach, the actual rate of sand transport will be less than the formulas predict. There is no shortage of formulas available to estimate bulk LST rates based on inputs such as wave conditions, beach profile shape, and grain size. Rather than present a comprehensive summary of bulk LST equations, this section will focus on the key formulas available, and their applicability to the Belgian coast.

The most common formula for calculating bulk rates is the CERC formula, presented in the Shore Protection Manual (USACE 1984). This formula was used by Svasek (2012) to estimate a net longshore sediment transport rate near Cadzand of 200,000 m^3/year from west to east (400,000 east, 200,000 west) using a modelled wave climate. The formula assumes:

$$Q_{LST}\left[\frac{m^3}{yr}\right] = \frac{K_c \rho}{16(\rho_s - \rho)(1-a)}\sqrt{\frac{g}{\gamma}}H_b^{5/2}\sin(2\alpha_b) \quad (2)$$

Where,

$K_c = nondimensional\ empirical\ sand\ transport\ coefficient\ [0.39]$

$\rho_s = density\ of\ sediment\ \left[\sim 2650\frac{kg}{m^3}\ for\ quartz\ sand\right]$

$\rho = density\ of\ water\ \left[\sim 1025\frac{kg}{m^3} for\ sea\ water\right]$

$a = porosity\ index\ [0.4]$

$g = acceleration\ of\ gravity\ \left[9.81\frac{m}{s^2}\right]$

$\gamma = wave\ breaking\ index\ [0.78], which\ converts\ breaking\ wave\ depth\ to\ height$

$H_b = significant\ wave\ height\ at\ breaking\ [m]$

$\alpha_b = breaking\ wave\ angle$

In order to obtain breaking wave height and angle, it is usually necessary to transform offshore measured waves (e.g. at 10m water depth) to the wave breaking point (Gravens 1989).

The accuracy of the CERC formula is believed to be ±30-50%, and it does not include parameters such as breaker type and grain size, which have been shown to correlate with longshore transport (Wang et al 2002). It has often been found to overestimate bulk transport rates, and many attempts have been made to modify the coefficient or improve the formula itself (Kamphuis 1991, Schoonees and Theron 1996, Wang et al 2002, Smith et al 2004, Bayram et al 2007, Mil-Homens et al 2013).

Kamphuis (1991) proposed a different formula that considers grain size, wave period, and beach slope, which are all known to influence sediment transport rates (Wang et al 2002). The Kamphuis formula generally results in lower estimates of LST compared to the CERC formula. This is partly explained by the lower order exponent on the significant wave height: 2 rather than 5/2 in the CERC formula.

$$Q_{LST}\left[\frac{m^3}{yr}\right] = K_k H_b^2 T_p^{1.5} m_b^{0.75} D_{50}^{-0.25} \sin^{0.6}(2\alpha_b) \tag{3}$$

Where,

$K_k = nondimensional\ empirical\ sand\ transport\ coefficient\ [6.4 * 10^4]$

$T_p = peak\ period\ for\ offshore\ wave\ spectrum\ [s]$

$m_b = beach\ slope\ in\ the\ breaking\ zone\ (between\ shoreline\ and\ area\ where\ waves\ are\ breaking)$

$D_{50} = characteristic\ median\ grain\ size\ [m]$

$And\ other\ variables\ as\ defined\ above\ for\ equation\ (2)$

Limber et al (2008) warn that the littoral cut-off diameter, a grain size threshold below which sand will not remain on a given beach in any significant quantity (even if it falls within the conventional range representing sand), should be considered when developing sediment budgets. Otherwise, volume inputs to the system may be greatly overestimated.

Schoonees and Theron (1996) recalibrated the Kamphuis (1991) formula using a database containing nearly all available field data (up to 1993) and prioritizing them by quality. This resulted in 273 field estimates of bulk transport rates (compared to the 41 used for the CERC formula, and only lab tests used for the Kamphuis 1991 formula). They recommend a new transport coefficient that improves the R^2 fit of the equation by 118% and the standard error by 20%.

Bayram et al (2007) point out that the CERC and Kamphuis (1991) equations only consider wave-generated currents and disregard wind and tidal currents. They propose a new equation based on the assumption that waves stir up sediment, maintaining a sediment concentration it in the water column, and then currents (from waves, wind, tides) transport it away. The key parameter is a transport coefficient, ε, which expresses the efficiency of waves keeping sediment in suspension:

$$Q_{LST}\left[\frac{m^3}{s}\right] = \frac{\varepsilon}{(\rho_s - \rho)(1-a)g w_s} F\bar{V} \tag{4}$$

$$\varepsilon = \left(9.0 + 4.0\frac{H_b}{w_s T_P}\right) * 10^5$$

Where,

$$\varepsilon = transport\ coefficient\ [-]$$

$$F = flux\ of\ wave\ energy\ towards\ the\ shore\ \left[\frac{kg*m}{s^3}\right]$$

$$\bar{V} = mean\ longshore\ current\ velocity\ over\ the\ surf\ zone\ \left[\frac{m}{s}\right]$$

$$w_s = fall\ velocity\ \left[\frac{m}{s}\right]$$

$$And\ other\ variables\ as\ defined\ above\ for\ equations\ (2)\ and\ (3)$$

The equation was calibrated using six high quality datasets, including both field and lab data. Esteves et al (2009) compared the Bayram et al (2007) formula with CERC and Kamphuis (1991), and found that Bayram (2007) had the best fit with modelled sediment transport rates (modelled using LT-MOD). This method has not been implemented in the present study, as there are not enough field measurements to validate the equations.

Mil-Homens et al (2013) recently tweaked the CERC, Kamphuis (1991), and Bayram (2007) formulas to better match the same set of data used in the Bayram (2007) analysis. They found that the Kamphuis (1991) formula performed best, followed by Bayram (2007).

The present sediment budget uses the CERC and Kamphuis equations to estimate sediment transport along the Belgian coast, in combination with results from the Wang et al (2015) numerical modelling. The results and discussion of longshore sediment transport rates estimated and used in the present study are described in detail in Section 2.4.

1.4.1.1.3. Onshore and offshore sediment transport rates (T)

Few studies have been done to quantify cross-shore transport rates along the Belgian coast. Transport around Zeebrugge Harbour (with transport offshore on the west and onshore on the east side of the harbour) has been analysed in a few studies. A 2D sand transport model, including tidal forcing but not waves, showed a net transport from the Zeebrugge Harbour entrance to the Baai Van Heist (Van Lancker et al, 2007). Trouw et al (2015) estimated that approximately 200,000 m^3/year of mostly fine sediments enter the area just east of Zeebrugge Harbor from the offshore, based on morphological evolution. Most of this is likely coming from the erosion zone in front of the Zeebrugge Harbour. This study suggests that construction of the harbour led to a replacement in alongshore transport (to the east side of Zeebrugge) with input from the offshore. Lanckneus et al (2001) measured bedload transport and estimated a transport of 0.05 m^3/m/day from the north (offshore) towards Baai van Heist (extended over a year, and assuming a 1000m width gives approximately 18,000 m^3/year transport in bedload).

In the Netherlands, van Rijn (1997) found that onshore-directed transport (at the -20 m contour) was in the range of 0 to 15 m^3/m/year (based on a UNIBEST model). This agrees with a study by Roelvink and Stive (1990) that calculated onshore transport at the -8 m line on the order of 10 m^3/m/year. Dijkman et al (1990) estimated cross-shore transport to be +6 m^3/m/year at the -5 m line (based on an equilibrium profile 2-line model).

Sea level rise is generally treated as an offshore sediment sink in sediment budget studies (de Ruig and Louisse 1991, Wolters 1995, van Rijn 1997, Rosati et al 1999, Rosati and Kraus 1999).

1.4.1.1.4. Aeolian transport rates

Aeolian sand transport can account for significant sediment transport in the coastal zone. Aeolian sand transport is poorly investigated at the Belgian coast, and just one study provides quantitative estimates at one location using numerical modelling (Teurlincx et al 2009). Anthony et al (2006) investigated aeolian sand transport at the neighboring French coast, where they found that

significant transport takes place from the shoreface to the dune area. The wind regime favours longshore sand transport and plays an important role in defining the morphology of the intertidal beach (Anthony et al. 2006). However, the data was not sufficient for estimating average annual aeolian sand transport towards the dunes (too short of a measuring period), as would be needed for the sediment budget.

Most aeolian transport occurs within the active beach zone, so this is contained within the sediment budget cells as they are defined in the present project (see section 2.3). However, some transport can also occur between the dunes and the beach, in both directions. Along most parts of the Belgian coast, the dunes and the beach are separated by a road or tram line. In many places, the dunes have been developed or no longer exist. Where they do exist, they are often well stabilized by vegetation. Therefore, we assume that most aeolian sand transport occurs from the beach towards the dunes. Furthermore, much of the landward transport does not reach the dunes, as it first builds up in the road/tramline, where it is regularly cleared by local authorities (and presumably not returned to the coastal zone). The volume of sand removed from the road/tram line are not measured/documented, so no absolute estimate of this loss could be made.

1.4.1.1.5. Sea level rise

Relative sea level rise is an increase in mean sea level relative to land level (caused by changing water level, land level, or both). As sea level rises relative to the land, the equilibrium beach profile will adjust by shifting upwards and landwards to reach a new location that is once again in equilibrium with sea level. This profile shift requires sediment input to raise the profile. Therefore, sea level rise should be included as a sediment sink in the sediment budget equation (Rosati 2005, USACE 1984).

Table 1 presents observed trends in mean sea level for sites in Belgium, as well as the North Sea and globally. The estimates for Oostende, Zeebrugge, Nieuwpoort, and the North Sea were all made using linear regressions on tide gage records (Van Cauwenberghe 1999, Van den Eynde et al 2011, Wahl et al 2013). Wahl et al (2013) compiled data from 30 tide gages around the North Sea to estimate mean sea level rise in the North Sea over different time periods. The Oostende tide gage, which is used to estimate most of the observed sea level trends in Belgium, has records dating back to 1927 (with significant gaps during World War 2). Older records were collected, dating back as far as 1820, but this data is either incomplete, lost, or consists only monthly mean values of high and low water, which is not sufficient to calculate the mean sea level trend (Van Cauwenberghe 1999).

Table 1 – Observed mean sea level trends from linear fits of tide gage records.

Study	**Location**	**Time Period**	**MSL Trend** (mm/year)
Long-term			
IPCC 2013	Global	1901 – 2010	1.7 ± 0.18
Wahl et al 2013	North Sea average	1900 – 2009	1.54 ± 0.11
Van Cauwenberghe 1999	Oostende tide gage	1927 – 1998	1.44
Van den Eynde et al 2011	Oostende tide gage	1927 – 2006	1.69
Medium-term			
IPCC 2013	Global	1971 – 2010	2.0 ± 0.3
Wahl et al 2013	North Sea average	1950 – 2009	1.62 ± 0.29
Wahl et al 2013	Oostende tide gage	1950 – 2011	2.1 ± 0.3
Wahl et al 2013	Oostende tide gage	1980 – 2011	2.5 ± 0.7
Van Cauwenberghe 1999	Zeebrugge tide gage	1964 – 1998	1.50
Van Cauwenberghe 1999	Nieuwpoort tide gage	1967 – 1998	2.77

Short-term			
IPCC 2013	Global	1993 – 2010	3.2 ± 0.6
Wahl et al 2013	North Sea average	1993 – 2009	4.0 ± 1.53
Van den Eynde et al 2011	Oostende tide gage	1992 – 2006	4.41
Wahl et al 2013	Oostende tide gage	1993 – 2011	3.5 ± 1.4

While the above table only presents mean sea level trends, Van Cauwenberghe (1999) also found that the mean high water level at Oostende increased more (~50% more) than the mean sea level over the 70 year time period. At the same time, low water level increased less (~40% less) than the mean sea level. This means that the average tide range at Oostende has been growing (similar trends were observed for the Zeebrugge and Nieuwpoort gages). However, for the purposes of this sediment budget exercise, we assume that the equilibrium profile response to sea level rise is driven by the mean sea level, and therefore we will select an appropriate mean sea level trend that takes into account the timeframe of the sediment budget.

The sediment required to lift the profile in response to sea level rise can be estimated using the Bruun Rule (Bruun 1962, Bruun 1988, e.g. Rosati et al 1999, Rosati and Kraus 1999, van Rijn 1997). The transfer of sediment from the top of the beach profile to the bottom of the beach profile (resulting in shoreline erosion and lifting of the profile) is shown in Figure 5.

Figure 5 – The Bruun Rule – translation of the beach and bottom profile resulting in shore recession and deposition of sediments (Source: Bruun, 1988).

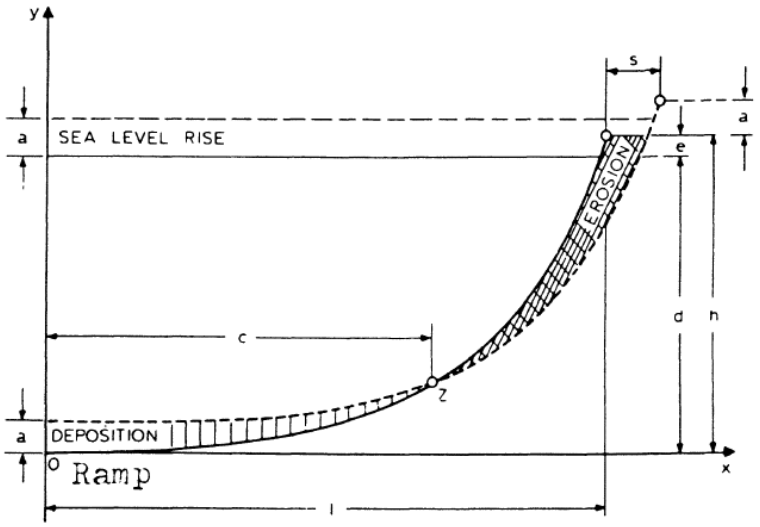

Note: the letters representing dimensions in this figure do not correspond with the letters in the equations below.

The basic Bruun Rule for shoreline recession due to sea level rise is as follows:

$$\Delta y_{slr} = \frac{L}{B + D_c} S \tag{5}$$

Where,

$\Delta y_{slr} = the\ long - term\ beach\ recession\ due\ to\ sea\ level\ rise\ [m]$

$L = the\ cross - shore\ distance\ from\ closure\ depth\ to\ the\ beach\ berm\ crest\ [m]$

$B = beach\ berm\ height\ above\ vertical\ datum\ [m]$

$D_c = depth\ of\ closure\ (relative\ to\ the\ same\ vertical\ datum, a\ positive\ value)[m]$

$S = amount\ of\ sea\ level\ rise\ [m]$

This equation can then be used to estimate the volume of sand that must be added to the system to counteract this shoreline recession (i.e. the sediment "sink" caused by sea level rise):

$$Q_{SLR}\left[\frac{m^3}{m*yr}\right] = \frac{\Delta y_{slr}}{t} * (B + D_c) \quad (6)$$

Where,

$Q_{SLR} = sand\ sink\ due\ to\ sea\ level\ rise\ \left[\frac{m^3}{m*yr}\right]$

$t = time\ over\ which\ sea\ level\ rise\ occurred$

If the sediment budget is done with multiple cross-shore cells, then the volume loss due to sea level rise must be divided by the cross-shore cells (e.g. van Rijn 1997).

Example: Assume sea level rose at a rate of 3 mm/year from 1990 to 2010 (t = 20 years). This is a total of 0.06 m of sea level rise. Assume an overall profile slope of 1:100 (i.e. the $L/(B+D_c)$ term). This corresponds to a profile recession of 6 meters. Assuming an overall profile height of 8 meters ($B+D_c$), and a 67 km-long coastline. This results in an annual sediment sink of $1.6*10^5$ m^3/year.

The Bruun Rule has had many critics over the years (e.g. Dubois 1992, Cooper and Pilkey 2004, Ranasinghe et al 2012, Rosati et al 2013), who argue that the relation is too simplistic, makes incorrect assumptions, lacks supporting field data, and omits important processes. However, it is exactly its simplicity that makes it ideal for this sediment budget exercise. The alternatives would be detailed numerical modelling, probability studies, and complex empirical equations. The uncertainties inherent in the longshore sediment transport rates (Section 1.4.1.1.2), which sometimes span multiple orders of magnitude, are likely greater than those resulting from the Bruun Rule. Therefore, we will use it here, with caution, to estimate the sediment sink created by sea level rise.

1.4.2 Placements and removals (P and R)

Placements and removals, represented by the P- and R-terms in Equation (1), are sediment quantities that are deliberately added or removed from the sediment cell by humans rather than natural processes. Removals usually result from sand mining or dredging. Placements usually occur in the form of nourishment projects (both on the shoreface or beach). There are two common types of beach nourishments on the Belgian coast: beach nourishment using sand from locations other than the active beach, and beach "lifts" (in Dutch: badstrandophogingen). In the latter, sand is taken from the intertidal beach and shoreface (from 2.5 m TAW and below) and placed up on the dry beach.

Houthuys (2012) presents a description of morphological trends along the Belgian coast between 1983 and 2011, including trends corrected for placement and removal of sediment. The placements and removal volumes are documented by coast stretch (see 2.5) and year, and are based on reports and data from, primarily, the Coastal Division. The report also documents any assumptions that were made about the sediment volume and/or date of occurrence. For example, in order to calculate volume changes in each of the vertical elevation zones resulting from a beach "lift" nourishment, it was assumed that 50% of the sand was taken from the intertidal beach zone and 50% from the shoreface (IMDC (2010)). Section 2.5 describes how the Houthuys (2012) placement and removal data was incorporated into the current sediment budget.

1.4.3 Volume changes (ΔV)

The volume change term, ΔV in Equation (1), represents the change in sediment volume over the time period of interest. There are many ways to calculate the volume change in a cell. Often, shoreline change rates are combined with the shoreface height (from profile surveys) to calculate a volume change over time (e.g. Rosati et al 1999). If detailed beach profile data is available, these can be compared from year to year and multiplied by the longshore distance to estimate the volumetric change (e.g. van Vessem and Stolk 1990, de Ruig and Louisse 1991, Houthuys 2012). It is also possible to derive volume changes from shoreline positions or topographic/bathymetric survey data.

This study uses bathymetric and topographic surveys conducted by the Flemish government (Coastal Division[3]). The surveys are available almost every year between 1997 and 2010, though the spatial extent does not always cover the entire Belgian coast. The topographic surveys extend roughly from the dune toe to low water, and the bathymetric surveys extend from low water to 1.5 km offshore. Since 1998, the topographic surveys have been conducted using airborne LiDAR during low tide. The LiDAR data is post-processed to remove vegetation and structures, and has a reported accuracy on the order of ±10 cm (Janssens et al 2013). The bathymetric surveys are collected by either a hovercraft or catamaran equipped with an echo sounder. Data is collected in shore-perpendicular transects at 100-meter spacing along the coast, and the estimated accuracy is ±10 cm (Janssens et al 2013).

In order to calculate the volume changes from these survey data, it is necessary to interpolate the data to a digital elevation model. This has been done in two previous studies: Houthuys 2012 and Janssens et al 2013. Both studies started with the same input data provided by Afdeling Kust, xyz text files representing (1) the ground-based LiDAR survey points and (2) bathymetric transect survey points. The Houthuys 2012 study constructed digital elevation models by building a triangulated irregular network (TIN) out of the points and then converting to a 2- or 10-meter raster for the beach and shoreface surveys, respectively. Janssens et al (2013) used the Natural Neighbor interpolation technique in ArcGIS, creating 2-meter grids for both the beach and shoreface surveys.

As part of the Houthuys 2012 study, volume changes, relative to a starting date that varies along the coast, were calculated for each zone and section (see 1.3.2), to approximately 1500m offshore (the typical limit for the shoreface bathymetric surveys). The volumes, aggregated into coast stretches (see 1.3.2) were made available for use in this study.

Section 2.6 describes how these DEMs and the derived volumes were used for input to the sediment budget along the Belgian Coast.

1.5 Combining uncertainties in sediment budgets

Each of the terms in the sediment budget equation has an associated level of uncertainty. Section 2, Methods, describes how uncertainty was estimated for each of the inputs. Once uncertainties are estimated for each of these terms, they must be combined in order to estimate the uncertainty of the solved unknown. This was done using conventional rules for combining uncertainties when adding, subtracting, multiplying, or dividing terms:

When terms are added:

$$X = x + y - z \ldots$$

Then the best estimate of uncertainty (root-mean-squared error, where δ represents the uncertainty of a term) is:

[3] Afdeling Kust, in Dutch.

$$\delta X_{best} = \sqrt{(\delta x)^2 + (\delta y)^2 + (\delta z)^2}$$

When terms are multiplied or divided:

$$X = \frac{xy}{z} \ldots$$

Then the best estimate of uncertainty is:

$$\frac{\delta X_{best}}{X} = \sqrt{\left(\frac{\delta x}{x}\right)^2 + \left(\frac{\delta y}{y}\right)^2 + \left(\frac{\delta z}{z}\right)^2}$$

For a detailed explanation about how to combine uncertainties from various sources, we refer the reader to Kraus and Rosati 1998.

2 Methods

This section describes the methods used to develop and apply a sediment budget for the Belgian coastline. These methods are based on the literature and data available, as described in Chapter 1. The first section presents a simplified version of the sediment budget equation presented in section 1.3, which was then applied for the Belgian coast.

2.1 The sediment budget equation on the Belgian coast

For the present sediment budget, we reorganize the sediment budget equation (1) in applying it to the Belgian coast (Figure 6). The simplified equation (7) is presented below, with an accompanying figure to explain the sign conventions. A term is positive if it leads to the sediment in the cell increasing. As is described in later sections, the onshore/offshore transport is not well documented or understood, so the residual is set to zero and the offshore/onshore transport, T, is solved for.

$$\Delta V = \Delta L + P - R + T \tag{7}$$

Where:

ΔV = Observed change in volume (+ is net increase in volume, - is net decrease in volume)

ΔL = L_{in}-L_{out} = Net longshore sediment transport into the cell (+ is accumulation, - is erosion)

P = Volume of sand added to the cell in the form of nourishments/dredge placement

R = Volume of sand removed from the cell during dredging/mining

T = Net transport into or out of the cell via cross-shore transport (including exchange with the offshore *and* inland areas).

Figure 6 – Simplified sediment budget schematic for one cell along the Belgian coast.

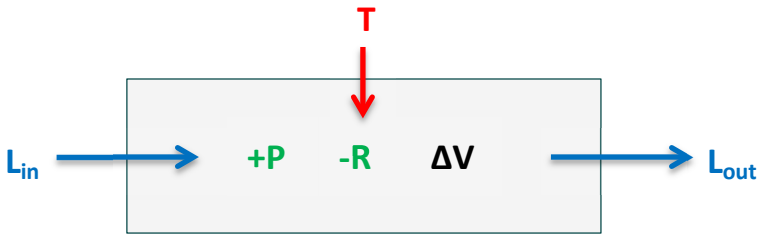

Another term that is sometimes used in developing the sediment budget is the "natural evolution" volume change, ΔV', which is the observed volume (ΔV) corrected for any placement or removal volumes:

$$\Delta V' = \Delta V - (P - R) = \Delta L + T \tag{8}$$

2.2 The sediment budget tool

While simple, single-celled, sediment budgets can be calculated by hand, more complex sediment budgets are better solved using computer-based tools. For example, the Sediment Budget Analysis System (SBAS), developed by the U.S. Army Corps of Engineers (USACE) is an ArcGIS extension tool (though a stand-alone version also exists) that can document, calculate, and visualize a multi-celled sediment budget (USACE 2012).

For this study[4], a spreadsheet tool was built that is tailored to the data collected along the Belgian coast. The tool, built in a Microsoft Excel spreadsheet, solves the sediment budget equation (see Section 1.3, assumes Residual = 0) using a set of macros and user inputs. The tool works according to the following general steps:

1. The user enters the available information about sediment added or removed from the system by human interventions (Section 1.4.2) and measured volume changes derived from survey data (Section 1.4.3).
2. The user specifies the sediment budget time frame (within the span of the input data).
3. The user specifies how the 277 along-shore sections and the 4 cross-shore zones should be aggregated for the purposes of the sediment budget. For example, the user could group the 4 cross-shore zones together to look at the overall sediment budget along the coast (but not attempting to resolve the sediment budget across the shore). See section 1.3.2 for a description of how the alongshore sections were grouped in the present budget.
4. The tool then provides an empty array, where the user inputs the longshore (Section 1.4.1.1) and cross-shore (Section 1.4.1.1.3) sediment transport rates and their associated uncertainties for each of the aggregated regions.
5. The tool then verifies whether the system of equations (one sediment budget equation for each aggregated region) is solvable. It reports how many extra unknowns there are for each aggregated region. The user is then referred to another tab, where the missing terms must be filled in before the system of equations can be solved.
6. Once the correct number of variables have been defined, the user runs the tool, which uses Excel macros to solve the system of equations, assuming that the residual is equal to 0.

The result is a set of tables reporting longshore and offshore transport rates, volume changes, and their associated uncertainties for each aggregated region. Values that were provided as inputs are formatted differently from values that were solved for by the tool, making it easy for the user to see the difference. These results should then be assessed for reality using judgement and any additional datasets that were not already used to develop inputs to the model.

The sediment budget tool follows the rules described in Section 1.5 to combine uncertainties of each of the input parameters to estimate the uncertainty of the solved-for variable. The exact implementation of uncertainty calculations is explained in detail in the sediment budget tool manual (attached as Appendix A, in Dutch).

[4] Developed in 2013 in a previous phase of this project.

2.3 Defining the analysis cells

This section describes how the analysis cells (Figure 7) were selected for the current sediment budget, in the longshore and cross-shore directions. Refer to section 1.3.2 for an explanation of the existing longshore and cross shore divisions that formed the basis of the cells described below.

Figure 7 – Nine sediment budget analysis cells (and their constituent stretches) along the Belgian Coast.

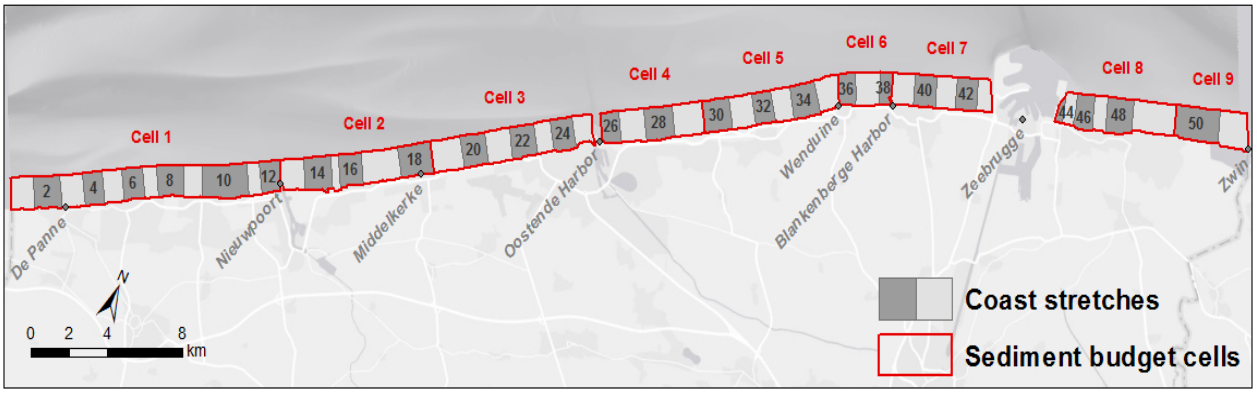

2.3.1 Longshore divisions

The coast stretches were grouped into analysis cells for the sediment budget based primarily on harbors. In some cases the distance between the harbour was divided in approximately half, based on a change in longshore sediment transport rate or key landmark. Table 2 presents the longshore cells (groups of sections) selected for this study.

Table 2 – Alongshore divisions for the sediment budget.

Cell #	Stretches	Sections	Length (km)	Description
1	1-12	2-59	14.3	De Panne to Nieuwpoort Harbour
2	13-18	60-87	8.0	Nieuwpoort Harbour to Middelkerke
3	19-25	88-117	8.6	Middelkerke to Oostende
4	26-29	119-139	5.4	Oostende Harbour through Bredene-aan-Zee
5	30-35	140-172	7.2	De Haan to Wenduine
6	36-38	173-184	2.7	Wenduine to Blankenberge Harbour
7	39-43	185-216	5.3	Blankenberge Harbour to Zeebrugge Harbour
8	44-49	217-241	6.4	Zeebrugge Harbour to Knokke Zoute
9	50-51	242-255	3.9	Knokke Zoute to Het Zwin

2.3.2 Cross-shore divisions

While volume change and placement/removal estimates are available on a zone basis (see section 1.3.2), estimating long- and cross-shore sediment transport rates between individual zones (e.g. between the shoreface and the beach) would introduce significant uncertainty to the resulting sediment budget. While estimating longshore sediment transport rates for an entire beach profile is already a challenge (see sections 1.4.1, 2.4, and 2.7), estimating cross-shore transport rates between,

say, the shoreface and the beach, is even more difficult (less documented/studied). Estimating the individual longshore sediment transport rates for the shoreface, beach, and dunes separately, as well as the cross-shore transport rates between them, would introduce much more error/uncertainty than the benefit that would be gained by presenting results at such a high resolution.

Therefore, this study combines all cross-shore zones into a single zone that (ideally) includes the entire active beach profile (Figure 7). This transforms the sediment budget into a 1D string of cells spanning the Belgian coast.

2.3.3 Onshore limit

Ideally, the onshore limit of this study would extend to the inland limit of the active littoral system (e.g. dunes). However, the ability to do this is limited by the available survey data. The onshore limit for this study was taken as the maximum inland extent of survey data (i.e. the maximum inland extent which all surveys used for the volume calculations reached). This generally results in an inland limit somewhere in the dunes, in the case of a natural coastline, or just beyond the seawall, where development exists.

2.3.4 Offshore limit

The offshore limit of the analysis cells is the most challenging to define, as the limit should be a location where we have an understanding of the sediment transport occurring across it. Ideally, offshore limit of the coastal cell should is define as the area where offshore sediment transport is negligible in comparison with longshore transport. As described in section 1.3.2, previous studies used an elevation contour (-4.11m TAW) to define the lower limit of the shoreface. In order to check this assumption, we applied the Hallermeier (1981) equation, which is based on linear wave theory, to estimate the "closure depth," or seaward limit of significant profile change (Sabatier et al 2004). The Hallermeier equation is as follows:

$$D = 2.28H_e - 68.5\left(\frac{H_e^2}{gT_e^2}\right) \tag{9}$$

Where,

$D = closure\ depth\ [m]$

$H_e = extreme\ significant\ wave\ height\ (occurring\ 12hrs\ or\ 0.137\%\ of\ the\ time)[m]$

$T_e = extreme\ significant\ wave\ period\ corresponding\ with\ H_e\ [s]$

This equation was applied using the nearshore (approximately 5 m depth) wave data time series described in section 2.4. The resulting longshore variation in closure depth is shown in Figure 8.

The results suggest that an appropriate lower elevation bound would be around -5 m TAW. Figure 9 shows the extent of the volume calculations in the previous/present study ("sediment budget cells") and the depth of closure contour based on the Hallermeier equation. This figure shows that in most cases, the sediment budget cell contains the depth of closure (and further offshore). However, in some cases (parts of cell 1, cell 4, cell 7, and cell 8) the surveys did not extend far enough offshore to reach this depth. Ultimately, the entire surveyed area, which extends to approximately 1500 m offshore, was considered in the sediment budget, rather than limiting to a certain depth (which was not possible since many of the surveys did not extend to -5m depth). This also made it possible to use volumes calculated in previous studies (Houthuys 2012). The closure depth is the deepest zone where the waves, occurring over a certain time period, can influence the morphology of the sea floor. This imply a rather constant slope of the beach profile, but for the Belgian coast often it is not the case. In many cases after reaching a maximum depth the beach profile becomes shallower due the proximity of the coastal banks and thus the closure depth concept cannot be applied. However,

since the active beach is bound offshore by the closure depth we calculated this depth for the same period as the rest of data used to build the sediment budget, 2000 – 2009 inclusively. Furthermore, the results were proved consistent with the offshore boundary selection of -5 m TAW.

Figure 8 – Closure depth (in m TAW) along the Belgian coast, as calculated with Hallermeier 1981.

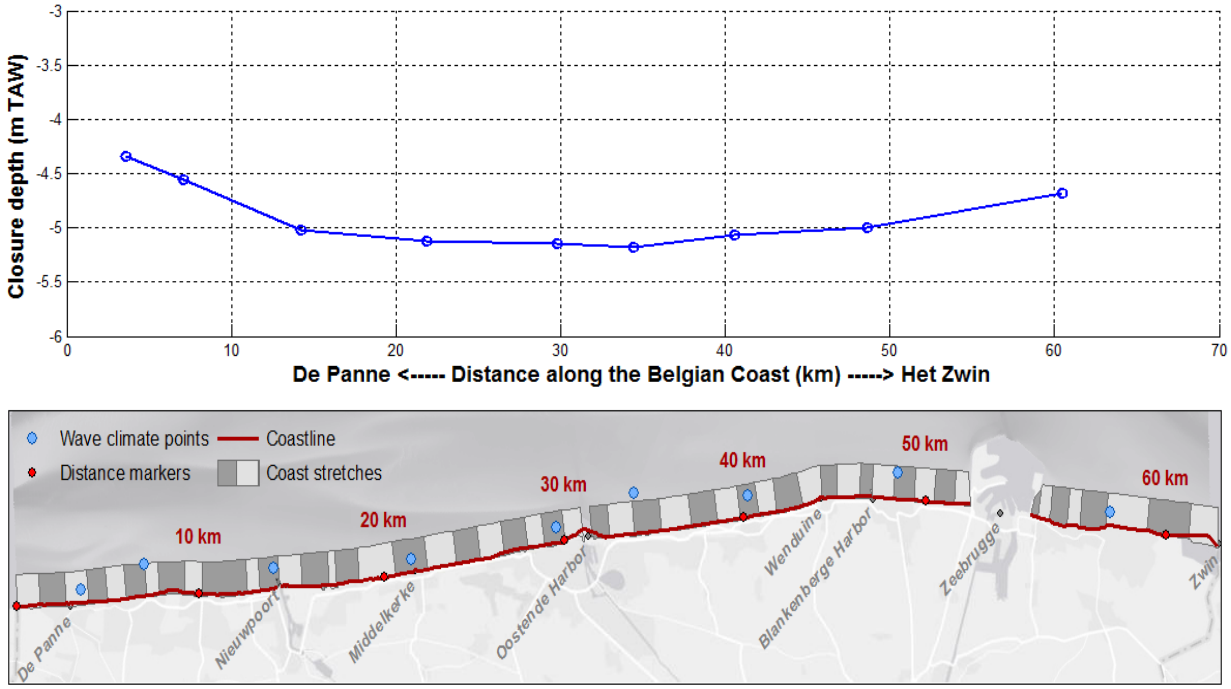

Figure 9 – Depth of closure contour (closest contour to shore) and export line for longshore sediment transport (see section 2.4.3).

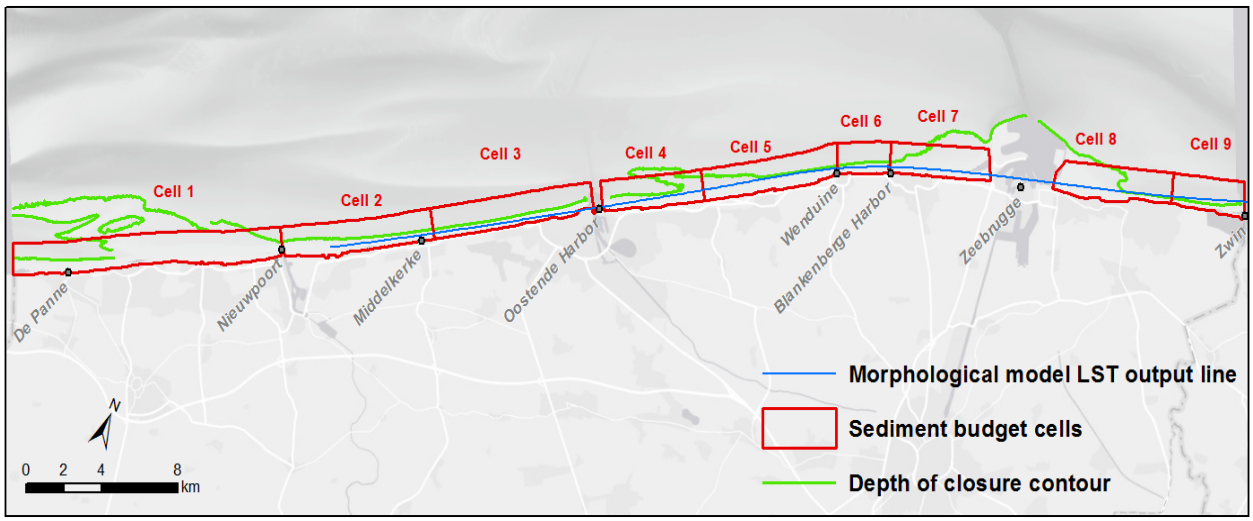

2.4 Estimating longshore sediment transport rates (L)

The longshore sediment transport rate along the Belgian coast was estimated using three different methods: two empirical equations (see section 1.4.1.1.2) and a numerical morphological model of the Belgian coast. Each of these estimates are described in the subsequent sections, with the last section comparing the different methods and explaining which values were used in developing the sediment budget for the Belgian coast.

2.4.1 CERC equation

The main inputs to the CERC equation (Equation (2)), described in section 1.4.1.1.2, are the breaking wave height and angle. For this project, the CERC equation was applied to a representative wave climate, which reports the frequency of occurrence for a set of wave height (0.25 m), period (1 second), and directional (5 degree) bins. The CERC equation was applied to each bin of data, and the resulting longshore transport rates were multiplied by the corresponding frequency and then summed to obtain the average annual longshore transport rate.

Wave data for this project was obtained from a SWAN model developed by IMDC for Flanders Hydraulics Research between 2005 and 2009 (IMDC 2009a, IMDC 2009b). The model domain includes the entire Belgian coast between France and the Netherlands and has a spatial resolution of 250 x 250 meters. Nearshore time series (significant wave height, period, and direction) from 1996 to 2005 were readily available for 9 points (5 m water depth) along the coast (Figure 10). 21% of the time series was missing due to measurement gaps in one or more input wave buoys. Since much of the missing data occurs in winter, these data gaps could not be ignored, as these months are usually stormier and contribute more significantly to the longshore transport rates. First, small gaps (<4 hour duration) were linearly interpolated in time. Average monthly wave climates were developed by averaging the individual wave climates of months containing at least 75% data. Then, the average annual wave climate was estimated by combining the average monthly wave climates (weighted by the number of days per month). The result was a percent occurrence for each wave height, period, and direction bin.

The next step was to estimate the breaking wave height and angle for each wave bin. This was done using the refraction, shoaling, and breaking equations described in Kamphuis 2010. This analysis did not consider wave diffraction, which is particularly important near harbour jetties of Zeebrugge, Oostende, and Nieuwpoort, as well as beach groins. See section 2.4.4 for further discussion. The result was breaking wave height, angle, and depth for each wave bin.

Finally, the CERC equation could be implemented to calculate the average annual longshore sediment transport rate for each of the wave bins. We assumed a sediment density of 2650 kg/m^3, sea water density of 1025 kg/m^3, and a voids ratio of 0.6 (volume voids/total volume). Since each of the wave bins occurs only a fraction of the time, the LST rates were multiplied by their respective fractions and summed together to obtain a total average annual LST rate for each of the 9 nearshore locations (Figure 15).

2.4.2 Kamphuis equation

The Kamphuis equation (Equation (3), described in section 1.4.1.1.2) was applied using the same wave data (bins, corrections for missing wave data, breaking wave heights) as the CERC equation (see previous section). The Kamphuis equation required three more inputs than the CERC equation: peak wave period, average beach slope in the wave breaking zone, and grain size (D_{50}) in the wave breaking zone. The peak period was already available in the same wave dataset described above.

The average slope was calculated using representative profiles from each beach section. The representative profiles were a combination of beach and shoreface data from 2010 LiDAR and 2009 surveys, respectively. The slope was calculated as the linear trend between mean low water (MLW) and mean high water (MHW), as reported at the nearest available tide station (Table 3).

Figure 10 – Location of nearshore wave data output points.

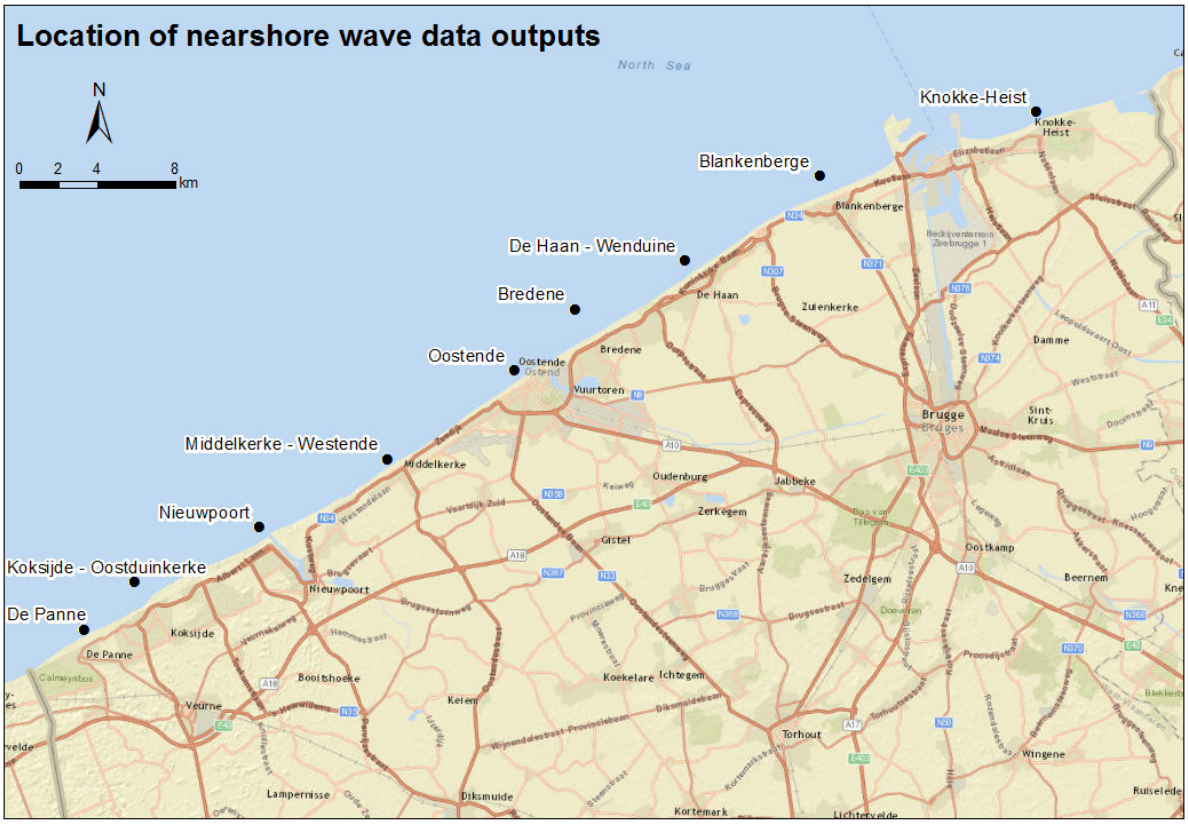

Figure 11 presents the beach slope variability along the Belgian Coast. The beach is relatively flat in the vicinity of De Panne, but gradually steepens as it approaches Oostende Harbor, with a sudden steepening in the sections adjacent to the breakwater. On the east side of the harbour, the beach slope is relatively constant until it approaches Blankenberge and Zeebrugge Harbour, where it continues to flatten. Beaches east of Zeebrugge Harbour are initially very flat, but steepen quickly in the vicinity of Het Zwin. The shoreface slopes are used to estimate sediment volumes "lost" due to sea level rise, as described in section 2.7.1.

Beach grain size data are available at approximately 50 evenly spaced (approximately every 1.5 km) cross-shore transects along the Belgian coast. The data was collected by VITO for the Belgian Coastal Division in 2003. Samples were collected at up to 4 locations along each transect, based on beach surface elevation (1, 2, 3, and 4 m TAW). At each location, up to 3 samples were collected, at the surface, 50 cm depth, and 80 cm depth. The samples were analysed for grain size and organic content. The D_{50} in the surf zone was approximated by averaging the samples from all depths for the 1 m TAW sample location. This is the lowest sampling location in elevation along the transect, and therefore the closest available to the break zone. Each beach section was assigned the average grain size for the sample collected nearest to it (Figure 12).

Table 3 – Belgian Tidal Datums (m TAW).

Datum	Description	Nieuwpoort	Oostende	Zeebrugge
HOWL	Highest observed water level	6.730	6.660	6.690
MHWS	Mean high water spring	4.842	4.700	4.583
MHW	Mean high water	4.420	4.302	4.209
MHWN	Mean high water neap	3.876	3.790	3.730
MTL	Mean tide level	2.374	2.359	3.645
MSL	Mean sea level	2.313	2.294	2.294
MLWN	Mean low water neap	0.769	0.816	0.919
MLW	Mean low water	0.328	0.416	0.564
MLWS	Mean low water spring	-0.016	0.100	0.281
LOWL	Lowest observed water level	-1.100	-1.090	-0.830
	Tide range (spring)	4.858	4.600	4.302
	Tide range (mean)	4.092	3.886	3.645
	Tide range (neap)	3.107	2.974	2.811

Figure 11 – Beach slopes along the Belgian Coast.

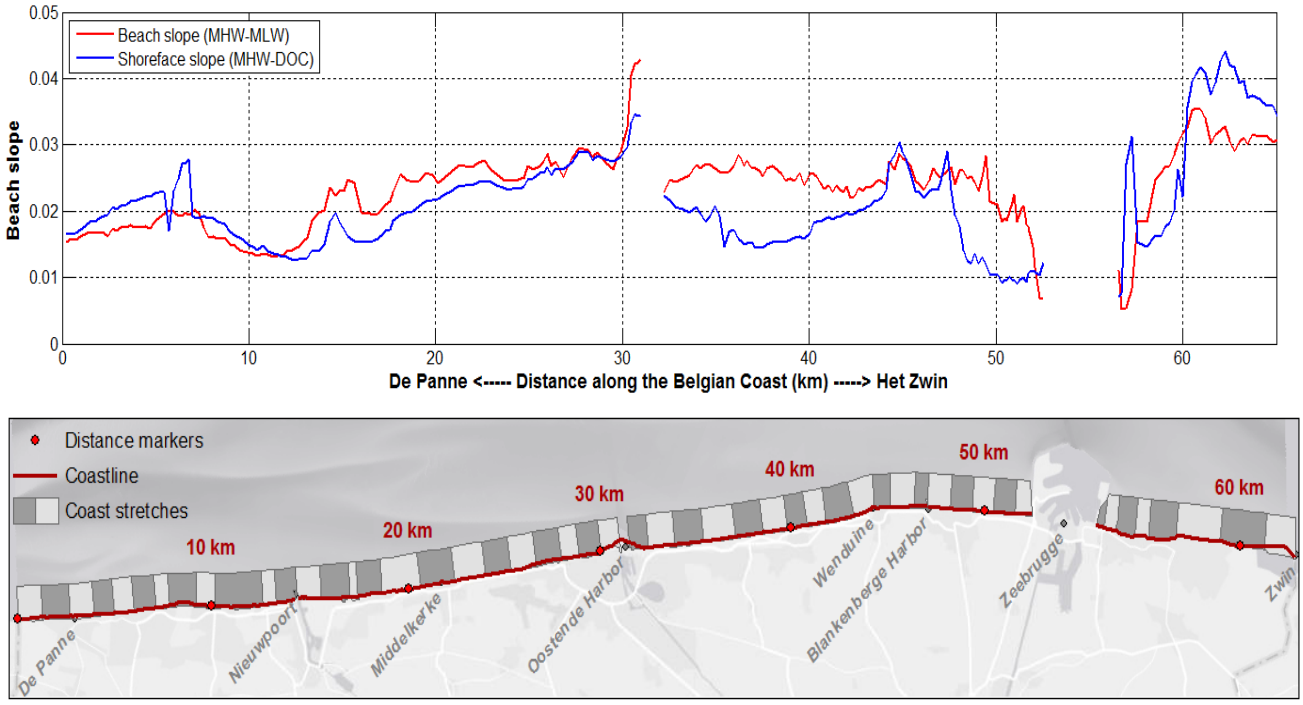

Finally, the Kamphuis equation could be implemented to calculate the average annual longshore sediment transport rate for each of the wave bins. We assumed a sediment density of 2650 kg/m^3, sea water density of 1025 kg/m^3, and a voids ratio of 0.6 (volume voids/total volume). Since each of the wave bins occurs only a fraction of the time, the LST rates were multiplied by their respective fractions and summed together to obtain a total average annual LST rate for each of the 9 nearshore locations (Figure 15).

Figure 12 – Grain size along the Belgian Coast.

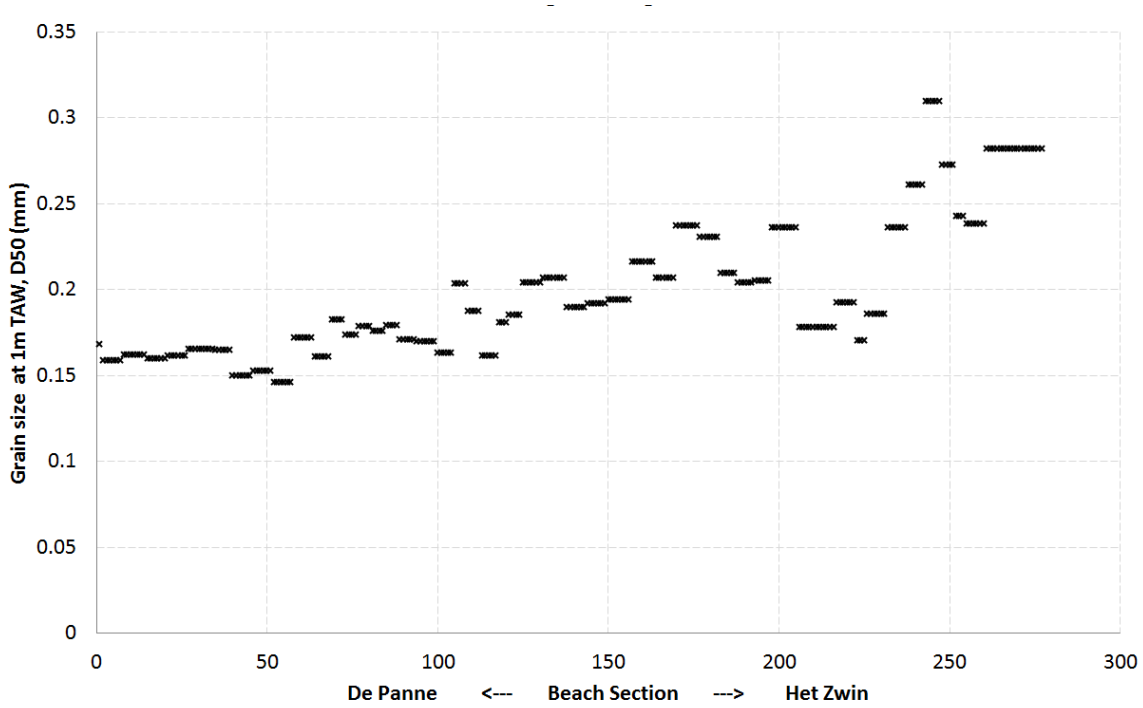

2.4.3 Long term morphological model

A 2D numerical model was developed during a previous study (Wang et al 2015) for most of the Belgian coast, from Nieuwpoort to the Zwin, to estimate longshore sediment transport in the surf zone. The model was found to capture long term morphological changes reasonably well for most of the coast, except in the Baai van Heist area. Long-term average annual sediment transport was calculated for two past time horizons (1986 – 1996 and 1999 – 2009) and one future projection (2009 – 2019). The results from the 1999 – 2009 time horizon are presented here, as they best match the time frame of the present sediment budget (Figure 15, solid blue line).

The study was primarily focused on estimating longshore transport due to breaking waves, and therefore assumed that the transport beyond the surf zone was negligible. The longshore transport rates are derived from the model by integrating the transport along a cross-shore profile from the beach (landward limit of model) to a line offshore. The offshore limit of the integration, shown in Figure 13 is based on a line of grid cells in the model domain, rather than a fixed distance from the coastline or elevation contour.

Along much of the coast, the depth of closure contour and the LST integration line are relatively close together (Figure 9). However, there are a few locations where the integration line falls with within the depth of closure contour. Therefore, the longshore transport reported by the model likely underestimates the true longshore transport rate. Figure 15 shows conceptual cross-shore distributions of longshore transport (Q) for a grain size of 0.2 mm, which is close to the average along the Belgian coast. Peak transport generally occurs just onshore of the breaking wave line, and tapers off further offshore, so it is likely that for most wave conditions, the model estimate includes most of the peak and only cuts off the outermost tail. However, it is possible that for larger wave events, when the peak shifts offshore, part of the LST was not captured.

Figure 13 – Offshore limit of the longshore transport calculation (pink line) (source: Wang et al 2015).

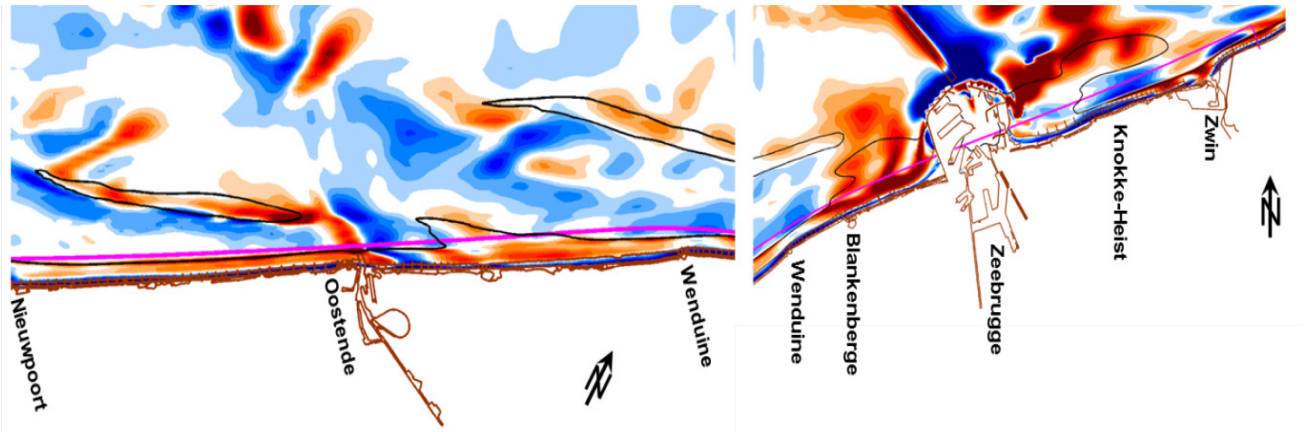

Figure 14 – Distribution of the littoral transport over a conceptual coastal profile.

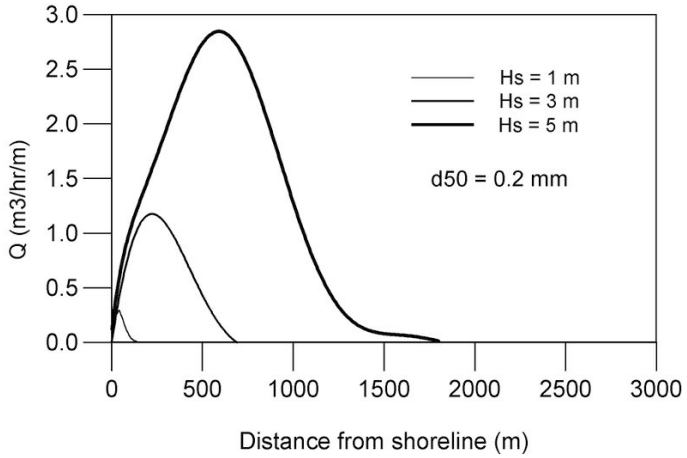

For grain size d50 = 0.2 mm, wave heights H_s = 1, 3, 5m, angle of incidence 30° and for an equilibrium profile corresponding to the grain size. Calculated using LITPACK. Source: http://www.coastalwiki.org/wiki/Coastal_Hydrodynamics_And_Transport_Processes

2.4.4 Comparison of longshore sediment transport estimates

Figure 15 presents a comparison of the potential average annual longshore sediment transport rate along the Belgian coast from seven sources: two from observations (Verwaest et al 2010, Trouw et al 2015), three empirical equations (CERC and Kamphuis 1991 in this study and Svasek 2012), and two numerical models (Wang et al 2012, Wang et al 2015). The results from the empirical equations bound the results from the numerical models and observations. The least sophisticated estimate, from the CERC equation, appears to overestimate the longshore transport rate compared to the other methods. The Kamphuis empirical equation, which is generally smaller in magnitude from the other studies, does not take into account the local effects of diffraction in the vicinity of the harbours, which likely explains much of the difference between this equation and the morphological model in the vicinity of Zeebrugge. Additionally, the empirical equations only consider wave-driven longshore transport. Tidal current-driven transport may also play a role along the Belgian coast, though the magnitude is not known. The morphological model, does, however, model tidal currents, and therefore is thought to be the best available estimate of average annual longshore sediment

transport rates along the Belgian coast (since real measurements are lacking). Therefore, we propose to use the results from the recent morphological model (Wang et al 2015) for developing the sediment budget for the Belgian coast.

Since the morphological model did not extend past Nieuwpoort, we extended the results using the Kamphuis equation, shifted to match the morphological model data at Nieuwpoort. Beyond the limits of the morphological model (for the short distance to the French border), the Kamphuis estimates were extrapolated assuming a constant longshore sediment transport rate. These extended estimates are shown in Figure 15 as the blue dashed line.

2.4.5 Using the LST rates in the sediment budget tool

The sediment budget tool requires as an input the longshore sediment transport rates into/out of each of the analysis cells (see section 2.3). Using the location (along the Belgian coast, in km) of the western edge of each cell, the LST rate was identified from the continuous plot derived from modelling (see blue line, Figure 15). These rates were then input to Step 3 in the sediment budget tool (see section 2.2).

Figure 15 – Potential longshore sediment transport rates along the Belgian Coast.
Uncertainty bands are included when available.

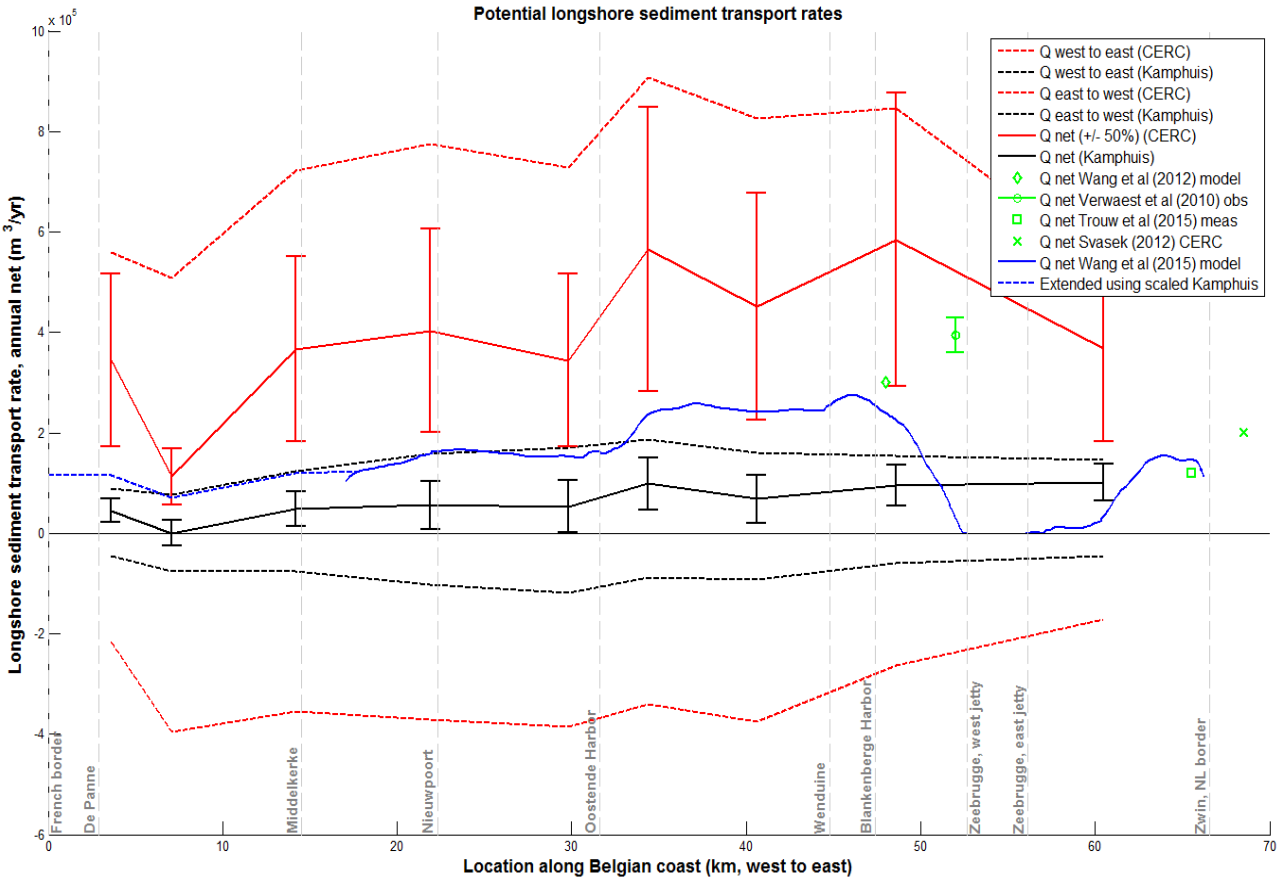

2.4.6 Uncertainty in LST rates

As explained in section 2.4.4, the longshore sediment transport (LST) rates derived from numerical modelling were used in this analysis. However, no confidence intervals were reported alongside the LST rates estimated from this model. Therefore, it is necessary to estimate the uncertainty of the LST rates independently.

Independent of the model accuracy, year-to-year variability in longshore transport rates cannot be ignored. Since the modelled longshore transport rates were not reported on a year-to-year basis (only an average over a 10-year period), an empirical equation was used to estimate the relative year-to-year variability of LST along the Belgian Coast. The Kamphuis equation (see section 2.4.2) was used to estimate the net LST rate for each year from 1996 through 2005 (Figure 16a). This analysis suggests that there was a slight net westward transport in 1996. 1998 and 1999 are the years with the highest net transport of approximately $12x10^4$ m^3/year (Figure 16a). These are rough estimates, as certain years were missing more wave data than others. Missing data for each year was interpolated assuming that the LST rate for the rest of that year was representative of the missing data. The goal was to coarsely estimate the year-to-year variability in LST rates rather than make accurate estimates of LST in each year.

Figure 16b plots the standard deviation of the annual longshore transport rates at each location along the coast. The year-to-year variability is largest around the central part of the Belgian coast, and is reduced towards the French and Dutch borders.

For the three locations west of Nieuwpoort, no modeled longshore transport rates are available. As described in the previous sections, the modeled longshore transport rates were extended to the French border using the Kamphuis data. In order to reflect this added uncertainty in the LST rates beyond Nieuwpoort, the uncertainty derived from the annual variability was doubled for the three wave points beyond Nieuwpoort (see blue shaded area in Figure 16c). This figure presents the resulting longshore transport rate and associated uncertainties used as input to the sediment budget.

This method of estimating an uncertainty in LST considers the year-to-year variability, but furthermore assumes that the model results are ideal. Therefore it can be considered an optimistic estimate of uncertainty for the modeled LST rates.

Figure 16 – (a) Annual net longshore transport rate (Kamphuis 1991) for each year. (b) Annual variability (standard deviation) of longshore transport rates along the coast. (c) The longshore transport rate (red line) and associated uncertainty (shaded area) used in the sediment budget. (d) Map showing distance along the coast.

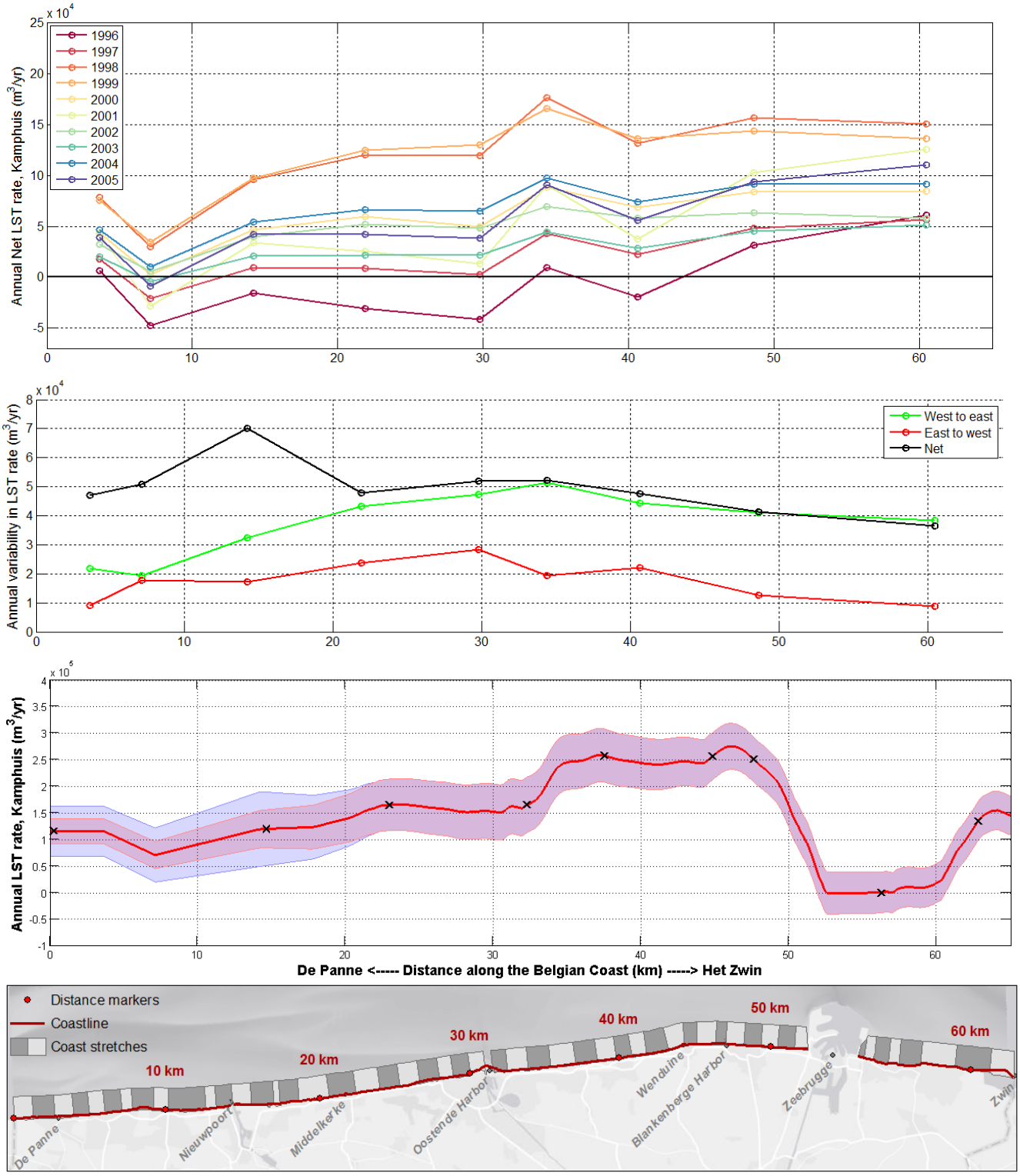

The blue shaded area shows how the uncertainty was doubled in the east, where the LST rate was extrapolated.
The black **x** represent budget cell boundaries, where longshore transport rates are identified and input to the sediment budget.

2.5 Estimating placements and removals (P and R)

The placement and removal data, described in section 1.4.2, was further catalogued according to the month of occurrence and by location along the Belgian coast: by stretches(s) and by whether the placement was above or below the low water line (i.e. in the seafloor/shoreface zones or in the beach/dune zones). Each quantity was assigned to the correct zone(s) and stretches(s) based on the reported location of the placement or removal (e.g. shoreface nourishment or beach nourishment), whenever possible. If location was unknown, it was assumed that the quantity was distributed equally across the zones and/or stretches in question, in proportion to the alongshore width of the section. Figure 17 presents the placement and removal volumes on an average annual basis for the sediment budget time period (2000 – 2009).

Figure 17 – Average annual placement/removal volumes by coast stretch (2000 - 2009).

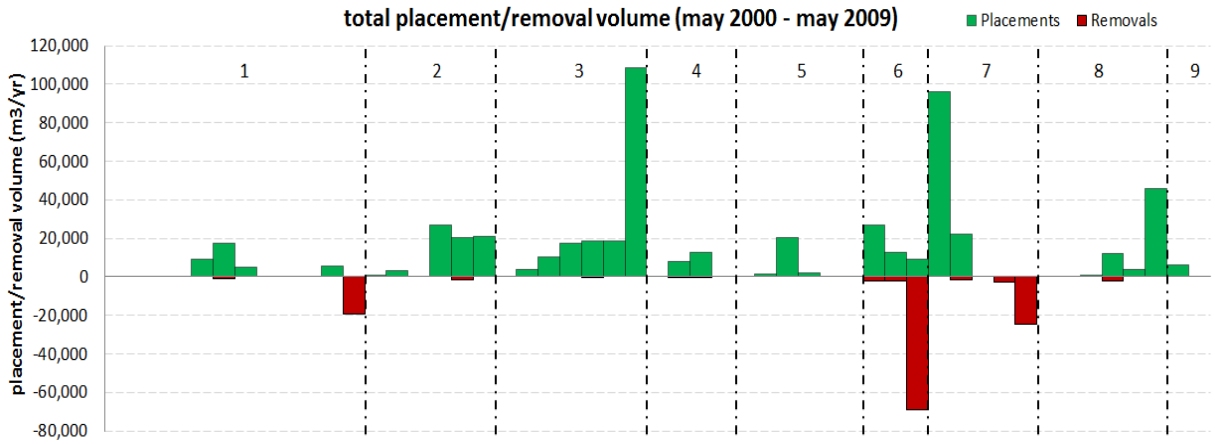

Removals are due to dredging in the harbor area to maintain navigation or bypass/transfer the sand down drift.
Placements are due to beach maintenance which take place periodically at the most vulnerable parts of the Belgian coast.

2.5.1 Uncertainty in placements and removals

Estimates of sand volumes that are placed or removed from a sediment budget cell are subject to many sources of uncertainty (Kraus and Rosati, 1998):

- ***Uncertainty in the volume-estimation process***. For example, when using a hopper dredge, it may filter out fine sand by being filled to overflowing, allowing the fines to be moved away by currents, thus using capacity volume of dredge may *underestimate volumes*. Also, if only the permitted volume is available for reference, this is usually an underestimate of what is usually dredged. The uncertainty in the pre- and post-dredging surveys, if this is how volumes are estimated, also contributes uncertainty to the dredged volume.
- ***Unquantified shoaling that occurs between pre- and post-dredging surveys***. The time elapsed may introduce uncertainty in that natural volume changes may have occurred in parallel with volume changes due to the dredging, leading to either an *over- or underestimate of the dredged volume*.
- ***Failure to include dredging that was not paid***. Volume dredged outside of a dredging design template is generally not paid, and therefore is not reported in payment statements, *underestimating the dredged volume*. It is easier to dredge inside the specified template during calm seas, so rough conditions can increase this uncertainty (e.g. from 20% to 100%).

- ***Changes in bulk density*** between the dredged and placed sediments.

Some rough estimates of uncertainty associated with different measurement types, as reported by Kraus and Rosati (1998) are:

- Hopper volume based on distance from top of hopper to top of sand: ± 10%
- Nuclear-density meter on a dredged slurry: ± 30%

Generally, shore-protection beach nourishment projects are constructed according to design drawings, as confirmed by surveys during the project. The sediment volume estimates from these types of project generally have low uncertainty. On the other hand, in beneficial-use projects, the nourishment is not usually surveyed in place, so the volume must be estimated from the dredging process, introducing larger uncertainty.

Based on the brief descriptions of uncertainty/assumptions that accompanied each of the placement/removal data points[5], a qualitative uncertainty (low/medium/high) was assigned to each data point, as follows:

1. **Low uncertainty**: when the magnitude, date, and location of the placement/removal are known/documented reasonably well.
2. **Medium uncertainty**: when uncertainty in the magnitude is not too large and/or the uncertainty in the dates is on the order of months.
3. **High uncertainty**: when the numbers provided are only rough estimates of the magnitudes, dates, and/or locations.

The relative uncertainty was then used to assign a relative uncertainty (in percent) to each qualitative uncertainty category. For this study, low, medium, and high uncertainties were assigned relative uncertainties of 20%, 35%, and 50%, respectively. For example, a beach nourishment of 10,000 m^3 with a medium level of uncertainty was assigned a quantitative uncertainty of +/- 3,500 m^3. The low relative uncertainty was set at 20%, because even when the date and location of placement are well documented, placement volumes can still be quite uncertain due to inaccurate volume estimates, undocumented discrepancies, uncertainty in pre- or post-project surveys, and changes in bulk density. The high uncertainty was set at 50% to reflect the potentially large uncertainties when the exact location, timing, and/or volumes are not known. The medium uncertainty was set as the midpoint between the low and high uncertainties.

2.6 Estimating volume changes (ΔV)

As described in section 1.4.2, digital elevation models (DEMs) were available from two previous studies (Janssens et al 2013 and Houthuys 2012). Both datasets were considered as part of this study.

Section 2.6.1 describes how the Janssens et al 2013 DEMs were processed to derive volume changes over time for input to the sediment budget. The next section, 2.6.2, explains why the decision was made to use the Houthuys 2012 DEMs in the present study. Section 2.6.3 describes two ways to calculate the volume change (using the start and end datasets, and using a complete time series of datasets). Sections 2.6.4 and 2.6.5 describe uncertainty in calculating the volume change using the start and end elevation models and in using a linear regression, respectively.

[5] Here, a "data point" refers to the volume of sand placed or removed from a specific coast stretch and zone during a specific period.

2.6.1 Calculating volumes from Janssens et al 2013 DEMs using GIS

The Janssens et al 2013 DEMs span the years between 1997 and 2010. During the interpolation process, in which raw survey data was converted to an ArcGIS raster digital elevation model, some areas were extrapolated outside the limits of the input data. For the surveys between 1999 and 2010, these DEMs were available in a second version, in which the extrapolated data had been manually removed through a clipping process in GIS. Ultimately, a time span from 2000 to 2009/2010 (2009 for shoreface, 2010 for beach) was selected, as the 1999 beach data does not cover the full alongshore extent of the Belgian coast.

A tool was built in ArcGIS (using ModelBuilder) to calculate the volumes for each of the 4 cross-shore elevation zones and 255 longshore sections described in section 1.3.2. A GIS shapefile showing the dividing lines for the longshore sections is available for download from KustAtlas[6]. These lines were extended to 1.5 km offshore in order to make bounding boxes for the section volume calculations (Figure 18). The tool iterates through each longshore section, clipping the digital elevation model to the section boundary and calculating the volume of sediment above the relevant elevation (e.g. the elevation dividing dry beach from dunes, +6.89 m TAW). These volumes are written to a text file, which is later post-processed in Matlab to calculate the volumes within each zone's elevation band.

The bathymetric surveys were used to estimate the volume of the shoreface zone, while the beach and dune volumes were derived from the topographic surveys. The GIS volume tool was therefore applied to the shoreface and beach digital elevation models separately (since these are separate DEMs).

In some cases, the beach DEM did not extend completely to landward side of the section box (Figure 19). For the 2000 and 2010 surveys, 1.3% and 0.4% of the total beach area was missing, respectively, so the gaps that had to be filled were small compared to the total beach area. These areas were filled in using the beach survey, closest in time, that did contain valid data. For the first time point, the spring 2000 beach survey was used, and the gaps were filled using the fall 2001 survey (the fall 2000 and spring 2001 surveys do not cover much larger area than the spring 2000 survey). For the last time point, the spring 2010 survey was used, and gaps were filled using the spring 2008 survey.

[6] http://www.coastalatlas.be/en/home/

Figure 18 – Section boundaries from KustAtlas (blue) extended 1.5 km offshore (red) to create section boundaries for the volume calculations.

Figure 19 – Example of beach survey not extending to the back of the section boundary. These areas are filled in using data from another survey (the nearest in time).

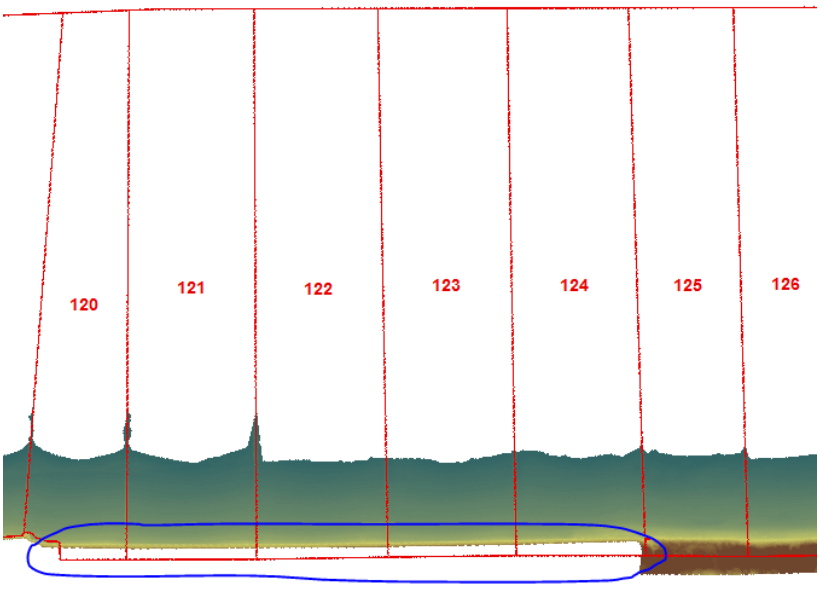

2.6.2 Selection of volume change data

The Houthuys 2012 DEMs had already been processed in a previous study, so volume changes through time for each coast stretch were already available, making it unnecessary to conduct the steps described in section 2.6.1. The only disadvantages of this dataset were that the zone limits were fixed (i.e. elevations defining zones could not be changed), but this was ultimately not an

important issue, as this study aims to be consistent with previous studies and that the volumes were aggregated into coast stretches (rather than more detailed sections). Moreover, the coast stretches were selected to reflect similar morphologies (important for this study), and they were aggregated into coarser cells for the purposes of the sediment budget.

The volume changes obtained using the Janssens et al 2013 DEMs were compared with the volume changes in the Houthuys 2012 study to determine which dataset to use for input to the sediment budget. Upon comparison, and in collaboration with Rik Houthuys, it became clear that there was a datum conversion issue in the 2000 shoreface DEM from Janssens et al. 2013. The 2000 data provided by aMT had the Z vertical elevation datum, while all subsequent datasets used TAW. In order to convert from Z to TAW, it is necessary to subtract 0.11m. However, it appears that the 2000 shoreface DEM from Janssens et al 2013 was shifted the wrong way, resulting in a DEM which was approximately 0.22 m too high.

Because of this discrepancy, the decision was made to use the volume changes from the Houthuys 2012 study rather than the Janssens et al 2013 DEMs. Figure 20 shows the volume change rate (end point rate) between 2000 and 2009 based on the Houthuys 2012 data.

Figure 20 – End point volume change rates (ΔV) between 2000 and 2009 based on volumes from the Houthuys 2012 study.

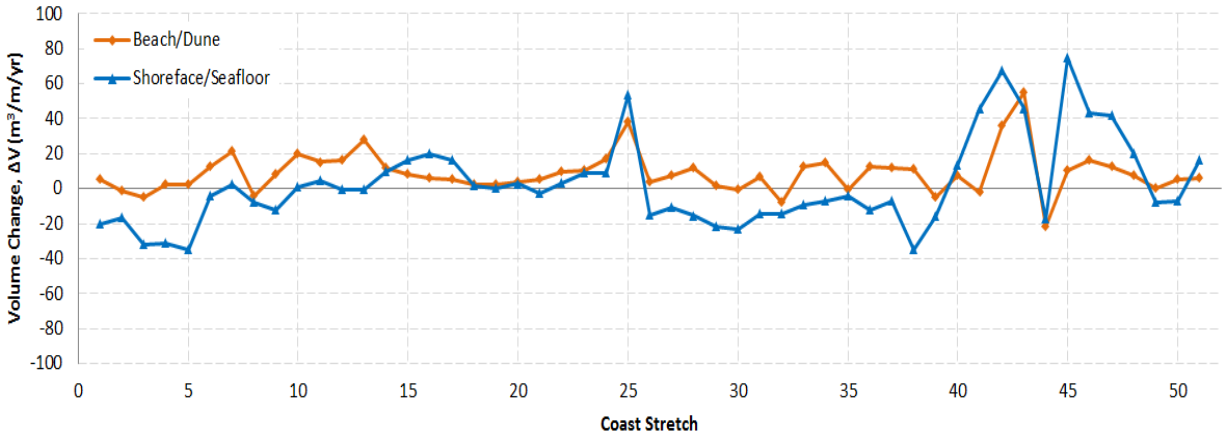

See Figure 7 for a map with the coastal stretch numbering. These values have not been corrected for placement volumes.

2.6.3 Volume changes from end point rate vs. linear trends

Two methods for estimating the volume change were investigated in developing the sediment budget. The first, called *end point change*, uses only the starting and ending digital elevation models, and simply calculates the difference between the two time moments. The second approach, called *linear regression change*, uses all survey data between 2000 and 2009 and estimates an average change rate over the 9 year period using a linear regression. The Houthuys 2012 data includes additional beach surveys every year and bathymetric surveys in 2003 (most of the coast), 2004 (in a few locations), 2007, and 2008, making it possible to apply this linear regression technique.

Figure 21 shows an example of how each approach is calculated. The black line plots the beach volume relative to 2000. In this case, the beach appears to be relatively stable, with a small amount of growth. However, a cumulative total of 160,000 m^3/km of sand was placed on the beach over the 9 year period (green line). The “natural evolution” volume, plotted in dark orange, is the observed volume change with beach nourishments removed. Annexe B presents plots similar to Figure 21 for each of the along coast cells, for the above low water (beach surveys) and below low water (bathymetric surveys) separately. The above and below low water data is processed separately

(because the survey dates differ), and the separate volume changes are later combined to give the total volume change for the cell.

Next step was to use the two methods to estimate the volume change that occurred over the 9 year period:

4. **End point change**: The volume change is the difference between the 2000 and 2009 digital elevation models. This is depicted in black. The volume is then corrected within the sediment budget (ΔV – P = ΔV') to give a "natural evolution" end point volume change.
5. **Linear regression change**: The previous approach only uses the start and end point data. This approach fits a linear regression to the natural evolution volume (dark orange) line, to try and estimate the "background" volume trend. Then, the difference between the start and end of the linear trend line provides another estimate of the natural evolution volume change, based on the complete time series of surveys. The linear fit is applied to the natural evolution volume series (rather than the observed volume series) to remove perturbations caused by nourishment or dredging.

Figure 21 – Example of estimating volume changes in two ways: using the start and end point, and using the slope of a linear trend through all measurements.

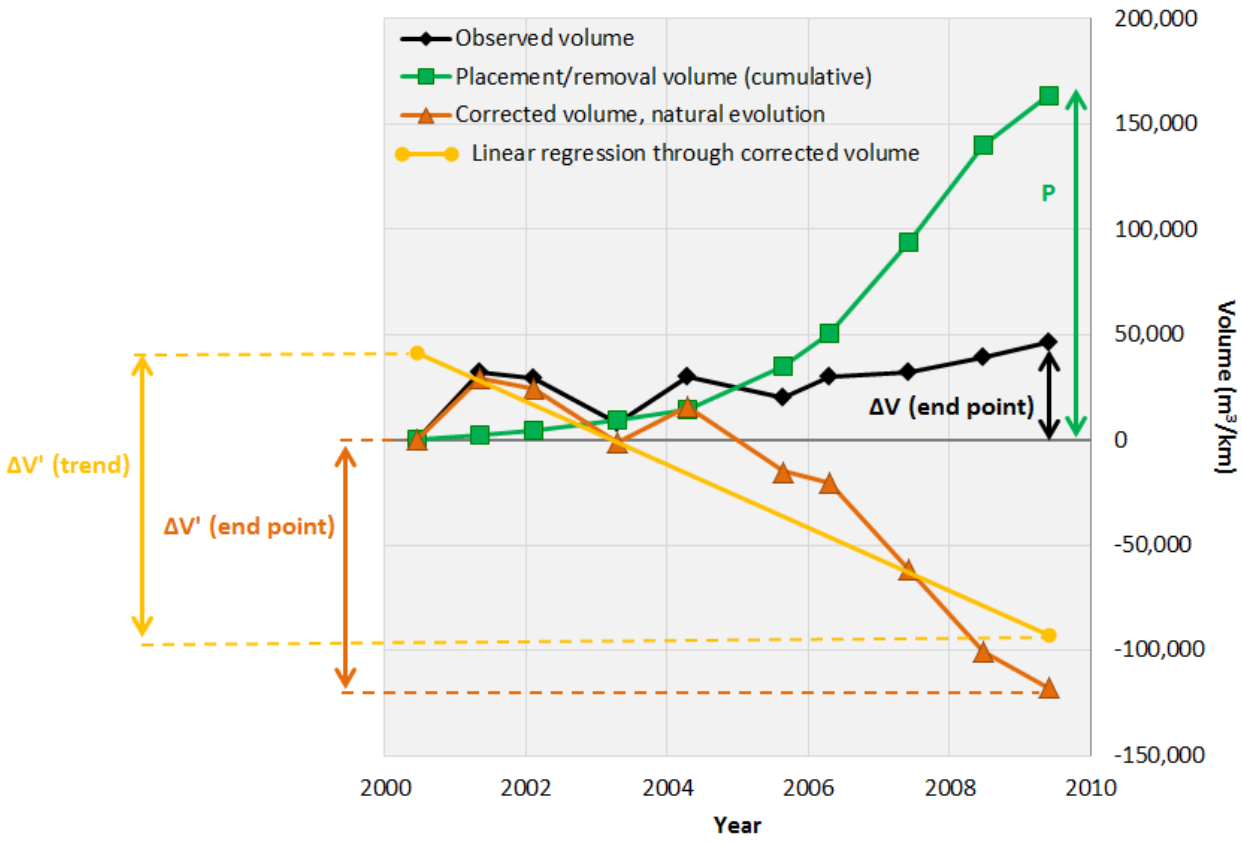

Each method has its own merits. The benefit of the method 1 is that it involves a transparent, straight-forward conservation of volume equation. Taking this approach, the DEMs available between the start (2000) and end (2009) time points are not used. This approach depends heavily on the starting and ending survey data, while ignoring intermediate survey data. If the start and end surveys were perfect (i.e. no uncertainty/bias), then method 1 would be the most accurate, as it is a volume-balance approach. If either the start or end surveys had any bias/error problems, then

method 2 might give a more reliable estimate of the volume change. However, if the beach naturally experiences a lot of natural variability, then method 2 may artificially smooth the long-term evolution of the coast and not represent the volume change well.

Figure 22 presents the natural evolution volume change rates for the dune/beach and shoreface/seafloor for each coast stretch derived using both methods. The endpoint rate and the linear regression rate for the dune/beach give essentially the same results. For the shoreface/seafloor, however, the endpoint rate is consistently lower than the linear regression rate. A closer look at the shoreface/seafloor data for year 2000 shows that the shoreface was higher/wider this year than would be expected from the regression trend, causing the end point rate to be skewed low. However, the same is not true for the dune/beach datasets derived from LiDAR, so this difference may be due to the measurement technique/accuracy of the 2000 bathymetric surveys.

Figure 22 – Natural evolution volume change (ΔV') by coast stretch using the end point rate and linear regression trend methods.

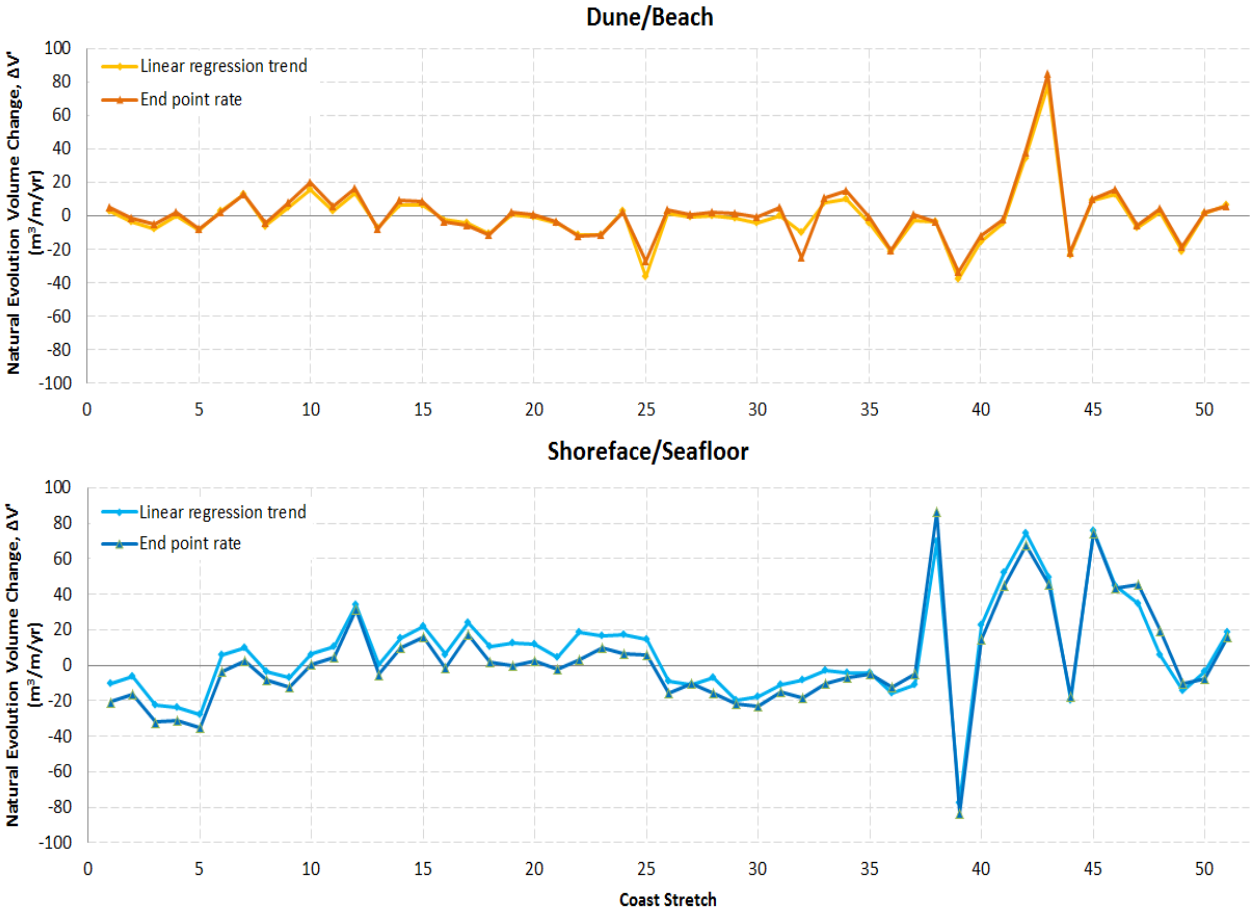

In summary, both sets of volume changes were considered in developing the sediment budget, and both resulting sediment budgets are presented later in this report.

2.6.4 Uncertainty in volume changes – end point change

The uncertainty associated with estimating volume changes by comparing start and end DEMs depends on:

- The accuracy and spatial extent of the surveys used to create the DEMs.
- The interpolation method used to make the DEMs.
- Seasonal variability that may mask long-term trends in volume changes.

The volume change data available from the Houthuys 2012 study was not accompanied by uncertainty estimates for each individual survey. Therefore, it was necessary to develop a method to assign an absolute uncertainty to each survey volume, for input to the sediment budget. As described in section 1.4.2, the reported accuracy of the LiDAR DEMs and bathymetric surveys is on the order of ±10 cm. However, the LiDAR survey acceptance reports seem to indicate that the absolute error is closer to 3 cm, based on comparison with ground surveys (Houthuys, personal communication, 23/5/2016). Therefore, an uncertainty of +/- 3 cm was assumed for the beach and dune zones, and +/- 10 cm for the zones below low water. Average area above and below low water in each coastal stretch were estimated using the 2000 and 2009 DEMs from the Houthuys 2012 study. Then, these areas were multiplied by the uncertainty (3 or 10 cm) to calculate the absolute volume uncertainty in each stretch .

2.6.5 Uncertainty in volume changes – linear regression change

In the end point volume change, the uncertainty was based on the individual uncertainties of the 2000 and 2009 survey data (see section 2.6.3). This approach cannot be used when the linear trend is used to estimate the volume change. Instead, the standard error was calculated for each regression equation using the Microsoft Excel STEYX function. This function returns the standard error of the predicted volume for each year in the regression. This standard error was applied to the starting (2000) and ending (2009) volumes predicted from the linear regression equation. Following the rules for combining uncertainties described in section 1.5, this would result in an error of the volume change equal to √2*standard error.

2.7 Estimating cross-shore sediment transport rates (T)

Since the cross-shore sediment transport rate is the least known component of the sediment budget, this term is solved for rather than input to the budget. Below we describe some potential contributors to cross-shore sediment transport, including offshore losses due to sea level rise and windblown sand transport across the inland cell boundary.

2.7.1 Estimating volume “losses” from sea level rise

Equation (5), in section 1.4.1.1.3, was used to estimate the volume losses to the offshore that could potentially be attributed to sea level rise. In this equation, the term $\frac{L}{B+D_c}$ is equivalent to the shoreface slope, or the slope between the beach berm and the depth of closure. Since we do not have an accurate estimate of beach berm crest along the coast, mean high water was used as a proxy for the berm crest elevation. Shoreface slopes were estimated using the same methods as for beach slopes, described in section 2.4.2. Figure 11 presents the shoreface slope by section along the coast. The general trend of the shoreface slope matches that of the beach slope, with the exception of sections 120 to 160 (from Oostende Harbour to De Haan), where the shoreface slope becomes flatter. Around Wenduine the two slopes converge and steepen together. Then, the shoreface slope

flattens again up to Zeebrugge Harbour. Beyond the harbour the shoreface slope is initially very flat (in the area of accumulation just adjacent to the harbour), but then steepens for the rest of the Belgian coast, just flattening again at Het Zwin.

The next term in Equation (5) is the mean sea level trend. A low and high sea level trend of 2 and 4 mm/year were selected based on the summary in Table 1 in order to bound the potential losses due to sea level rise over the sediment budget timeframe.

2.7.2 Estimating aeolian transport across the backshore cell boundaries

As mentioned before, there are no systematic studies of the aeolian sand transport along the Belgian coast. Currently, under the framework of the CREST project, aeolian sand transport is being measured at two locations, with results expected in 2018-2019. Since the sediment budget equation can solve for only one unknown, assumptions have to be made regarding the sand volume loss/gain at the onshore and offshore boundaries of each cell (both of which are unknown). The first assumption we make is that aeolian transport is the only process causing a gain or loss of sand across the inland limit of each cell. According to De Lijn, the company operating the Kusttram, most of the sand landing on the tram tracks comes from the beach, so it is a loss from the system. Unfortunately, there is no measurement of the volume of sand removed from the tram line. Therefore we assume that the volume of sand lost or gained at the offshore boundary of the cells is much larger than the aeolian losses across the inland limit. We approximate that a total of 1000 to 2000 m^3 of sand is removed from the tram lines every year[7] along the entire coast, which is multiple orders of magnitude less than the 10^5 to 10^6 m^3/year exiting or entering at the offshore limit of the cells.

2.7.3 Uncertainty in cross-shore transport rates

Uncertainty in the volume losses from sea level rise is addressed by considering a low and high observed sea level trend (see section 2.7.1).

Uncertainty in the volume of windblown sediment across the landward cell boundary was assumed to be very high as there are no exact measurements. However, the total volume of sand removed from the system at the inland limit of the cells is in the order of few thousands m^3 for the entire coast for one year.

[7] Assuming that a truck carries 10 m^3 of sand, this is equivalent to 100 to 200 truck trips per year.

3 Results and Discussion

3.1 The Sediment Budget

The final sediment budget is presented in two forms: as a map (Figure 23) and as a graph (Figure 24). The combined uncertainties, as computed in the present study, for each term of the sediment budget equation are also presented in Figure 24 as vertical bars. The values and uncertainties are also presented in Table 4. The individual components of the sediment budget are presented in the sections in section 2. The longshore transport rate estimates are described in section 2.4, the volume changes in section 2.6, the placement and removal volumes in section 2.5, and a discussion of the onshore/offshore transport rates in section 2.7. To understand the sign conventions of each of the terms, please refer to the simplified sediment budget equation for the Belgian coast in section 2.1.

3.1.1 Longshore sediment transport rate, L

The net longshore sediment transport (LST) was calculated using two formulas and compared with results of a numerical model (Figure 15). Due to more detailed input and calculation at finer resolution the results of the model were selected as input for the sediment budget. However, results of the other two formulas were used to delimit the possible range variation for the net LST as well as to extrapolate the results for the cell 1 (Kamphuis results) which was not covered by the model. The net LST is oriented towards northeast direction and it ranges from 0 to approximately 260 000 m3/year. The gradient is increasing until Blankenberge harbour suggesting erosion of the coast, and then strongly decrease down to 0 at the Zeebrugge harbour indicating coastal accretion. Further down drift, after Zeebrugge the gradient is generally increasing down to the Dutch border. The trends are generally confirmed by observations and empirical estimations. The uncertainty of LST has two main sources: the annual variability and the extrapolation for the model results for cell 1 and partially cell 2 (Figure 16) and it can be considered **medium to low**.

3.1.2 Placements and removals, P-R

The placements refers mainly to beach nourishments while removals are dredging executed to maintain the navigation at the main harbors. This is confirmed by the location, the removals are mainly related to harbours Nieuwpoort, Zeebrugge, and, reaching a maximum, at Blankenberge (Figure 17). Significant volumes of sand were placed in several cells such as cells 2 and 3 for strengthening the coastal safety and in the cells 7 and 8 as bypass system for the sediments blocked by the harbours (Figure 23 and Figure 24). Uncertainty for placements and removals is mainly related to methods used for the volume estimation, shoaling and change in sediment density. Generally, the uncertainty related to placements and removals into the coastal system is **low** due to a rather good reporting and detailed evidence of the this operations.

3.1.3 Volume change, ΔV

The volume changes were derived by comparison of the topographic and bathymetric maps for the period 2000 – 2009 using available data and a triangulated irregular network. The results show large volume variations for cells 7 and 8 (containing harbors Blankenberge and Zeebrugge), medium volume for cells 2 and 3 (where nourishments were large too) and small for the rest of the cells (Figure 23 and Figure 24). The uncertainties related to the volume changes are due to a rather large number of factors: selection of start and end point of the surveys, interpolation method, maps accuracy and selection of boundaries. Generally, the uncertainty related to volume changes can be considered as **medium**, except for cell 6 where the large uncertainty is due to the small volume change.

Figure 23 – Sediment budget (conventional budget) for the Belgian Coast (2000 – 2009) in map form,
using volume change between two moments in time: year 2000 as starting moment and 2009 year as end year.

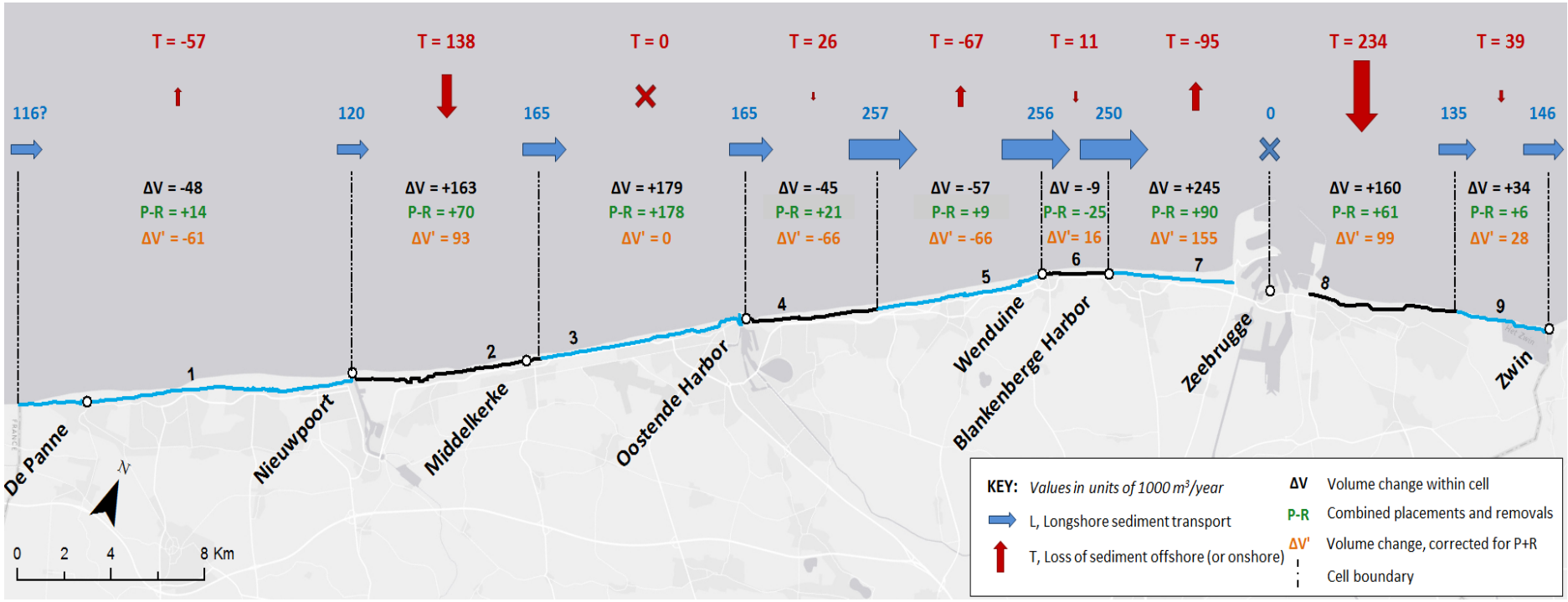

Units in 1000 m^3/yr. Longshore sediment transport next to French border more uncertain due to lack of exact calculations.

Figure 24 – Sediment budget (normalized per km) for the Belgian coast (2000 – 2009) in graph form, using volume change between 2000 and 2009. Units in m^3/yr/km.

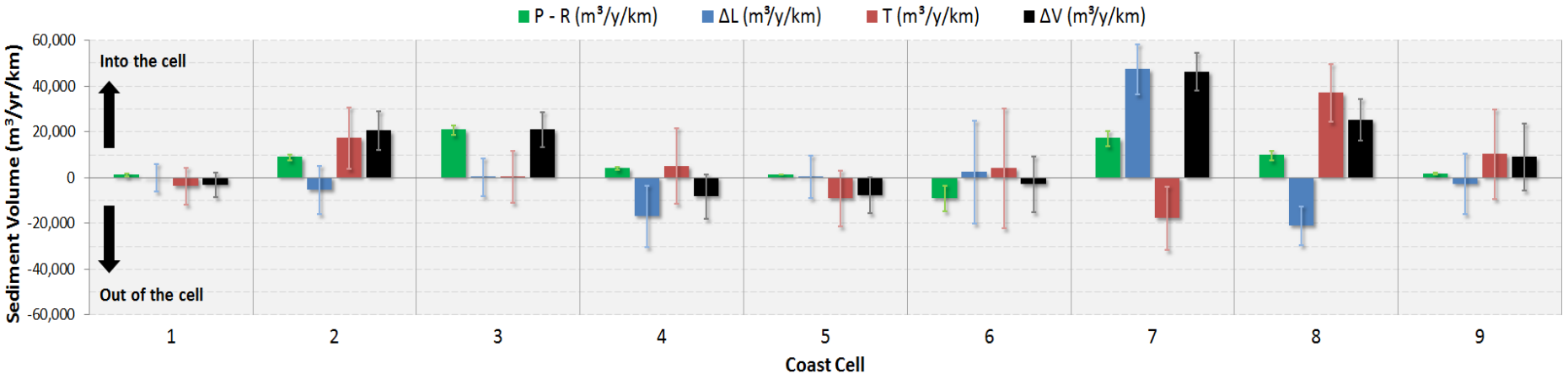

Table 4 – Sediment budget results summary table.

Cell characteristics	**Cell 1**	**Cell 2**	**Cell 3**	**Cell 4**	**Cell 5**	**Cell 6**	**Cell 7**	**Cell 8**	**Cell 9**
Sections	2 - 59	60 - 87	88 - 117	119 - 139	140 - 172	173 - 184	185 - 216	217 - 241	242 - 255
Stretches	1 - 12	13 - 18	19 - 25	26 - 29	30 - 35	36 - 38	39 - 43	44 - 49	50 - 51
Cell length (km)	14.3	8.0	8.6	5.4	7.2	2.7	5.3	6.4	3.9
Term in the sediment budget equation	**Absolute *rate* between 2000 - 2009 (1000 m^3/yr)***								
Volume change, ΔV	-48	163	179	-45	-57	-9	245	160	34
Placements - removals, P-R	14	70	178	21	9	-25	90	61	6
Longshore transport into cell, L_{in}	116	120	165	165	257	256	250	0	135
Longshore transport out of cell, L_{out}	120	165	165	257	256	250	0	135	146
Cross-shore transport, T**	-57	138	0	26	-67	11	-95	234	39
Term in the sediment budget equation	**Absolute *uncertainty* in the rate between 2000 - 2009 (1000 m^3/yr)**								
Volume change, ΔV	76	66	65	53	57	33	43	58	58
Placements - removals, P-R	11	10	17	4	1	15	18	13	2
Longshore transport into cell, L_{in}	47	69	48	52	50	44	42	38	37
Longshore transport out of cell, L_{out}	69	48	52	50	44	42	38	37	37
Cross-shore transport, T**	113	108	98	89	88	71	73	80	77
Term in the sediment budget equation	**Normalized *rate* between 2000 - 2009 (1000 m^3/yr/km)***								
Volume change, ΔV	-3.3	20.3	20.7	-8.4	-7.9	-3.2	46.2	25.1	8.8
Placements - removals, P-R	1.0	8.7	20.7	3.8	1.2	-9.2	17.0	9.5	1.6
Net longshore transport, ΔL (L_{in} - L_{out})	-0.3	-5.6	0.0	-17.1	0.2	2.1	47.2	-21.2	-2.9
Cross-shore transport, T**	-4.0	17.2	0.0	4.8	-9.3	3.9	-18.0	36.8	10.0
Term in the sediment budget equation	**Normalized *uncertainty* in the rate between 2000 - 2009 (1000 m^3/yr/km)**								
Volume change, ΔV	5.3	8.3	7.5	9.7	8.0	12.1	8.2	9.2	14.7
Placements - removals, P-R	0.8	1.3	2.1	0.7	0.2	5.6	3.4	2.0	0.5
Net longshore transport, ΔL (L_{in} - L_{out})	5.9	10.5	8.2	13.4	9.3	22.5	10.8	8.3	13.2
Cross-shore transport, T**	8.0	13.5	11.3	16.5	12.2	26.1	13.8	12.6	19.7

Notes

* Positive (green) values represent an increase in volume inside the cell (i.e. sand moving into the cell). Negative (red) are a movement of sand out of the cell.

** T is solved for in the sediment budget equation. All other terms are calculated independent of eachother.

3.1.4 Onshore/offshore transport, T

The results of the sediment budget obtained by using the linear regression method are shown in Figure 25. Both sediment budgets are in good agreement in terms of how each cell is balanced (i.e. the net losses or gains to the cell that are not accounted for in the volume change, placement/removals, and longshore transport). Table 4 presents a comparison of the balance in each cell across each of the Both sediment budgets. Cells 1, 3, 4, 6, and 9 are balanced in the sense that the offshore loss/gain term is not significantly different from 0. Cells 2 and 8 appear to be gaining sand in the cross-shore direction, while cells 5 and 7 appear to be losing sand in the cross-shore direction.

Figure 25 – Sediment budget for the Belgian coast using a linear regression to estimate the volume change between 2000 and 2009.

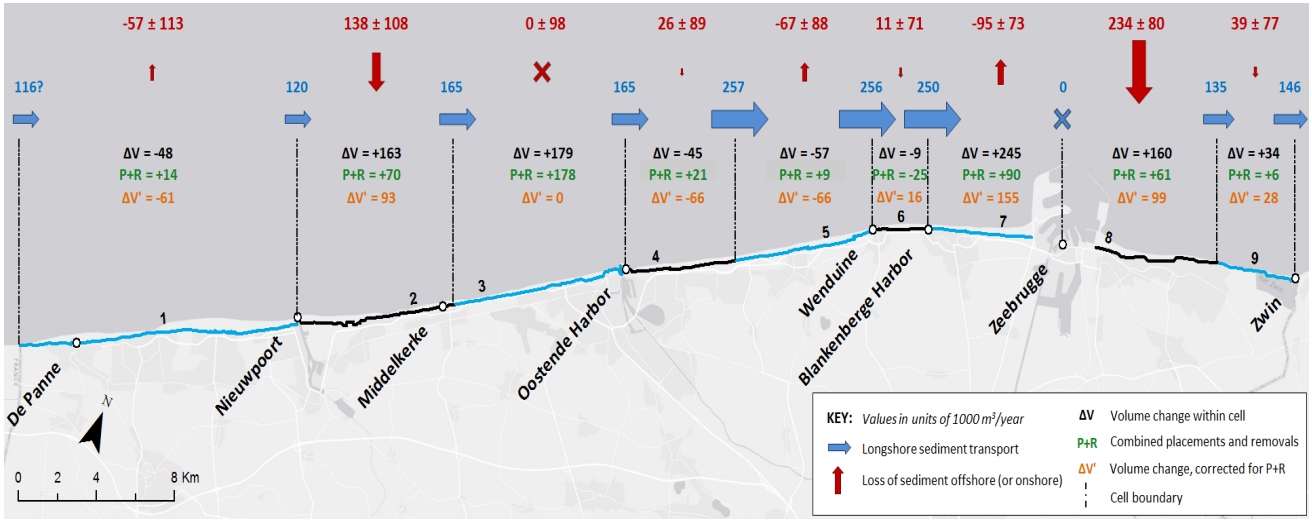

The range of "Loss of sediment offshore" reflects the results from two volume calculation methods, described in the Methods section.

Table 5 – Comparison of offshore/onshore term for different sediment budgets.

Cell	Conventional Budget	Linear Regression
1	Balanced (slight loss)	Balanced
2	Gain	Gain
3	Balanced	Balanced (slight gain)
4	Balanced (slight gain)	Balanced (slight gain)
5	Balanced (slight loss)	Balanced (slight loss)
6	Balanced (slight gain)	Balanced
7	Loss	Loss
8	Gain	Gain
9	Balanced (slight gain)	Balanced (slight gain)

Balanced = no significant loss or gain, based on uncertainty interval. Loss = sediment is lost to the offshore/onshore, Gain = sediment is gained from the offshore/onshore.

Since onshore and offshore transport are combined into one term that is solved for in the sediment budget, we can attempt to remove the losses due to sea level rise and aeolian transport (see sections 2.7.1 and 2.7.2) to isolate offshore losses. This is done in Table 6 below, for both sediment budgets. It is immediately clear that the losses to aeolian transport have little effect on the overall sediment budget. Losses to sea level rise are between 40 and 100 times greater than assumed aeolian losses, and can sometimes represent a significant portion of the net offshore/onshore losses. However, in general, removing losses due to sea level rise and aeolian transport does not affect the overall sediment balance (balanced, losing sediment, gaining sediment) of each cell.

Table 6 – Comparison of offshore/onshore losses/gains with sea level rise and aeolian transport losses.

	Cell								
	1	2	3	4	5	6	7	8	9
Offshore/onshore loss or gain	All values in 1000 m^3/year/km, (+ gain, - loss)								
Conventional budget	-4.0	17.2	0.0	4.8	-9.3	3.9	-18.0	36.8	10.0
Linear regression	0.4	15.7	6.4	4.9	-8.2	-3.9	-16.6	28.9	12.0
Losses to SLR									
Low estimate	-1.0	-1.0	-0.7	-1.0	-1.0	-0.7	-1.6	-0.9	-0.6
High estimate	-2.1	-2.0	-1.4	-2.1	-2.0	-1.5	-3.2	-1.7	-1.2
Losses to aeolian transport									
Low estimate	-0.02	-0.02	-0.02	-0.02	-0.02	-0.02	-0.02	-0.02	-0.02
High estimate	-0.03	-0.03	-0.03	-0.03	-0.03	-0.03	-0.03	-0.03	-0.03
Estimated offshore loss or gain (excluding losses to SLR and aeolian transport)									
Conventional budget (min)	-2.9	18.2	0.7	5.9	-8.2	4.7	-16.3	37.7	10.6
Conventional budget (max)	-1.9	19.2	1.5	7.0	-7.2	5.4	-14.7	38.6	11.3
Linear regression (min)	1.4	12.1	9.5	5.4	-10.6	-1.3	-16.7	31.4	13.3
Linear regression (max)	2.5	17.7	7.9	7.0	-6.2	-2.4	-13.3	30.7	13.3

The minimum and maxim values for both sea level rise and Aeolian transport were considered, hence the low and high estimates.

3.2 Results and discussions

The following sections describe the sediment results for each of the alongshore cells, and explains whether the inputs result in a net transport of sediment into or out of the cell that is not accounted for by longshore transport or placements/removals. It is easier to read this using the graph version of the sediment budget, which also shows the uncertainty ranges for each of the terms. The loss/gain of sediment offshore (or onshore) is depicted in red in Figures 23 and 24. This is the term that is solved-for in the sediment budget. The offshore and onshore components are grouped and discussed as one term, as neither of these quantities are well known or can be solved for independently. Estimates of various contributors to this term, such as sea level rise and aeolian transport, are discussed in section 2.7.

Each of the four coastal harbours in Belgium (Nieuwpoort, Oostende, Blankenberge, and Zeebrugge) is also given its own description in the following section. While reading the results for each harbour, the reader can refer to Figures 23 and 24 (and the accompanying graphs), which show the sediment budget results derived from two different methods.

3.2.1 Cell 1 – De Panne to Nieuwpoort

This cell includes coastal sections 2 to 59. This is the longest cell and spans from De Panne to Nieuwpoort. The incoming longshore sediment transport is relatively uncertain, as the modelled longshore transport rates did not extend past Nieuwpoort, and an empirical extrapolation was used. As described in section 2.4.6, the uncertainty (which was based on seasonal variability) was doubled to reflect this uncertainty in extrapolation. The net longshore transport is almost constant displaying a slight increase, so the contribution of this transport is minimum to the sand volume of the cell. This cell shows slight erosion between 2000 and 2009. There is beach nourishment carried out around Koksijde-Bad and dredging west of Nieuwpoort Harbour, resulting in a slightly positive net placement volume. The result is a net transport of sediment out of the cell, most probably towards offshore, though taking into account the uncertainty bands, it appears that this cell is **relatively balanced**.

The uncertainty of longshore sediment transport is rather large due to both extrapolation of the model's result to the French border, but also due to the relatively small amplitude. Uncertainty related to the offshore transport and to the volume differences are medium and similar for both methods of calculations. Uncertainty of the placements and removal is very small due to precise records of these activities (Figure 26).

Figure 26 – Results and uncertainties for cell 1.

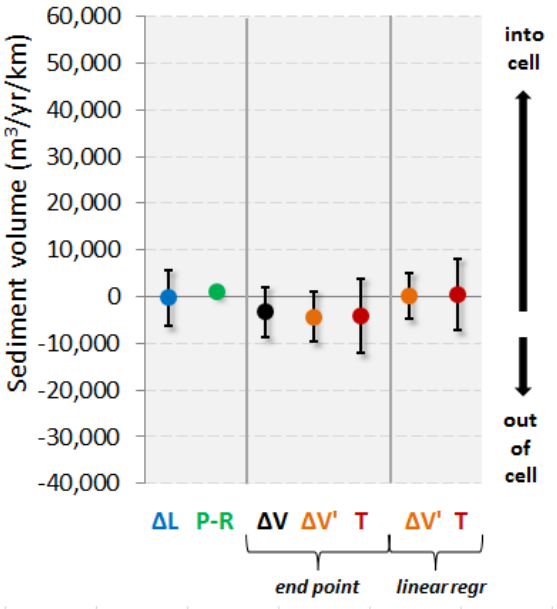

3.2.2 Nieuwpoort Harbour

Nieuwpoort harbour is located between cells 1 and 2 (sections 59 and 60). The net longshore transport rate from cell 1 to cell 2 is estimated to be ~120,000 m^3/year. As can be seen in Figure 27, the volume calculations were done both adjacent to and in front of the harbour. Therefore, the portion of the sediment that is dredged in front of the harbour (mostly sand, Houthuys 2012) is taken into account as a removal of volume from cell 1. Dredging that occurs inside the harbour is not taken into account, as this material is primarily mud (Houthuys 2012). A portion of the sand that is dredged from in front of the harbour is placed in sections 73-76, which is taken into account in as a placement in cell 2. Both methods of calculating the sediment budget show that cell 2 is accreting while cell 1 is stable or slightly erosive (Table 4).

Figure 27 – Volume calculation limits for the sections near Nieuwpoort Harbour.

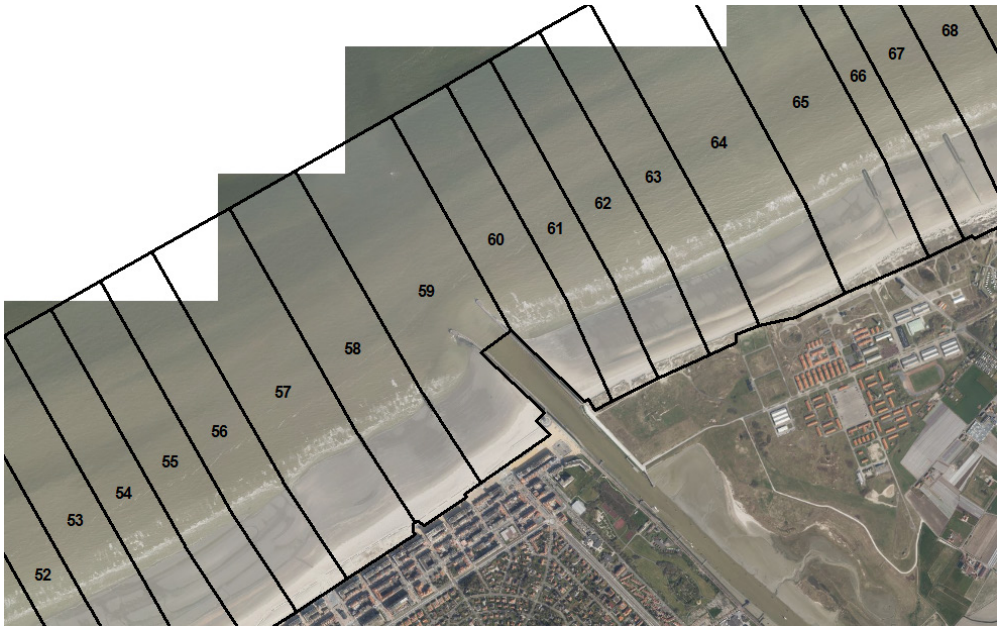

3.2.3 Cell 2 – Nieuwpoort to Middelkerke

This cell includes coastal sections 60 to 87. More beach nourishment took place here, especially close to Middelkerke. The longshore transport rates are a result of a numerical model and the uncertainty is related to the year-to-year variability of the wave climate. This cell experienced accretion from 2000 to 2009, but it cannot be entirely explained by the net longshore transport (more out than in) or placements and removals (net positive, but not enough). The gradient of the longshore transport is positive, this transport adding approximately 45,000 m^3 of sand into the cell yearly.

The uncertainty is rather large, but keeping the same trends as in the previous cell (Figure 28). Sediment appears to be entering the cell from the offshore or from the inland areas. Therefore, this cell is **unbalanced, with incoming net transport**.

Figure 28 – Results and uncertainty for cell 2.

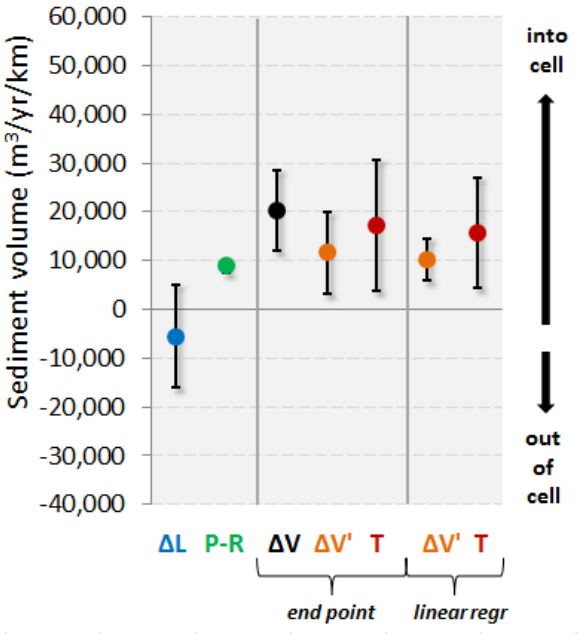

3.2.4 Cell 3 – Middelkerke to Oostende

This cell includes coastal sections 88 to 117. This cell experienced similar accretion as cell 2, but it appears to be more balanced, as the placement volumes are essentially equal to the volume change, and the net longshore transport is zero. There was intense beach nourishment in this cell, especially in Oostende centrum. Therefore, the sediment budget shows a **balanced** cell, with no net transport to the offshore/inland areas. The uncertainties are medium when compared with the previous two cells (Figure 29).

Figure 29 – Results and uncertainty for cell 2.

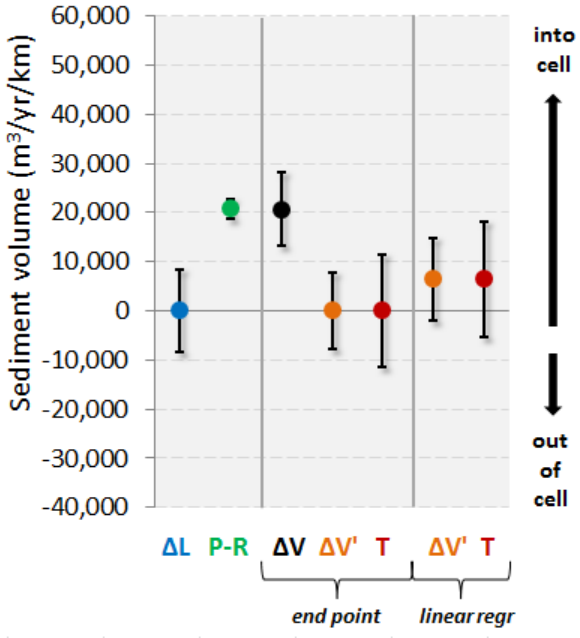

3.2.5 Oostende Harbour

Oostende Harbour is located at the border between cells 3 and 4 (sections 117 and 119, Figure 30). The estimated net rate of longshore transport is 165,000 m^3/year. Since 2005, a significant amount of sand has been placed in cell 3, most of which is just updrift of the harbour (both on the shoreface and on the beach, Figure 24). Section 118 is not included in the sediment budget, as no volumes were reported for this section in Houthuys 2012. Since the entrance channel to Oostende harbour goes through section 118, no dredging volumes were taken into account for Oostende harbour. This results in the assumption that the longshore transport from one side of the harbour to the other is the modelled rate of 165,000 m^3/year (i.e. the harbour is not a major impediment to longshore transport). With this assumption, cell 4 still imports a small volume (24,000 to 26,000 m^3/year) from the offshore in order to be balanced.

Figure 30 – Volume calculation limits for the sections near Oostende Harbour.

Photo on the left shows the actual situation, with the new harbor jetties built in 2011.
On the right side the old configuration of the harbor, as it was during the considered period (2000 – 2009) for the sand budget.

3.2.6 Cell 4 – Oostende to Bredene-aan-Zee

This cell includes coastal sections 119 to 139. This cell experienced a slightly negative volume change, even though some nourishment was conducted. This appears to be explained by a gradient in longshore sediment transport, with more sediment leaving from the eastern boundary than coming in along the western boundary. In fact, the longshore sediment transport is main sand contributor for the cell with 92,000 m3 yearly. Uncertainties are rather large for this section, especially for sediment transport along and offshore (Figure 31). Given the range of uncertainty, this cell is **relatively balanced**.

Figure 31 – Results and uncertainty for cell 4.

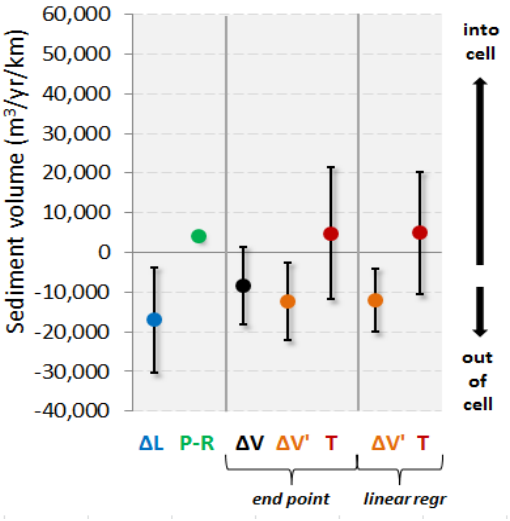

3.2.7 Cell 5 – De Haan to Wenduine

This cell includes coastal sections 140 to 172. This cell experienced slight erosion over the sediment budget timeframe, but this cannot be explained by placements/removals (almost none) or longshore sediment transport which maintain similar level for the entire cell . Therefore, there appears to be a slight loss of sediment to the offshore, resulting in a cell that is **slightly unbalanced with net transport out**. However, given the uncertainty of the longshore transport and volume estimates (Figure 32), this net transport is not significant and could be interpreted as a **balanced** cell.

Figure 32 – Results and uncertainty for cell 5.

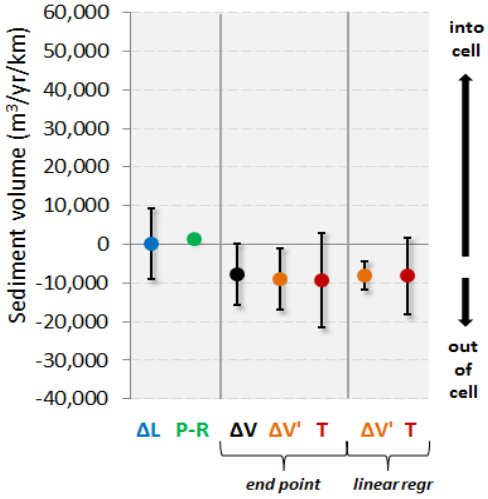

3.2.8 Cell 6 – Wenduine to Blankenberge Harbour

This cell includes coastal sections 173 to 184. This is the shortest cell, spanning less than 3km. This area experiences some of the largest longshore transport, with the strong year-to-year variability, but with rather mild gradient. However, volume of sand entering is almost equal with the one leaving the cell. This section experienced little to no volume change between 2000 and 2009. This cell experiences some beach nourishment in parallel with significant dredging of deeper sediments. Probably part of the dredged sand was due to bypassing, which is the transfer of the sand from the up drift side of the harbour, where sand is accumulating (SW of Blankenberge in this case) to the eroding downdrift side (NE). This cell is more or less **balanced** considering the uncertainty of the longshore transport rates, placement/removal volumes, and volume change. The uncertainiy level is rather large especially for the offshore and longshore transport (Figure 33).

Figure 33 – Results and uncertainty for cell 6.

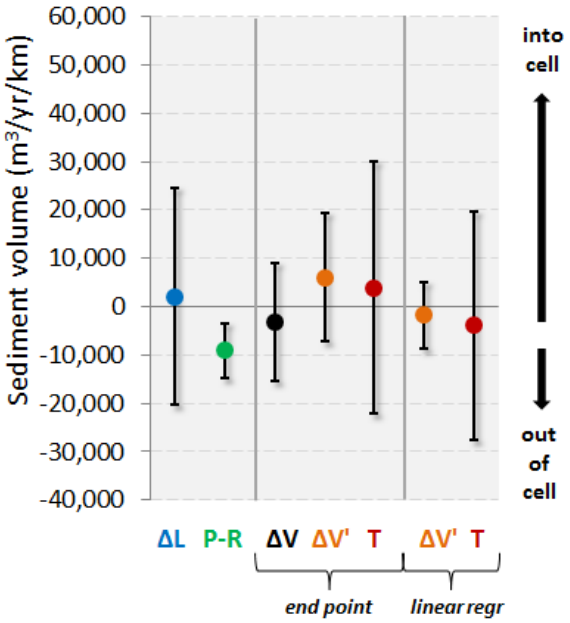

3.2.9 Blankenberge Harbour

Blankenberge harbour is located between cells 6 and 7 (sections 184 and 185, Figure 34). Many detailed studies exist that focus on the sediment budget for this harbour (Houthuys et al 2014, Teurlincx et al 2009, Wang et al 2012), so we refer the reader to these references for a more in-depth analysis. The longshore transport rates in these studies are in good agreement with the rates used in the Wang et al 2012 and Houthuys et al 2014 studies.

Figure 34 – Volume calculation limits for the sections near Blankenberge Harbour.

3.2.10 Cell 7 – Blankenberge Harbour to Zeebrugge Harbour

This cell includes coastal sections 185 to 216. This very dynamic cell experienced significant accretion between 2000 and 2009. This can be explained by a combination of net sediment placement from dredging/bypassing around Blankenberge Harbour and net longshore transport into the cell (it is assumed that no sand leaves the cell along the boundary with the harbour The cell is **unbalanced, with net transport out**. Therefore, it appears that a significant volume of sand moves offshore after it builds up against Zeebrugge Harbour. This is also due to the offshore limit of the surveys not extending far enough to capture the full shoreface zone. Considering the large volumes of sediments involved in the budget of this cell the uncertainties are small (Figure 35).

Figure 35 – Results and uncertainty for cell 7.

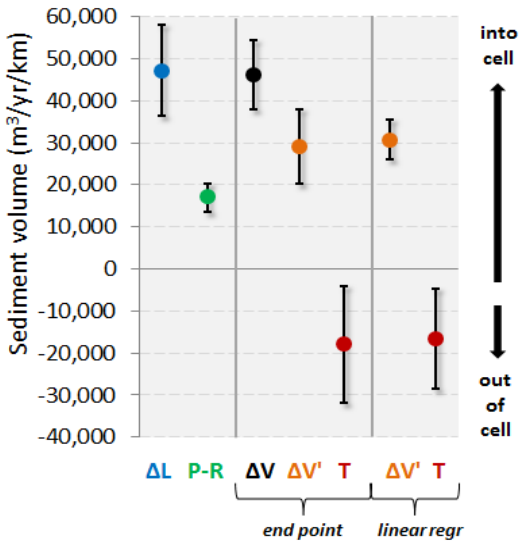

3.2.11 Zeebrugge Harbour

Zeebrugge Harbour is located at the border between cells 7 and 8 (section 216 and 217, Figure 36). Compared with the other harbours, the longshore transport rates around Zeebrugge have been relatively well studied (see section 1.4.1.1.1 for more details). The longshore transport rate from cell 7 to 8 is effectively 0, as the harbour acts as a complete block to longshore transport. Average net transport into cell 7, west of Zeebrugge harbour, is 250,000 m^3/year (from the morphological model). The observed volume change over the 10 year analysis period ranges from 163,000 to 251,000 m^3/year, depending on the method used to calculate volume change (see section 2.6). An average of approximately 94,000 m^3/year of sand was placed in this cell between 2000 and 2009 (this was a combination of placements and removals). The result is that approximately 88,000 to 97,000 m^3/year is moving offshore (assuming that inland transport is 0). East of the harbour, in cell 8, approximately 135,000 m^3/year is leaving the cell through longshore transport. At the same time, the volume in the cell has increased between 47,000 and 160,000 m^3/year, depending on how the volume change is calculated. Only ~61,000 m^3/year of this increase can be attributed to sediment entering the cell. This means that a large amount of sand (between 182,000 and 234,000 m^3/year) is coming in from the offshore (assuming input from the upland area is negligible). This is in agreement with previous studies (Van Lancker et al 2007, Trouw et al 2015), as described in section 1.4.1.1.3. These studies suggest that the incoming sediment primarily comes from an erosion area in front of Zeebrugge Harbour. Dredging volumes removed from Zeebrugge Harbour were not taken into account in the sediment budget since the harbour itself is not included in the analysis cells. For a more detailed analysis of the sediment budget and morphological trends in the vicinity of Zeebrugge, refer to Houthuys et al 2014 and Trouw et al 2015.

Figure 36 – Volume calculation limits for the sections near Zeebrugge Harbour.

3.2.12 Cell 8 – Zeebrugge Harbour to Knokke Zoute

This cell includes coastal sections 217 to 241. According to the volumetric analysis, this area experienced significant net sediment accretion between 2000 – 2009 (though not as much as cell 7). Part of this may be explained by beach nourishments around Knokke. However, the net longshore transport is significantly negative, with no sand coming in from the border with Zeebrugge harbour and significant sand going out along the eastern border. This results in cell that is **unbalanced, with net transport in,** likely from offshore Zeebrugge Harbour. This is in agreement with past studies of the sediment balance in this area (see discussion in section 1.4.1.1.1). Compared with the rest of the cells the uncertainties are small to medium (Figure 37).

Figure 37 – Results and uncertainty for cell 8.

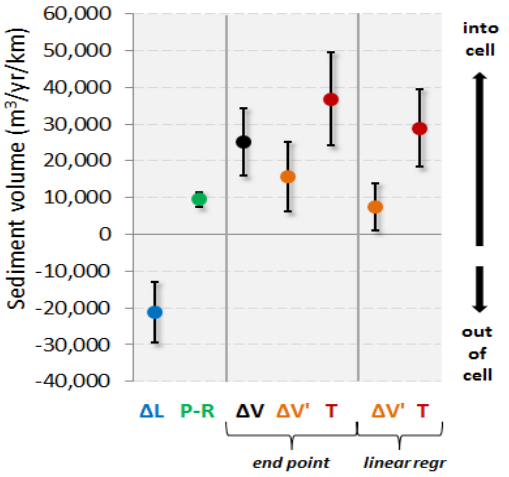

3.2.13 Cell 9 – Knokke Zoute to Het Zwin (Dutch border)

This cell includes coastal sections 242 to 255. This cell experienced a slight accretion from 2000 to 2009, though not significant within the uncertainty of the volume measurements. The net longshore transport across the zone is slightly negative, but this is also not significant, especially since the Dutch border was not included in the numerical modelling of longshore transport rates, resulting in an extrapolation being used. There were some very minor beach nourishment works near Knokke Zoute. In summary, this cell is **slightly unbalanced, with net transport in**, but it is not significant. The uncertainties are rather large (except for the placements and removals) probably due to lack of connection to the sediment transport from the Netherlands (Figure 38).

Figure 38 – Results and uncertainty for cell 9.

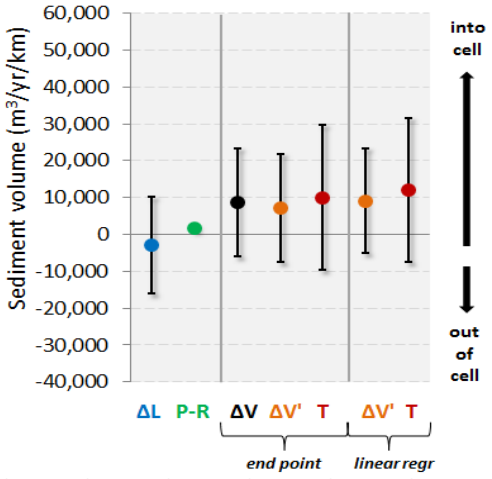

4 Conclusions

A comprehensive sediment budget for the entire nearshore part of the Belgian coast was constructed in the frame of this project. The sediment budget equation was applied using existing data to compute the sand volumes entering or exiting from the considered coastal system at onshore and offshore boundaries. An Excel tool, developed in a previous phase of this project, was used to optimise the computation of the sediment budget and to calculate the associated uncertainties. Uncertainties were assigned to each of the inputs, allowing an estimate of uncertainty for the results.

A timeframe of 10 years was selected to represent existing conditions and to guarantee sufficient coverage of input data: hydrodynamics, sediment transport, and human interventions. The spatial scale was selected based on both sediment transport limits such as the closure depth at the offshore boundary and dykes or road at the onshore boundary as well as on data availability. Next, we calculated the longshore sediment transport using bulk formulations such as those from CERC and Kamphuis and the results of a numerical model (Wang et al 2012). After comparison, the latter was used as the main input for the sediment budget.

Volume changes for both dry and submerged beach were calculated along with the associated uncertainties for the period between 2000 and 2009. The main input data were sand volumes on the beach and in the nearshore areas (1.5 km) reported in Houthuys 2012 for multiple years between 2000 and 2009. Volume change estimates are subject to many uncertainties. Therefore, two sediment budgets were developed using different approaches to calculate the volume change. The first sediment budget was based on the volume change between the 2000 and 2009, independent of data from intermediate years. This approach has the advantage of respecting the conservation of volume equation, but is sensitive to the start and end measurements. In order to minimize the effects of such possible error a second sediment budget was developed using a linear trend on all volume measurements, both corrected and uncorrected for human interventions. The second sediment budget shows no different trends for the cells, but small differences for the sediment volume. The similarity with the main sediment budget increase the confidence on the final results.

Finally, brief reference was made to the role of the harbours in the sediment budget without great detail since there are reports describing the sediment budget for each harbour, but also because their budgets mainly involve finer sediments.

The present sediment budget covers a period of 10 years for the entire Belgian coast and it is the first study to provide a clear overview on the sediment status for nearshore area. The coast is generally balanced in terms of loss and gain of sand, excepting the area downdrift and updrift of Zeebrugge harbour, but this situation was anticipated due to the disturbance induce by the large harbour.

The results of this study are not without uncertainty. While the quality of some of the data, such as the topography, bathymetry, and sand placement/removal volumes, is difficult to improve, there are opportunities to improve the accuracy of the sediment budget in other ways. Improving the understanding of longshore transport rates, especially near the border with France, may have a large impact on the sediment budget. Moreover, a detailed and accurate longshore transport model for the entire Belgian coast should be built and this model should account for sediment transport induced by all wave conditions. Better understanding the closure depth, and ensuring that the closure depth is reached in regular bathymetric surveys, would allow for a more complete understanding of volume changes occurring in each cell. Refining estimates of aeolian transport, while highly uncertain, is unlikely to have a significant impact on the overall sediment budget, since this term is expected to remain fairly small. Finally, the sediment budget in Belgium is complicated by the presence of offshore sandbanks on the Belgian continental shelf. Eventually, an integrated sediment budget, which explore the interaction between the shelf and the nearshore zone, should be developed.

5 References

Anthony, E.J. (2000). Marine sand supply and Holocene coastal sedimentation in northern France between the Somme estuary and Belgium. Geological Society, London, Special Publications 2000, 175, 87-97.

Beck, C., P. Claubaut, S. Dewez, O. Vicaire, H. Chamley, C. Augris, R. Hoslin, and A. Caillot (1991). Sand bodies and sand transport paths at the English Channel – North Sea border: morphology, hydrodynamics and radioactive tracing. Proceedings of the International Colloquium on the environment of epicontinental seas, Lille, 20-22 March, 1990. Oceanologica Acta, 11, 111-121.

Bayram, A., M. Larson, and H. Hanson (2007). A new formula for the total longshore sediment transport rate. Coastal Engineering, 54, 700-710.

Bowen, A.J. and D.L. Inman (1966). Budget of littoral sand in the vicinity of Point Arguello, California. U.S. Army Coastal Engineering Research Center, Technical Memorandum No. 19, 56 p.

Bray, M.J., D.J. Carter, and J.M. Hooke (1995). Littoral cell definition and budgets for Central Southern England. Journal of Coastal Research, 11(2), 381-400. Fort Lauderdale, Florida.

Bruun, P. (1962). Sea level rise as a cause of shore erosion. Journal of Waterways and Harbours Division, American Society of Civil Engineers, 88, 117-130.

Bruun, P. (1988). The Bruun Rule of erosion by sea-level rise: A discussion of large-scale two and three-dimensional usages. Journal of Coastal Research 4, 627-648.

Church, J.A., P.U. Clark, A. Cazenave, J.M. Gregory, S. Jevrejeva, A. Levermann, M.A. Merrifield, G.A. Milne, R.S. Nerem, P.D. Nunn, A.J. Payne, W.T. Pfeffer, D. Stammer and A.S. Unnikrishnan (2013). Sea Level Change. In: Climate Change 2013: The Physical Science Basis. Contribution of Working Group I to the Fifth Assessment Report of the Intergovernmental Panel on Climate Change [Stocker, T.F., D. Qin, G.-K. Plattner, M. Tignor, S.K. Allen, J. Boschung, A. Nauels, Y. Xia, V. Bex and P.M. Midgley (eds.)]. Cambridge University Press, Cambridge, United Kingdom and New York, NY, USA.

Cooper, J.A.G. and O.H. Pikley (2004). Sea-level rise and shoreline retreat: time to abandon the Bruun Rule. Global and Planetary Change, 43, 157-171.

Cooper, N.J., J.M. Hooke, and M.J. Bray (2001). Predicting coastal evolution using a sediment budget approach: a case study from southern England. Ocean & Coastal Management, 44, 711-728.

de Ronde, J.G. (2008). Toekomstige langjarige suppletiebehoefte. Deltares Report, Z4582.24. Deltares: [s.l.]. 36 pp. [in Dutch]

de Ruig, J.H.M. and C.J. Louisse (1991). Sand budget trends and changes along the Holland coast. Journal of Coastal Research, 7(4), 1013-1026.

Deronde, B., R. Houthuys, W. Debruyn, D. Fransaer, V. Van Lancker, and J. Henriet (2006). Use of airborne hyperspectral data and laserscan data to study beach morphodynamics along the Belgian coast. Journal of Coastal Research, 22(5), 1108-1117. http://www.jstor.org/stable/4300377.

Dewez, S., P. Clabaut, O. Vicaire, C. Beck, H. Chamley, and C. Augris (1989). Transits sedimentaires resultants aux confins Manche-mer du Nord. Bulletin de la Societe Geologique de France, 8, 1043-1053 [in French].

Dijkman, M.J., W.T. Bakker, and J.H. de Vroeg (1990). Prediction of coastline evolution for the Holland Coast. Proceedings of the 22nd Coastal Engineering Conference (Delft), Volume 2, Chapter 146, pp. 1935-1947.

Dubois, R.N. (1992). A re-evaluation of Bruun's rule and supporting evidence. Journal of Coastal Research, 8(3), 618-628. Fort Lauderdale, Florida.

Esteves, L.S., J.J. Williams, and M.A. Lisniowski (2009). Measuring and modelling longshore sediment transport. Estuarine, Coastal and Shelf Science, 83, 47-59.

Eurosense (1991a) Evaluatiestudie "Stabilisatie van het onderwaterstrand d.m.v. vertikale kunststofdoeken" – Knokke-Zoute en Zwin – Beginsituatie Voorjaar 1990 – Administratie Waterinfrastructuur en Zeewezen. Dienst der Kusthavens: Oostende.

Eurosense (1991b) Evaluatiestudie "stabilisatie van het onderwaterstrand d.m.v. vertikale kunststofdoeken": Knokke-Zoute en Zwin. Situatie zomer 1991: bodemtransport, duikersverslagen en side-scan sonarregistraties. Administratie Waterinfrastructuur en Zeewezen. Dienst der Kusthavens: Oostende.

Eurosense (1991c) Evaluatiestudie "stabilisatie van het onderwaterstrand d.m.v. vertikale kunststofdoeken": Knokke-Zoute en Zwin. Situatie zomer 1991: hydrodynamica en sedimentologie. Administratie Waterinfrastructuur en Zeewezen. Dienst der Kusthavens: Oostende.

Eurosense (1994a). Bufferzone Heist Sedimentdynamica. Metingen van spring- naar doodtij (9-16 feb. 1993) enbij storm (18-20 feb. 1993). Tekst & Figuren. KDN 94.004, Eurosense, Wemmel.

Eurosense (1994b). VooroeverZwin, Sedimentdynamica. KDN 94.005>

Fettweis, M. and D. Van den Eynde (1999). Bepaling van de sedimentbalans voor de Belgische kustwateren (SEBAB), Activiteitsrapport I: Literatuurstudie. MUMM Rapport SEBAB/i/XX/199912/NL/AR/1, 37 pp. (in Dutch).

Fettweis, M., B. Nechad, F. Francket, and D. Van den Eynde (2002). Bepaling van de sedimentbalans voor de Belgische kustwateren (SEBAB-III), Activiteitsrapport 1: Dynamica van het gesuspendeerd particulair materiaal (SPM) op het Belgisch Continentaal Plat. MUMM Rapport SEBAB/3/MF/200212/NL/AR/1, 30 pp. (in Dutch).

Fettweis, M., D. Van den Eynde, F. Francken, and B. Nechad (2008). Monitoring en Modellering van het cohesive sedimenttransport en evaluatie van de effecten op het mariene ecosysteem ten gevolge van bagger- en stortoperatie (MOMO). Activiteitsrapport 4 (1 october 2007 – 31 maart 2008). MOMO/3/MF/200805/NL/AR/4, 56 pp. (in Dutch).

Fremout, A. (2002). Overzicht van de tijwaarnemingen langs de Belgische kust: Periode 1991-2000 voor Nieuwpoort, Oostende, en Zeebrugge. Afdeling Kust, Oostende. (in Dutch)

Gravens, M.B. (1989). Estimating potential longshore sand transport rates using WIS Data. Coastal Engineering Technical Note CETN-II-19, U.S. Army Engineer Waterways Experiment Station, Coastal and Hydraulics Laboratory, Vicksburg, MS.

Hallermeier, R.J. (1981). A profile zonation for seasonal sand beaches from wave climate. Coastal Engineering, 4, 253-277.

Hequette, A., Y. Hemdane, and E.J. Anthony (2008). Sediment transport under wave and current combined flows on a tide-dominated shoreface, northern coast of France.

Houthuys, R. (2011). A sedimentary model of the Brussels Sands, Eocene, Belgium. Geologica Belgica, 14(1-2), URL: http://popups.ulg.ac.be/1374-8505/index.php?id=3205.

Houthuys, R. (2012). Morfologische trend van de Vlaamse kust in 2011. Agentschap Maritieme Dienstverlening en Kust. Afdeling Kust: Oostende. 150 pp. (in Dutch)

Houthuys, R., K. Trouw, N. Zimmermann, B. De Maerschalck, R. Delgado, T. Verwaest, and F. Mostaert (2014). Scientific support regarding hydrodynamics and sand transport in the coastal zone: Update of the sediment budget for the nearshore of Blankenberge-Zeebrugge. Version 3_0. WL Rapporten, 00_072. Flanders Hydraulics Research & IMDC: Antwerp, Belgium.

International Marine & Dredging Consultants (IMDC) (2009a). Deelrapport 4: Technisch Wetenschappelijke Bijstand: Eindrapport. Afstemming Vlaamse en Nederlandse voorspelling golfklimaat op ondiep water. Voor de Vlaamse Overheid Departement Mobiliteit en Openbare Werken – Afdeling Waterbouwkundig Laboratorium. I/RA/11273/09.030/SDO. (in Dutch)

International Marine & Dredging Consultants (IMDC) (2009b). Deelrapport 5: Rapportage jaargemiddeld golfklimaat. Afstemming Vlaamse en Nederlandse voorspelling golfklimaat op ondiep water. Voor de Vlaamse Overheid Departement Mobiliteit en Openbare Werken – Afdeling Waterbouwkundig Laboratorium. I/RA/11273/09.091/SDO. (in Dutch)

I**nternational Marine & Dredging Consultants (IMDC)** (2010). DO4: Morfologische evolutie van de Vlaamse kust ingedeeld in morfologisch homogene kuststroken, vanaf de eerste meetvlucht tot 2009, rekening houdend met de aangevoerde zandhoeveelheden. Agentschap Maritieme Dienstverlening en Kust. Afdeling Kust: Oostende. 86 pp. (in Dutch).Janssens, J., R. Delgado, T. Verwaest, and F. Mostaert (2013). Morfologische trends op middellange termijn van strand, vooroever en kustnabije zone langsheen de Belgische kust: Deelrapport in het kader van het Quest4D-project. Versie 2_0. WL Rapporten, 814_02. Waterbouwkundig Laboratorium: Antwerpen, Belgie. (in Dutch)

Janssens, J., R. Delgado, T. Verwaest, and F. Mostaert (2013). Morphologische trends op middellange termijn van strand, vooroever, en kustnabije zone langsheen de Begische kust: Deelrapport in het kader van het Quest4D-project. Versie 2_0. WL Rapporten, 814_02. Waterbouwkundig Laboratorium: Antwerpen, Belgie. (in Dutch)

Kamphuis, J.W. (1991). Alongshore sediment transport rate. Journal of Waterway, Port, Coastal, and Ocean Engineering, 117(6), 624-640.

Kamphuis, J.W. (2010). Introduction to coastal engineering and management, 2nd Edition. Advanced Series on Ocean Engineering – Volume 30. World Scientific. 525 pages.

Lanckneus, J., V.R.M. Van Lancker, G. Moerkerke, D. Van den Eynde, M. Fettweis, M. De Batist, and P. Jacobs (2001). Investigation of the natural sand transport on the Belgian Continental shelf: BUDGET (Beneficial usage of data and geo-environmental techniques) Scientific Support Plan for a Sustainable Development Policy (SPSD I): Programme "Sustainable Management of the North Sea" = Plan voor wetenschappelijke ondersteuning van een beleid gericht op duurzame ontwikkeling (PODO I): Programma "Duurzaam beheer van de Noordzee" Federal Office for Scientific, Technical and Cultural Affairs (OSTC): Brussel. 104 + 87 p. annexes pp.

Limber, P.W., K.B. Patsch, and G.B. Griggs (2008). Coastal sediment budgets and the littoral cutoff diameter: a grain size threshold for quantifying active sediment inputs. Journal of Coastal Research, 24(2B), 122-133. West Palm Beach, Florida.

Mercier, C. and E.J.M. Delhez (2007). Diagnosis of the sediment transport in the Belgian Coastal Zone. Estuarine, Coastal, and Shelf Science, 74, 670-683. Liege, Belgium.

Mil-Homens, J., R. Ranasinghe, J.S.M. van Thiel de Vries, and M.J.F. Stive (2013). Re-evaluation and improvement of three commonly used bulk longshore sediment transport fomulas. Coastal Engineering, 75, 29-39.

Ranasinghe, R., D. Callaghan, and M.J.F. Stive (2012). Estimating the coastal recession due to sea level rise: beyond the Bruun rule. Climatic Change, 110, 561-574.

Roelvink, J.A. and M.J.F. Stive (1990). Sand transport on the shoreface of the Holland coast. Proceedings of the 22nd Coastal Engineering Conference (Delft), Volume 2, Chapter 144, pp. 1909-1921.

Rosati, J.D. (2005). Concepts in sediment budgets. Journal of Coastal Research, 21(2), 307–322. West Palm Beach (Florida), ISSN 0749-0208.

Rosati, J.D., R.G. Dean, and T.L. Walton (2013). The modified Bruun rule extended for landward transport. Marine Geology, 340, 71-81.

Rosati, J.D., A.E. Frey, A.S. Grzegorzewski, C. Maglio, A. Morang, and R.C. Thomas (2015). Conceptual regional sediment budget for the U.S. North Atlantic coast. Conference paper for Coastal Sediments 2015, San Diego, CA.

Rosati, J.D., M.B. Gravens, and W.G. Smith (1999). Regional sediment budget for Fire Island to Montauk Point, New York, USA. Proceedings Coastal Sediments 1999, ASCE, pp. 802 – 817.

Rosati, J.D. and N.C. Kraus (1999). Formulation of Sediment Budgets at Inlets. Coastal Engineering Technical Note IV-15 (Revised September 1999). US Army Research and Development Center, Vicksburg, MS.

Ruz, M.H., E.J. Anthony, and L. Faucon (2005). Coastal dune evolution on a shoreline subject to strong human pressure: the Dunkirk area, northern France. Proceedings 'Dunes and Estuaries 2005' – International Conference on Nature Restoration Practices in European Coastal Habitats, Koksijde, Belgium. 441-449.

Schoonees, J.S. and A.K. Theron (1996). Improvement of the most accurate longshore transport formula. 25th International Conference on Coastal Engineering, Vol. 3. ASCE, Orlando, FL, 3652-3665.

Sebatier F., M.J.F. Stive, and F. Pons (2004). Longshore variation of depth of closure on a micro-tidal wave-dominated coast. Proceedings of the 29th International Conference on Coastal Engineering, 3, 2327-2339.

Smith, E.R., B.A. Ebersole, and P. Wang (2004). Dependence of total longshore sediment transport rates on incident wave parameters and breaker types. US Army Corps of Engineers, ERDC/CHL CHETN-IV-62, September 2004.

Stive, M.J.F. (1989). Voorspelling ontwikkeling kustlijk 1990-2090. Kustverdediging na 1990, Technisch Rapport 5, Rijkswaterstaat, Den Haag.

Svasek (2012). Morfologie Zwakke Schakel Cadzand-Bad, ref. 1638/U12221/SPo/B.

Teurlincx, R., K. Van der Biest, J. Reyns, T. Verwaest, and F. Mostaert (2009). Haven van Blankenberge – vermindering van de aanzanding van de havengeul en het voorpleind. Eindrapport. WL Rapporten WL2009R643_12_rev1_1, 127 p. (in Dutch)

Trouw, K., N. Zimmerman, L. Wang, B. De Maerschalck, R. Delgado, T. Verwaest, and F. Mostaert (2015). Scientific support regarding hydrodynamics and sand transport in the coastal zone: Literature and data review coastal zone Zeebrugge – Zwin. Version 4_0. WL Rapporten, 12_107. Flanders Hydraulics Research. Antwerp, Belgium.

U.S. Army Corps of Engineers (USACE) (1984). Shore Protection Manual, Volume 1, Chapter 4 – Littoral Processes.

U.S. Army Corps of Engineers (USACE) (2012). Sediment Budget Analysis System (SBAS) for ArcGIS 10 – User's Guide. Available at http://cirp.usace.army.mil/products/sbtools.php.

Van Cauwenberghe, C. (1999). Relative sea level rise along the Belgian Coast: Analyses and conclusions with respect to the high water, the mean sea, and the low water levels. Infrastructuur in het Leefmilieu, pp. 513 – 539.

Van de Rest, P. (2004). Morfodynamica en hydrodynamica van de Hollandse kust. TUDelft Faculty of Civil Engineering, MSc Thesis. May 2004. (in Dutch)

Van den Eynde, D., R. De Sutter, L. De Smet, F. Francken, J. Haelters, F. Maes, E. Malfait, J. Ozer, H. Polet, S. Ponsar, J. Reyns, K. Van der Biest, E. Vanderperren, T. Verwaest, A. Volckaert, and M. Willekens (2011). Evaluation of climate change impacts and adaptation responses fr marine activities "CLIMAR". Final Report Brussels: Belgian Science Policy Office, 121 p. (Research Programme Science for a Sustainable Development).

Van Lancker, V., M. De Batist, M. Fettweis, G. Pichot, and J. Monbaliu (2007). Management, Research And Budgetting Of Aggregates In Shelf Seas Related To End-Users - Marebasse (SPSD II project).

Verwaest, T., R. Delgado, J. Janssens, and J. Reyns (2010). Longshore sediment transport along the Belgian coast. Paper abstract submitted for the Coastal Sediments conference, Miami, US, 2-6 May 2011.

Vincent, C.E., A. Stolk, and C.F.C. Porter (1998). Sand suspension and transport on the Middelkerke Bank (southern North Sea) by storms and tidal currents. Marine Geology, 150, 113-129.

Wahl, T., I. Haigh, F. Albrecht, D. Dillingh, J. Jensen, R. Nicholls, R. Weisse, P.S. Woodworth, G. Wöppelmann (2013). Observed mean sea level changes around the North Sea coastline from 1800 to present. Earth Science Reviews, 124, 51–67.

Wang, P., B.A. Ebersole, and E.R. Smith (2002). Longshore Sand Transport – Initial Results from Large-Scale Sediment Transport Facility. US Army Corps of Engineers ERDC/CHL CHETN-II-46, March 2002.

Wang, L., N. Zimmermann, K. Trouw, B. De Maerschalck, R. Delgado, T. Verwaest, F. Mostaert (2015). Scientific support regarding hydrodynamics and sand transport in the coastal zone: Calibration of a Long term morphological model of the Belgian shelf. Version 4.0. WL Rapporten, 12_107. Flanders Hydraulics Research & IMDC: Antwerp, Belgium.

Wang, L., N. Zimmermann, K. Trouw, R. Delgado, F. Toro, T. Verwaest, and F. Mostaert (2012). Scientific support regarding hydrodynamics and sand transport in the coastal zone: Longshore modelling : Realistic Blankenberge case. Version 1_0. WL Rapporten, 744_30. Flanders Hydraulics Research & IMDC: Antwerp, Belgium.

Yu, C.S. (1993). Modelling shelf sea dynamics and estuarine circulations. Ph.D. Thesis. KULeuven.

Annexe 1 Sediment Budget Calculation Tool for the Belgian Coast

This annexe was written by Job Janssens in a previous phase of this project (in 2012/2013). The tool was used as developed (and described below) in developing the sediment budget for the Belgian coast described in the main report.

A.1 Inleiding

Deze appendix vormt een handleiding bij het Excelbestand “sedment_budget_calculation_tool_v3.xlsm” dat is opgemaakt in het kader van het project Vlaamse Baaien – Sedimentbalans kust (12_155).
Dit Excelbestand bevat enerzijds de benodigde data voor het uitvoeren van een sediment budget (voornamelijk volumes voor de verschillende secties langs de Belgische kust), en is anderzijds ook een rekentool die toelaat om op geautomatiseerde wijze het sediment budget uit te rekenen. Deze handleiding zal dan ook enerzijds toelichten welke datasets gebruikt zijn en hoe deze verwerkt , en anderzijds

A.2 Definities

Definities:

Het uitrekenen van een sediment budget langsheen de Belgische kust bestaat erin van voor een bepaalde indeling van de Belgische kust in verschillende cellen de omvang van de onbekende sedimenttransporten tussen verschillende aangrenzende cellen te berekenen, en dit op basis van gekende sedimenttransporten, en de over een bepaalde periode optredende volumeveranderingen en extern toegevoegde volumes binnen de cellen. Deze berekening bestaat in feite voor elke cel uit het boekhoudkundig bijhouden van inkomende en uitgaande sedimenthoeveelheden.

In de Exceltool wordt uitgegaan van een raster van min of meer rechthoekige cellen, bestaande uit m rijen en n kolommen. Figuur 39 geeft een schematisch overzicht van een deel van zulk een raster, samen met de mogelijke sedimenttransporten (rode pijlen). Per conventie wordende horizontale lijnen in het raster zoveel mogelijk kustparallel genomen. Verder is sedimenttransport positief indien het de zin van de pijlen zoals aangegeven in Figuur 39 volgt, d.w.z. positief sedimenttransport gaat in de kustparallelle richting van Frankrijk naar Nederland en in de kustdwarse richting van zee naar land.

Figure 39 – Schematisch overzicht van een raster van cellen met de mogelijke sedimenttransporten tussen aangrenzende cellen.

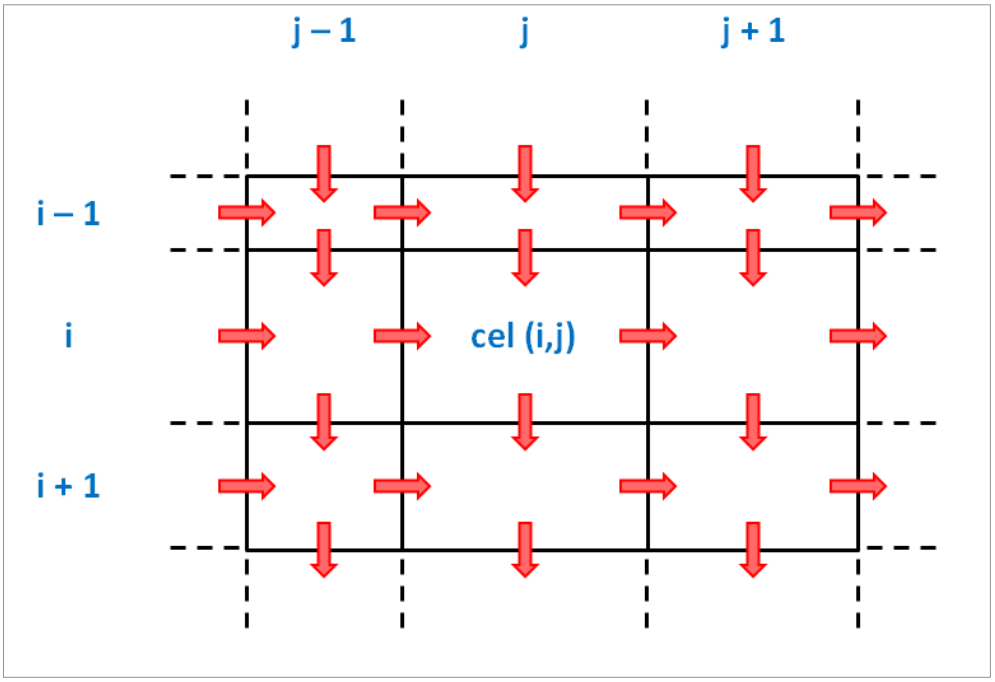

Figuur 40 geeft een schematische voorstelling van een enkele cel met coördinaten (i,j), samen met de conventies betreffende de naamgeving van de verschillende fysische grootheden. Deze grootheden zijn de volgende:

$\Delta V_{ij} = V_{ij}(t_b) - V_{ij}(t_a)$ is in cel (i,j) het verschil tussen het volume op tijdstip t_b en het volume op tijdstip t_a. ΔV_{ij} wordt uitgedrukt in m³. t_b en t_a zijn de tijdstippen tussen dewelke het sediment budget wordt berekend.

P_{ij} = de hoeveelheid sediment die (in m³) die door menselijk ingrijpen is aangebracht in cel (i,j) tussen de tijdstippen t_b en t_a.

$\Delta t = t_b - t_a$ is het tijdinterval over hetwelk het sediment budget wordt uitgerekend.

L_{ij} = het gemiddeld sedimentdebiet (in m³/jaar) dat via de westelijke rand cel (i,j) binnenkomt, en bijgevolg ook het gemiddeld sedimentdebiet dat cel (i,j-1) verlaat via de oostelijke rand.

$L_{i,j+1}$ = het gemiddeld sedimentdebiet (in m³/jaar) dat via de oostelijke rand cel (i,j) verlaat, en bijgevolg ook het gemiddeld sedimentdebiet dat cel (i,j+11) binnenkomt via de oostelijke rand.

T_{ij} = het gemiddeld sedimentdebiet (in m³/jaar) dat via de noordelijke rand cel (i,j) binnenkomt, en bijgevolg ook het gemiddeld sedimentdebiet dat cel (i-1,j) verlaat via de zuidelijke rand.

$T_{i+1,j}$ = het gemiddeld sedimentdebiet (in m³/jaar) dat via de zuidelijke rand cel (i,j) verlaat, en bijgevolg ook het gemiddeld sedimentdebiet dat cel (i+1,j) binnenkomt via de noordelijke rand.

a_{ij} = de lengte (in m) van de westelijke rand van cel (i,j), en bijgevolg ook de lengte van de oostelijke rand van cel (i,j-1).

$a_{i,j+1}$ = de lengte (in m) van de oostelijke rand van cel (i,j), en bijgevolg ook de lengte van de westelijke rand van cel (i,j+1).

b_{ij} = de lengte (in m) van de noordelijke rand van cel (i,j), en bijgevolg ook de lengte van de zuidelijke rand van cel (i-1,j).

$b_{i+1,j}$ = de lengte (in m) van de zuidelijke rand van cel (i,j), en bijgevolg ook de lengte van de noordelijke rand van cel (i+1,j).

Indien de cel volmaakt rechthoekig is, geldt uiteraard $a_{ij} = a_{i,j+1}$ en $b_{ij} = b_{i+1,j}$. In het algemeen zullen de cellen echter niet volmaakt rechthoekig zijn.

De sedimenttransporten over de randen kunnen ook beschreven worden als fluxen, die hier gedefinieerd worden als debieten per lengte-eenheid:

l_{ij} = L_{ij}/a_{ij} is de gemiddelde (oostwaartse) sedimentflux (in m³/m/jaar) over de westelijke rand van cel (i,j), en bijgevolg ook de gemiddelde sedimentflux over de oostelijke rand van cel (i,j-1).

$l_{i,j+1}$ = $L_{i,j+1}/a_{i,j+1}$ is de gemiddelde (oostwaartse) sedimentflux (in m³/m/jaar) over de oostelijke rand van cel (i,j), en bijgevolg ook de gemiddelde sedimentflux over de westelijke rand van cel (i,j+1).

t_{ij} = T_{ij}/b_{ij} is de gemiddelde (landwaartse) sedimentflux (in m³/m/jaar) over de noordelijke rand van cel (i,j), en bijgevolg ook de gemiddelde sedimentflux over de zuidelijke rand van cel
(i-1,j).

$t_{i+1,j}$ = $T_{i+1,j}/b_{i+1,j}$ is de gemiddelde (landwaartse) sedimentflux (in m³/m/jaar) over de zuidelijke rand van cel (i,j), en bijgevolg ook de gemiddelde sedimentflux over de noordelijke rand van cel (i+1,j).

Figure 40 – Schematische voorstelling van een enkele cel, met de verschillende conventies betreffende naamgeving.

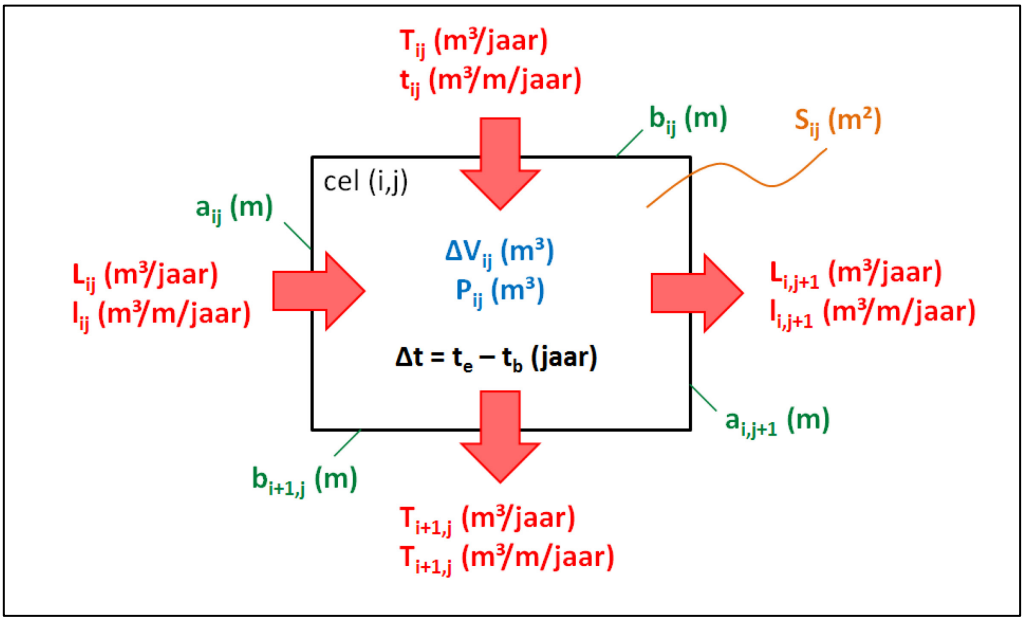

Met de hierboven gedefinieerde grootheden kunnen we nu een massabalans opmaken voor cel (i,j) voor de periode tussen t_b en t_a. Deze ziet er als volgt uit:

$$\frac{\Delta V_{ij}}{\Delta t} = \frac{P_{ij}}{\Delta t} + L_{ij} - L_{i,j+1} + T_{ij} - T_{i+1,j} \quad ,$$

of, indien we sedimentfluxen gebruiken i.p.v. sedimentdebieten:

$$\frac{\Delta V_{ij}}{\Delta t} = \frac{P_{ij}}{\Delta t} + a_{ij} \cdot l_{ij} - a_{i,j+1} \cdot l_{i,j+1} + b_{ij} \cdot t_{ij} - b_{i+1,j} \cdot t_{i+1,j} \quad .$$

Merk op dat bovenstaande formule zijn oorsprong vindt in de wet van behoud van massa, hoewel de formulering gebeurt in volumes. Dit betekent dat er impliciet van uitgegaan wordt dat de dichtheid gedurende de periode Δt niet verandert en voor alle processen (antropogene plaatsing en natuurlijk transport over de randen) identiek is.

Voor een m x n raster (met i gaande van 1 tot en met m en j gaande van 1 tot en met n) verkrijgen we dus in totaal m·n vergelijkingen (nl. voor elke cel een sedimentbalans zoals hierboven) en evenveel volumeveranderingen ΔV_{ij} en plaatsingen P_{ij}. Het aantal sedimentdebieten L_{ij} en T_{ij} bedraagt respectievelijk m·(n+1) en (m+1)·n. In totaal zijn er dus 2·m·n + m + n sedimentdebieten.

In de Excel rekentool wordt ervan uitgegaan dat de volumeveranderingen ΔV_{ij} en de sedimentplaatsingen P_{ij} gekend zijn. ΔV_{ij} kan immers berekend worden uit de verschillende beschikbare bodemopmetingen van de laatste 15 jaar, en P_{ij} is relatief goed geïnventariseerd voor deze periode. De tool is dan in staat van op basis van een aantal gekende sedimentdebieten (of -fluxen) andere niet gekende sedimentdebieten (of -fluxen) te berekenen. Voor een m x n raster betekent dit dat –om te komen tot een unieke oplossing van het stelsel van vergelijkingen bestaande uit de sedimentbalansen van alle cel– het aantal a priori gekende sedimentdebieten (of -fluxen) gelijk moet zijn aan m·n + m + n.

A.3 Overzicht van de verschillende stappen in de Excel rekentool

De Excel rekentool biedt de gebruiker enkele keuzes wat betreft de indeling van de kustzone, de periode waarover het budget uitgerekend moet worden, en verder ook enkele opties voor wat betreft de berekeningswijze. In dit hoofdstuk wordt een oplijsting gegeven van de verschillende stappen die in de Excel rekentool moeten doorlopen worden om de opties correct in te vullen en de tool het sediment budget te laten uitrekenen. Elke stap zal hierbij uitvoerig toegelicht worden.
In de Excel rekentool zijn slechts drie tabbladen relevant voor de gebruiker, nl. de tabbladen “SEDIMENTBUDGET”, “PARAMETERSTUDIE” en “INVULLEN ONTBREKENDE VOLUMES”. Deze tabbladen zijn voorzien van een groene tab. De overige tabbladen bevatten data of berekeningen en zullen later kort toegelicht worden.

A.3.1 Algemeen

Het belangrijkste tabblad is het tabblad “SEDIMENTBUDGET”. Hier bevinden zich de verschillende stappen die doorlopen moet worden voor het uitrekenen van het sediment budget. Deze stappen zijn:

1) periode sediment budget / parameters
2) indeling cellen Belgische kust
3) invullen debieten / fluxen
4) controleren oplosbaarheid
5) oplossen stelsel
6) debieten / fluxen per cel

Deze verschillende stappen zijn in het tabblad “SEDIMENTBUDGET” horizontaal naast mekaar geplaatst, en de gebruiker kan dus van de ene naar de andere stap overgaan door horizontaal te scrollen. Voor het gebruiksgemak zijn er echter ook enkele drukknoppen voorzien die het navigeren tussen de verschillende stappen makkelijker maken. Deze knoppen zijn bij elke stap aanwezig en bevinden zich bij normaal gebruik in een grijs vlak aan de linkerzijde. De huidige stap waarin de gebruiker zich bevindt heeft een knop met grijze i.p.v. zwarte tekst.

Figure 41 – Bij elke stap zijn in het grijze vak links drukknoppen aanwezig die helpen navigeren tussen de verschillende stappen.

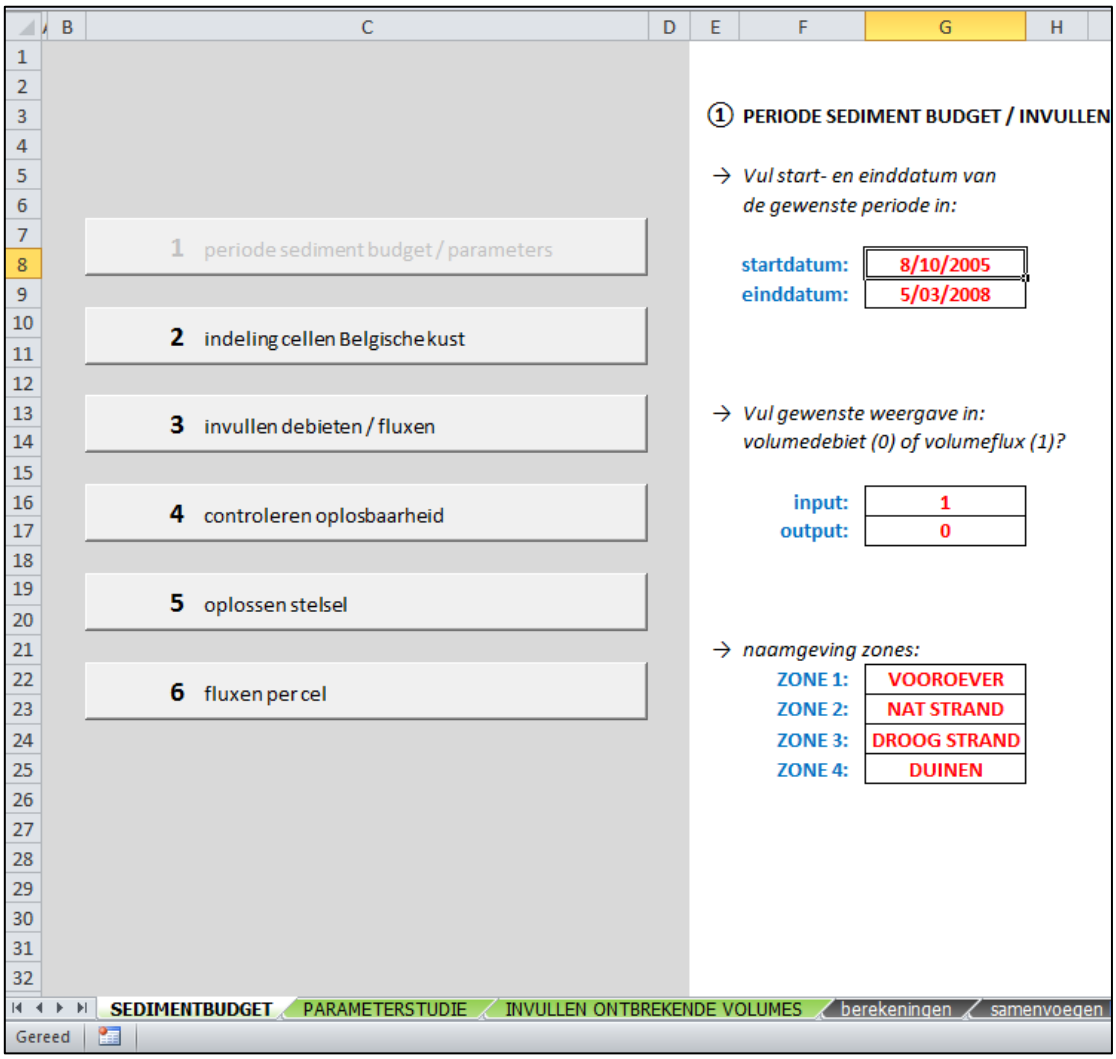

A.3.2 Stap 1: periode sediment budget / parameters

In stap 1 dient de gewenste periode voor de sediment budget berekening opgegeven te worden, samen met enkele parameters die invloed hebben op de berekeningsmethode. Op dit ogenblik heeft de gebruiker de indeling in cellen nog niet gemaakt. In stap 1 worden dan ook de sedimentvolumes binnen elke sectie en binnen elke zone berekend, en dit voor zowel begin- als einddatum van de gekozen periode. Tegelijk wordt voor elk volume een onzekerheid geschat.
In subparagraaf 0 worden de formules toegelicht die de rekentool aanwendt voor het bepalen van het verschil in sedimentvolume tussen twee door de gebruiker gekozen datums. Subparagraaf 0 geeft dan weer de formules gebruikt voor het berekenen van de onzekerheden op de sedimentvolumes. In subparagraaf 0

wordt getoond hoe de verschillende parameters voor stap 1 in de Excel rekentool dienen ingevuld te worden. In een laatste subparagraaf worden ten slotte enkele tips gegeven voor de keuze van de verschillende in te vullen parameters.

A.3.2.1 Berekening van de sedimentvolumes

De volumes per sectie en per zone zijn in principe reeds ingevoerd als basisdata in de Excel rekentool, toch dienen er nog berekeningen uitgevoerd te worden. Immers, de gekozen begin- en einddatum vallen in het algemeen niet samen met de opnamedatums van de basisdatasets. Om die reden zal de rekentool nadat gekozen is voor een begindatum interpoleren tussen de volumes van de basisdatasets waarvan de opnamedatums zo dicht mogelijk voor en na deze begindatum liggen. De interpolatieformule is als volgt:

$$V(t_b) \equiv V_b = \frac{\left(d_{b,l}\right)^N \cdot V_{b,v} + \left(d_{b,v}\right)^N \cdot V_{b,l}}{\left(d_{b,v}\right)^N + \left(d_{b,l}\right)^N} \ .$$

Hierbij is $V(t_b)$ het sedimentvolume voor een welbepaalde sectie en welbepaalde zone (indices hiervoor zijn weggelaten om de uitdrukking niet te overladen) op begindatum t_b. $V_{b,v}$ en $V_{b,l}$ zijn de sedimentvolumes voor die sectie en zone voor de respectievelijke opnamedatums $t_{b,v}$ en $t_{b,l}$, waarbij $t_{b,v}$ en $t_{b,l}$ ten opzichte van t_b respectievelijk de vroegere en latere dichtstbijzijnde opnamedatum zijn. Verder geldt $d_{b,v} = t_b - t_{b,v}$ en $d_{b,l} = t_{b,l} - t_b$. De parameter N is door de gebruiker vrij te kiezen en laat toe meer gewicht toe te kennen (door $N > 1$ te nemen) aan de meest nabije van de twee opnamedatums waartussen geïnterpoleerd wordt. Voor $N = 1$ gaat bovenstaande formule over in een lineaire interpolatie. Merk op dat bovenstaande interpolatie overeenkomt met de o.a. in ArcGIS vaak gebruikte IDW-interpolatiemethode (Inverse Distance Weighted), met dien verstande dat hier niet ruimtelijk wordt geïnterpoleerd maar langs de tijdsas.
Voor de interpolatie voor het bekomen van het volume $V(t_e)$ op einddatum t_e geldt uiteraard een analoge uitdrukking:

$$V(t_e) \equiv V_e = \frac{\left(d_{e,l}\right)^N \cdot V_{e,v} + \left(d_{e,v}\right)^N \cdot V_{e,l}}{\left(d_{e,v}\right)^N + \left(d_{e,l}\right)^N} \ .$$

Het is belangrijk op te merken dan verschillende datasets ofwel onvolledig zijn, ofwel onderling niet exact hetzelfde gebied bedekken (sommige basisdatasets reiken verder landwaarts of zeewaarts dan andere). Wanneer de basisdataset van een meest nabij gelegen opnamedatum onvolledig is voor een welbepaalde sectie en welbepaalde zone, zal voor die sectie en zone door de rekentool dan ook gezocht worden naar de eerstvolgende basisdataset die wel volledig is voor die sectie en zone. Om te bepalen of een basisdataset al dan niet als volledig kan beschouwd worden voor een bepaalde sectie en bepaalde zone wordt de oppervlakte van de basisdataset in die sectie en zone vergeleken met de oppervlakte van een referentiebasisdataset in die sectie en zone. Als referentiebasisdataset werd in de rekentool gekozen voor de meest recente dataset, voor strand is dat voor vooroever is dat kan aangepast worden verwijzen naar tabbladen en correcte kolom. Een basisdataset wordt voor een bepaalde sectie en zone als voldoende volledig beschouwd als aan volgend criterium is voldaan:

$$100 \cdot \left|\frac{S - S_{\text{ref}}}{S_{\text{ref}}}\right| \leq \text{tolerantie} \ .$$

Hierbij is S de oppervlakte van de beschouwde basisdataset in de sectie en zone in kwestie, S_{ref} is de referentieoppervlakte voor die sectie en zone. De tolerantie geeft aan welke procentuele afwijking tussen oppervlakte van de beschouwde basisdataset en referentieoppervlakte maximaal getolereerd wordt, en is een parameter die door de gebruiker ingesteld kan worden. Het is zinvol niet te eisen dat de oppervlakte van de basisdataset exact gelijk moet zijn aan de referentieoppervlakte, er kunnen immers kleine

afwijkingen optreden tussen oppervlaktes van datasets daar waar deze in theorie gelijk zouden moeten zijn (bijvoorbeeld door afrondingsfouten gemaakt bij het berekenen van sedimentvolumes in ArcGIS) Aan de andere kant mag de tolerantie uiteraard niet te hoog worden ingesteld, dit om te vermijden dat sedimentvolumes in gebieden van verschillende omvang worden vergeleken. Figuur 42 geeft het schematisch overzicht van de wijze waarop de verandering in sedimentvolume voor een bepaalde sectie en zone wordt berekend voor een door de gebruiker gekozen periode.

Figure 42 – Schematisch overzicht van de berekeningswijze van de wijziging in sedimentvolume voor sectie s en zone z voor een welbepaalde gekozen periode.

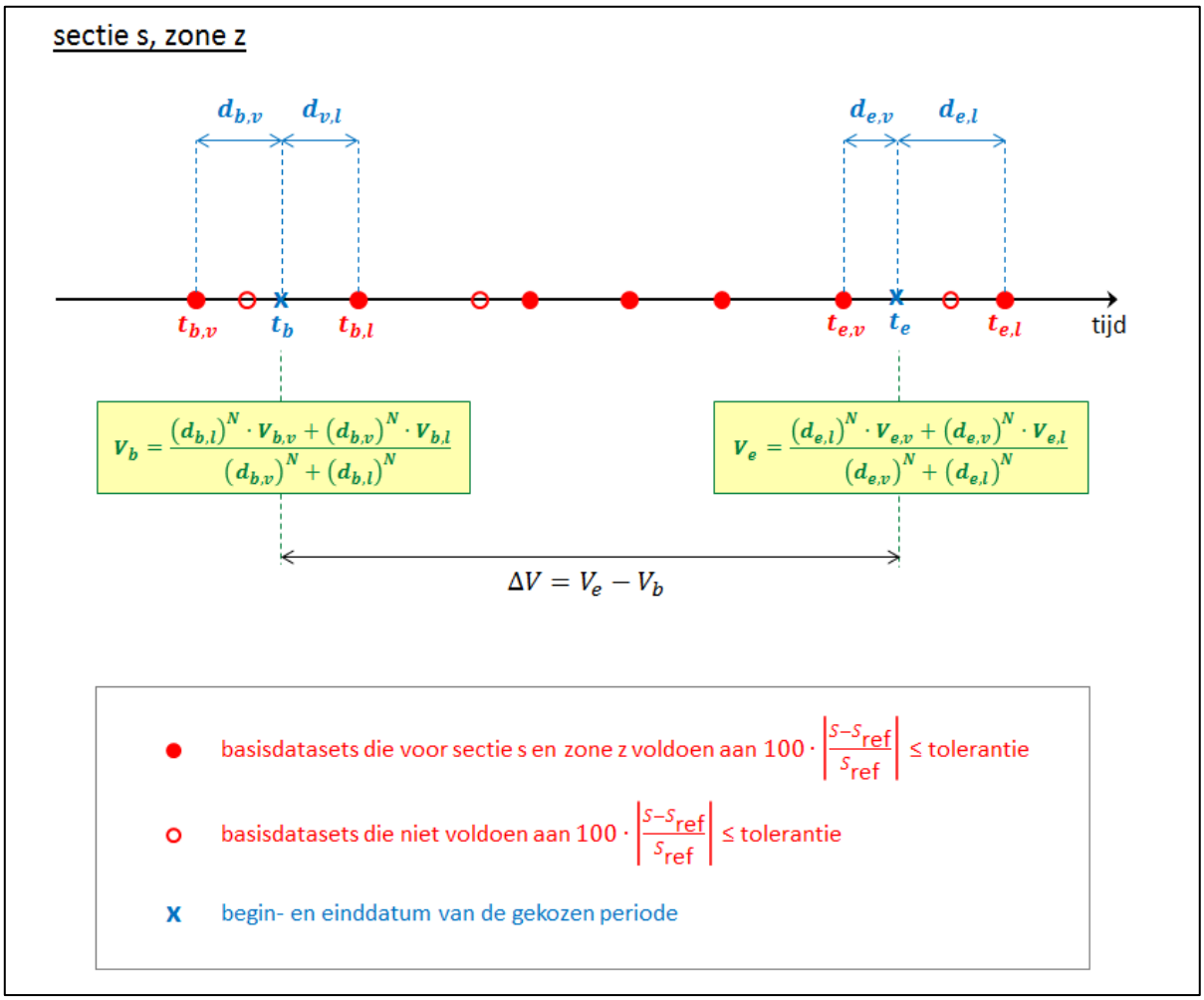

A.3.2.2 Inschatten van de onzekerheid op de sedimentvolumes

Hieronder wordt getracht een inschatting te maken voor de onzekerheid ΔV_b op het sedimentvolume V_b. Deze is enerzijds het gevolg van de onzekerheden op de grootheden waaruit V_b berekend wordt, maar anderzijds ook het gevolg van het feit dat V_b een geïnterpoleerde waarde is, en bijgevolg per definitie een benadering is.
Alle formules in deze subparagraaf gelden uiteraard ook voor de onzekerheid ΔV_e op V_e, de formules hiervoor kunnen bekomen worden door in onderstaande uitdrukkingen de index b te vervangen door e.

De fout ΔV_b op het geïnterpoleerd volume V_b bestaat uit 3 bijdragen:

$$(\Delta V_b)^2 = (\Delta V_{b,\,onz})^2 + (\Delta V_{b,\,int})^2 + (\Delta V_{b,\,int+onz})^2$$

Hierbij geldt:

1) $\Delta V_{b,\,onz}$ is de fout op het volume V_b t.g.v. onzekerheden $\Delta V_{b,v}$ en $\Delta V_{b,l}$ op de volumes $V_{b,v}$ en $V_{b,l}$ en de onzekerheden $\Delta d_{b,v}$ en $\Delta d_{b,l}$ op de tijdsintervallen $d_{b,v}$ en $d_{b,l}$ die doorgerekend worden in de interpolatieformule die V_b berekent uit $V_{b,v}$, $V_{b,l}$, $d_{b,v}$ en $d_{b,l}$.

   $\Delta V_{b,\,onz}$ wordt berekend door de gebruikelijke formule voor foutpropagatie toe te passen op de interpolatieformule. Dus toepassen van

$$\left(\Delta V_{b,onz}\right)^2 = \left(\frac{\partial V_b}{\partial V_{b,v}} \cdot \Delta V_{b,v}\right)^2 + \left(\frac{\partial V_b}{\partial V_{b,l}} \cdot \Delta V_{b,l}\right)^2 + \left(\frac{\partial V_b}{\partial d_{b,v}} \cdot \Delta d_{b,v}\right)^2 + \left(\frac{\partial V_b}{\partial d_{b,l}} \cdot \Delta d_{b,l}\right)^2$$

   op

$$V_b = \frac{\left(d_{b,l}\right)^N \cdot V_{b,v} + \left(d_{b,v}\right)^N \cdot V_{b,l}}{\left(d_{b,v}\right)^N + \left(d_{b,l}\right)^N}$$

   geeft een uitdrukking voor $\Delta V_{b,\,onz}$:

$$\left(\Delta V_{b,onz}\right)^2 = N^2 \; \frac{\left(d_{b,v} d_{b,l}\right)^{2N} \left(V_{b,v} - V_{b,l}\right)^2}{\left({d_{b,v}}^N + {d_{b,l}}^N\right)^4} \cdot \left[\left(\frac{\Delta d_{b,v}}{d_{b,v}}\right)^2 + \left(\frac{\Delta d_{b,l}}{d_{b,l}}\right)^2\right]$$

$$+ \quad \frac{\left(d_{b,v} d_{b,l}\right)^{2N}}{\left({d_{b,v}}^N + {d_{b,l}}^N\right)^2} \cdot \left[\left(\frac{\Delta V_{b,v}}{{d_{b,v}}^N}\right)^2 + \left(\frac{\Delta V_{b,l}}{{d_{b,l}}^N}\right)^2\right] .$$

2) $\Delta V_{b,\,int}$ is de fout op het volume V_b t.g.v. het interpolatieproces. Immers, zelfs indien de volumes $V_{b,v}$ en $V_{b,l}$ en de tijdsintervallen $d_{b,v}$ en $d_{b,l}$ exact gekend zouden zijn (en de onzekerheden $\Delta V_{b,v}$, $\Delta V_{b,l}$, $\Delta d_{b,v}$ en $\Delta d_{b,l}$ dus nul zouden zijn) zou er nog een onzekerheid bestaan op het volgens de interpolatieformule berekende volume V_b, daar de tijdsevolutie van het volume tussen tijdstippen $t_{b,v}$ en $t_{b,l}$ niet exact verloopt zoals voorgesteld door de interpolatieformule. De interpolatie is dus slechts een benadering.

   Hieronder wordt een model voorgesteld dat deze interpolatiefout $\Delta V_{b,\,int}$ tracht in te schatten. Dit model is opgebouwd rond volgende veronderstellingen:

   a) Bij $t_b = t_{b,v}$ ($t_b = t_{b,l}$) is het volume exact gekend (afgezien van onzekerheden op het volume van de basisdataset $\Delta V_{b,v}$ ($\Delta V_{b,l}$), die we hier buiten beschouwing laten omdat we trachten de onzekerheid in te schatten die louter het gevolg is van het interpolatieproces) en gelijk aan $\Delta V_{b,v}$ ($V_{b,l}$), en dus moet gelden:

$$\Delta V_{b,\,int}\left(t_b = t_{b,v}\right) = 0$$
$$\Delta V_{b,\,int}\left(t_b = t_{b,l}\right) = 0$$

      of equivalent daarmee en gebruik makend van de tijdsintervallen d_i en d_j als variabelen:

$$\Delta V_{b,\,int}\left(d_{b,v} = 0\right) = 0$$
$$\Delta V_{b,\,int}\left(d_{b,l} = 0\right) = 0$$

b) De onzekerheid op het volume moet groter worden naarmate tijdstip t_b verder verwijderd is van de tijdstippen $t_{b,v}$ en $t_{b,l}$. Bijgevolg moet $\Delta V_{b,\,\text{int}}$ van waarde nul bij $t_b = t_{b,v}$ stijgen tot een maximale waarde $\Delta V_{b,\,\text{int, MAX}}$ bij $t_b = (t_{b,v}+t_{b,l})/2$, om vervolgens terug te dalen tot waarde nul bij $t_b = t_{b,l}$.

Dus:

$$\Delta V_{b,\,\text{int}}\left(t_b = \frac{t_{b,v} + t_{b,l}}{2}\right) = \Delta V_{b,\,\text{int, MAX}}$$

of equivalent daarmee en gebruik makend van de tijdsintervallen $d_{b,v}$ en $d_{b,l}$ als variabelen:

$$\Delta V_{b,\,\text{int}}\left(d_{b,v} = d_{b,l}\right) = \Delta V_{b,\,\text{int, MAX}}$$

Bovenstaande twee veronderstellingen omtrent $\Delta V_{b,\,\text{int}}$ kunnen wiskundig geïmplementeerd worden door $\Delta V_{b,\,\text{int}}$ als volgt in een formule te gieten:

$$\Delta V_{b,\,\text{int}}\left(d_{b,v}\,, d_{b,l}\right) = \Delta V_{b,\,\text{int, MAX}} \cdot \frac{f\left(\frac{\left|d_{b,v} - d_{b,l}\right|}{2}\right) - f\left(\frac{d_{b,v} + d_{b,l}}{2}\right)}{f(0) \qquad - f\left(\frac{d_{b,v} + d_{b,l}}{2}\right)}$$

Hierbij stelt f een willekeurige functie voor, met als enige beperking dat f overal gedefinieerd en strikt monotoon moet zijn op het interval $\left[0, (d_{b,v} + d_{b,l})/2\right]$.

c) We veronderstellen verder dat de interpolatiefout $\Delta V_{b,\,\text{int}}$ toeneemt met het verschil $\left|V_{b,v} - V_{b,l}\right|$. Immers, des te groter de verandering in volume is tussen tijdstippen $t_{b,v}$ en $t_{v,l}$, des te groter is ook de onzekerheid op het via de interpolatie geschatte volume V_b op een tussenliggend tijdstip t_b. Bovendien mag verwacht worden dat de interpolatiefout ook groter zal zijn bij grote gebieden en zal toenemen met S_{ref}.

We implementeren bovenstaande door volgende wiskundige vorm voor $\Delta V_{b,\,\text{int, MAX}}$ voor te stellen:

$$\Delta V_{b,\,\text{int, MAX}} = A\left|\frac{V_{b,v} - V_{b,l}}{2}\right|^S + B(S_{\text{ref}})^T$$

Hierbij zijn A, B, S en T door de gebruiker te kiezen parameters, S_{ref} is de referentie-oppervlakte van de sectie/zone-combinatie in kwestie..

De volledige uitdrukking voor $\Delta V_{b,\,\text{int}}$ is nu als volgt:

$$\Delta V_{b,\,\text{int}}(d_{b,v}\,, d_{v,l}\,, V_{b,v}\,, V_{v,l})$$
$$= \left[A\left|\frac{V_{b,v} - V_{b,l}}{2}\right|^S + B(S_{\text{ref}})^T\right] \cdot \frac{f\left(\frac{\left|d_{b,v} - d_{b,l}\right|}{2}\right) - f\left(\frac{d_{b,v} + d_{b,l}}{2}\right)}{f(0) \qquad - f\left(\frac{d_{b,v} + d_{b,l}}{2}\right)}$$

Veronderstellen we nu nog dat $f(x) \sim x^R$, waarbij R een parameter is, dan kan deze uitdrukking verder uitgewerkt worden tot:

$$\Delta V_{b,\,\text{int}}\left(d_{b,v}\,, d_{v,l}\,, V_{b,v}\,, V_{v,l}\right) = \left[A\left|\frac{V_{b,v} - V_{b,l}}{2}\right|^{S} + B(S_{\text{ref}})^{T}\right] \cdot \left[1 - \left|\frac{d_{b,v} - d_{b,l}}{d_{b,v} + d_{b,l}}\right|^{R}\right]$$

3) $\Delta V_{b,\,\text{int+onz}}$ is de fout op het volume V_b t.g.v. onzekerheden $\Delta V_{b,v}$, $\Delta V_{v,l}$, $\Delta d_{b,v}$ en $\Delta d_{b,l}$ die doorgerekend worden in de bovenstaande formule die de interpolatiefout inschat. In die zin is $\Delta V_{b,\,\text{int+onz}}$ een "fout op een fout" of "onzekerheid op een onzekerheid".

$\Delta V_{b,\,\text{int+onz}}$ wordt berekend door de gebruikelijke formule voor foutpropagatie toe te passen op de hierboven gegeven formule voor de interpolatiefout.

Dus toepassen van

$$\left(\Delta V_{b,\text{onz}}\right)^2 = \left(\frac{\partial V_b}{\partial V_{b,v}} \cdot \Delta V_{b,v}\right)^2 + \left(\frac{\partial V_b}{\partial V_{b,l}} \cdot \Delta V_{b,l}\right)^2 + \left(\frac{\partial V_b}{\partial \mathrm{d_{b,v}}} \cdot \Delta \mathrm{d_{b,v}}\right)^2 + \left(\frac{\partial V_b}{\partial \mathrm{d_{b,l}}} \cdot \Delta \mathrm{d_{b,l}}\right)^2$$

op

$$\Delta V_{b,\,\text{int}}\left(d_{b,v}\,, d_{v,l}\,, V_{b,v}\,, V_{v,l}\right) = \left[A\left|\frac{V_{b,v} - V_{b,l}}{2}\right|^{S} + B(S_{\text{ref}})^{T}\right] \cdot \left[1 - \left|\frac{d_{b,v} - d_{b,l}}{d_{b,v} + d_{b,l}}\right|^{R}\right]$$

geeft

$$\begin{aligned}\left(\Delta V_{b,\,\text{int+onz}}\right)^2 &= \left(\frac{AS}{2}\right)^2 \left[1 - \left|\frac{d_{b,v} - d_{b,l}}{d_{b,v} + d_{b,l}}\right|^{R}\right]^2 \left|\frac{V_{b,v} - V_{b,l}}{2}\right|^{2S-2} \cdot \left[\left(\Delta V_{b,v}\right)^2 + \left(\Delta V_{b,l}\right)^2\right] \\ &+ R^2 \left[A\left|\frac{V_{b,v} - V_{b,l}}{2}\right|^{S} + B(S_{\text{ref}})^{T}\right]^2 \left|\frac{d_{b,v} - d_{b,l}}{d_{b,v} + d_{b,l}}\right|^{2R-2} \frac{4\left(d_{b,v}\, d_{b,l}\right)^2}{\left(d_{b,v} + d_{b,l}\right)^4} \\ &\cdot \left[\left(\frac{\Delta d_{b,v}}{d_{b,v}}\right)^2 + \left(\frac{\Delta d_{b,l}}{d_{b,l}}\right)^2\right]\end{aligned}$$

A.3.2.3 Invullen stap 1 in de Excel rekentool

Figuur 43 toont een schermafdruk van stap 1 in de Excel rekentool. Alle rode getallen zijn parameters die in principe ingevuld dienen te worden. De verschillende parameters worden hieronder overlopen.

Figure 43 – Stap 1 in de Excel rekentool: invullen van start- en einddatum en de interpolatieparameters.

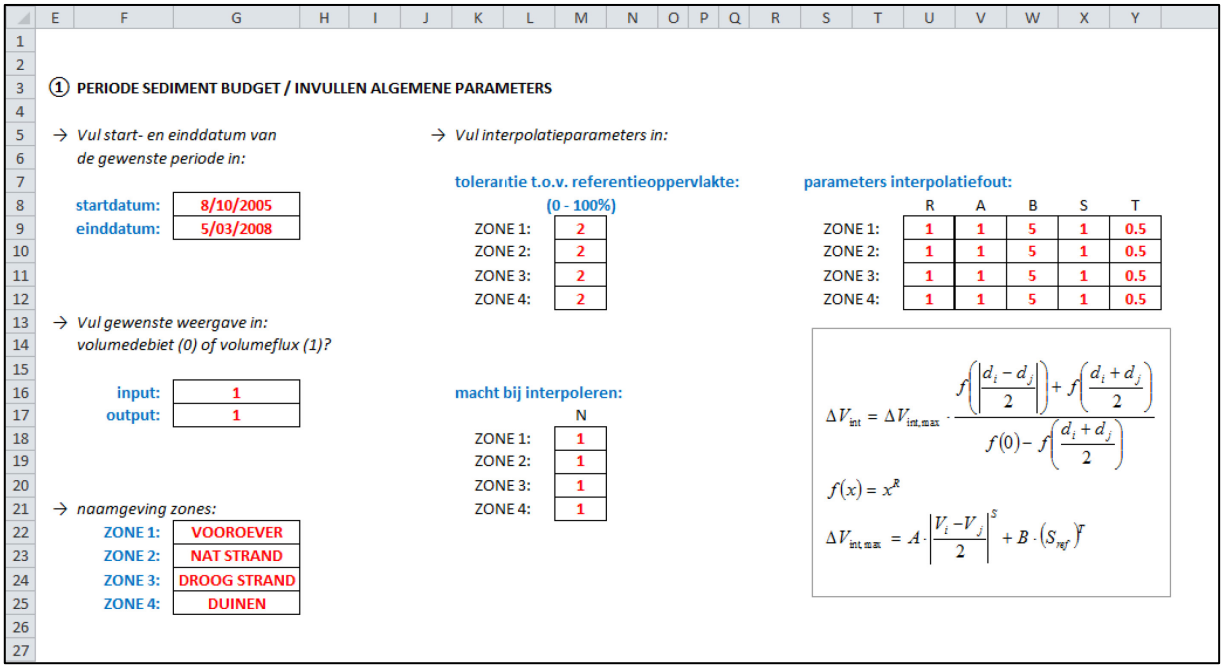

1) <u>Start- en einddatum (cellen G8-G9)</u>

   Hier dienen de start- en einddatum van de periode waarover men het sediment budget wenst uit te rekenen ingevuld te worden in het formaat dd/mm/jjjj.

2) <u>Gewenste weergave: volumedebiet of volumeflux (cellen G16-G17)</u>

   Voor zowel de in te geven als de te berekenen sedimentverplaatsingen over de celgrenzen kan de gebruiker ervoor kiezen om met volumedebieten (in m³/jaar) dan wel met volumefluxen (in m³/m/jaar) te werken. Indien de gebruiker wenst te werken met debieten, dient een 0 ingevuld te worden, en voor fluxen een 1. De afmetingen van de cellen, die nodig zijn voor de sedimentbalans indien men werkt met fluxen, zitten vervat in de Excel rekentool. Merk op dat het perfect mogelijk is om bij debieten op te geven bij de input, en fluxen te vragen als output.

3) <u>Naamgeving van de zones (cellen G22-G25)</u>

   Elk der vier zones kan een aparte naam toegekend worden. Het invullen van deze namen is echter geenszins nodig voor de goede werking van de rekentool. Deze naamgeving wordt enkel overgenomen in de tabbladen “berekeningen zone 1 (2, 3, 4)” en dient enkel als hulp bij het invoeren van de basisgegevens in deze tabbladen en te vermijden dat de basisgegevens van een bepaalde zone in het verkeerde tabblad terechtkomen.

4) <u>Interpolatieparameter: tolerantie t.o.v. referentieoppervlakte (cellen M9-M12)</u>

   Hier dient de maximale afwijking van de oppervlakte t.o.v. de referentieoppervlakte die de gebruiker wenst toe te laten ingevuld te worden. Indien een basisdataset met oppervlakte S in een bepaalde sectie en bepaalde zone niet voldoet aan

$$100 \cdot \left|\frac{S - S_{\text{ref}}}{S_{\text{ref}}}\right| \leq \text{tolerantie} ,$$

dan wordt deze basisdataset voor die sectie en zone genegeerd bij het berekenen van sedimentvolumes. S_{ref} is hierbij de referentieoppervlakte voor die sectie en zone (zie ook 0).
Merk op dat de rekentool erin voorziet om per zone een aparte tolerantie op te geven. Zo kan het zinvol zijn om voor bijvoorbeeld de meest zeewaarts gelegen zones een hogere tolerantie in te stellen: hier kunnen immers wel eens grotere verschillen optreden aangezien bepaalde datasets verder in zee reiken dan andere en een hogere tolerantie verhindert dat te veel datasets worden uitgesloten. Uiteraard dient men hiermee voorzichtig om te springen: bij een hoge tolerantie laat men immers de mogelijkheid toe dat sedimentvolumes van gebieden met ongelijke oppervlaktes worden vergeleken. Voor de meest landinwaarts gelegen zone geldt overigens dezelfde opmerking. Voor de tussenliggende zones is de bedekking door de meeste datasets nagenoeg volledig, een tolerantie van 0,3-0,5 % volstaat doorgaans om kleine afwijkingen geïntroduceerd door de ArcGIS calculaties te negeren.

5) Interpolatieparameter: macht bij het interpoleren N (cellen M18-M21)

Het gaat hier om de exponent N in de interpolatieformules (zie opnieuw 0)

$$V(t_b) \equiv V_b = \frac{\left(d_{b,l}\right)^N \cdot V_{b,v} + \left(d_{b,v}\right)^N \cdot V_{b,l}}{\left(d_{b,v}\right)^N + \left(d_{b,l}\right)^N}$$

$$V(t_e) \equiv V_e = \frac{\left(d_{e,l}\right)^N \cdot V_{e,v} + \left(d_{e,v}\right)^N \cdot V_{e,l}}{\left(d_{e,v}\right)^N + \left(d_{e,l}\right)^N} .$$

Ook deze parameter kan voor elke zone apart ingesteld worden.

Figuur 44 toont de interpolatiekromme voor enkele waarden van N. Voor N = 1 verkrijgen we een lineaire interpolatie, terwijl N > 1 (N < 1) ervoor zorgt dat meer gewicht wordt toegekend aan het volume van de dichtstbijzijnde (verst verwijderde) datum.

Op zich heeft de mogelijkheid om de parameter N te wijzigen weinig zin, bij ontbreken van enige a priori kennis omtrent de tijdsevolutie van sedimentvolumes kiest men best voor een lineaire interpolatie (N = 1). Enkel indien men aanwijzingen heeft dat sedimentvolumes tussen $t_{b,v}$ en $t_{b,l}$ volgens een bepaald verloop wijzigen kan men dit verloop trachten te benaderen door N aan te passen.

Figure 44 – Verloop interpolatiekromme voor enkele waarden van de parameter $\boldsymbol{N}$.

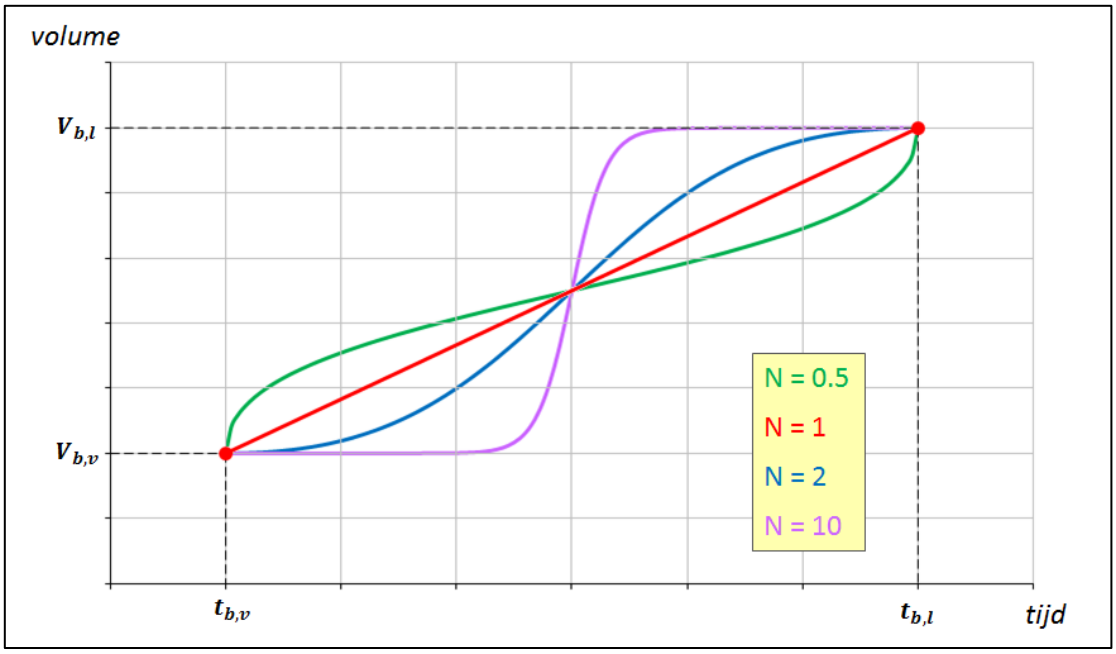

6) Parameters m.b.t. de interpolatiefout (cellen U9-X12)

Hier kan men verschillende waarden invullen voor de parameters R, A, S, B en T, die alle een invloed hebben op de manier waarop de interpolatiefout wordt ingeschat. Als geheugensteuntje staan de gebruikte formules voor het inschatten van de interpolatiefout in een kader bijgevoegd. Deze formule is (zie 0):

$$\Delta V_{b,\,\text{int}}\left(d_{b,v}\,,d_{v,l}\,,V_{b,v}\,,V_{v,l}\right)=\left[A\left|\frac{V_{b,v}-V_{b,l}}{2}\right|^{S}+B(S_{\text{ref}})^{T}\right]\cdot\left[1-\left|\frac{d_{b,v}-d_{b,l}}{d_{b,v}+d_{b,l}}\right|^{R}\right].$$

Opnieuw kunnen de parameters voor elke zone apart ingevuld worden. In de volgende subparagraaf worden enkele richtlijnen en nuttige wenken gegeven bij het kiezen van deze parameters.

Merk op dat in stap 1 geen macro's gebruikt worden, de interpolatie op basis van de ingegeven start- en einddatum en parameters gebeurt dus instantaan en de interpolatieberekening wordt dus onmiddellijk aangepast wanneer bijvoorbeeld een parameter wordt aangepast.

A.3.2.4 Het kiezen van de parameters m.b.t. de interpolatiefout: enkele richtlijnen en nuttige wenken

Figuur 45 toont in een aantal deelfiguurtjes de invloed van de verschillende parameters: in elk van de deelfiguurtjes wordt telkens slechts 1 parameter gevarieerd. De rode lijn toont telkens het verloop van V_b tussen $t_{b,v}$ en $t_{b,l}$ aan zoals ingeschat volgens een lineaire interpolatie (N = 1). We overlopen hieronder de verschillende parameters en trachten enkele richtlijnen te geven voor het zinvol inschatten van deze parameters. Merk op dat dit inschatten van de parameters geen exacte wetenschap is en deels intuïtief, deels volgens gezond verstand gebeurt. Verder is het nuttig te weten dat de interpolatiefout $\Delta V_{b,\,\text{int}}$ trachten in te schatten als zijnde de standaarddeviatie. Dit betekent dat het werkelijke sedimentvolume tussen de tijdstippen $t_{b,v}$ en $t_{b,l}$ ruwweg een 2/3 waarschijnlijkheid heeft om begrepen te zijn in het interval $[\,V_b-\Delta V_{b,\text{int}}\;;\;V_b+\Delta V_{b,\,\text{int}}\,]$ (uitgaande van een normale verdeling en afgezien van de onzekerheden die nog kunnen bestaan op de basisdata).

- Parameter A (deelgrafiek 1):

In deelgrafiek 1 zijn de parameters B = 0, S = 1 en R = 1 gekozen om zo goed mogelijk de invloed van A aan te tonen. R = 1 betekent dat de interpolatiefout begint bij waarde nul bij $t_b = t_{b,v}$, daarna lineair toeneemt en een maximale waarde bereikt bij $(t_{b,v} + t_{b,l})/2$, om vervolgens lineair af te nemen om opnieuw waarde nul te bereiken bij $t_b = t_{b,l}$.
Voor A = 1 zien we dat de onzekerheidsband rond V_b net niet boven de volumes $V_{b,v}$ en $V_{b,l}$ uitkomt. Hoewel het in theorie zeker niet onmogelijk is dat V_b onder $V_{b,v}$ daalt of boven $V_{b,l}$ uitstijgt, lijkt –rekening houdend met de hierboven vermelde interpretatie van 2/3 waarschijnlijkheid– toch te behoudsgezind om A > 1 te nemen. Op basis van deelgrafiek 1 lijkt 0,5 < A < 1 een goede keuze. Merk echter op dat de interpolatiefout eveneens afhangt van de overige parameters, en de exacte vorm van de onzekerheidsband is dan ook het gevolg van het samenspel tussen alle parameters (zie verder).

- Parameter S (deelgrafiek 2):
  De parameter S is de exponent van de volumeverandering $|V_{b,v} - V_{b,l}|$ in de eerste term van de eerste factor de formule voor $\Delta V_{b,\,\text{int}}$ (zie hierboven). Deelgrafiek 2 in Figuur 45 toont het verloop van de interpolatiefout voor enkele waarden van S. Merk op dat de bolle vorm van de onzekerheidsbanden in deelgrafiek 2 het gevolg zijn van de keuze voor R = 2, waar in deelgrafiek 1 nog R = 1 werd genomen.
  De meest logische keuze lijkt S = 1 te nemen, zodat de interpolatiefout recht evenredig wordt met het volumeverschil. Om te vermijden dat de interpolatiefout de pan uit swingt bij grote volumeverschillen $|V_{b,v} - V_{b,l}|$ wordt het ten stelligste afgeraden van S > 1 te nemen. Eventueel kan men S < 1 nemen, om zo voor grote volumeverschillen $|V_{b,v} - V_{b,l}|$ een enigszins verminderde interpolatiefout af te dwingen: het is immers niet onlogisch te veronderstellen dat grote volumewijzigingen $|V_{b,v} - V_{b,l}|$ stabieler en minder grillig in de tijd verlopen dan een kleine volumewijziging over hetzelfde tijdsinterval. De vraag blijft dan natuurlijk welke waarde precies voor S gekozen moet worden. In elk geval dient S dan in combinatie met A gekozen te worden om zo het gewenste verloop voor de interpolatiefout i.f.v. $|V_{b,v} - V_{b,l}|$ te bekomen. Bij ontbreken van verdere kennis hieromtrent blijft het evenwel aangeraden van S = 1 en 0,5 < A < 1 te nemen.

- Parameter B (deelgrafiek 3):
  De parameter B beïnvloedt de interpolatiefout via de term $B(S_{\text{ref}})^T$ in de eerste factor van de formule voor $\Delta V_{b,\,\text{int}}$. Deze term is toegevoegd om te vermijden dat bij $|V_{b,v} - V_{b,l}|$ = 0 de interpolatiefout zou terugvallen naar nul. Het feit dat er geen netto volumeverandering is tussen tijdstip $t_{b,v}$ en $t_{b,l}$ wil immers niet zeggen dat het volume op tussenliggende tijdstippen niet is afgeweken van de waarde $V_{b,v} = V_{b,l}$.
  Deelgrafiek 3 toont enkele onzekerheidsbanden voor verschillende waarden van B, waarbij T = 1 en $V_{b,v} = V_{b,l}$ is genomen. Bij T = 1 kan de volgende interpretatie aan B gegeven worden: B is een maat voor de fluctuaties op de gemiddelde hoogteligging van een gebied. Immers:

$$\Delta V_{b,\,\text{int}} \sim B \cdot S_{\text{ref}}$$

$$\Rightarrow\ B \sim \frac{\Delta V_{b,\,\text{int}}}{S_{\text{ref}}} \equiv \Delta h\ .$$

  Op basis van deze interpretatie kan de waarde voor B ingeschat worden in de grootteorde van ~cm. Een goede keuze lijkt dus van 0,005 < B < 0,05 te nemen.

- Parameter T (deelgrafiek 4):
  De parameter T treedt op in de term $B(S_{\text{ref}})^T$ in de eerste factor van de formule voor $\Delta V_{b,\,\text{int}}$. Voor de parameter T gelden dezelfde opmerkingen als voor parameter S: de keuze T = 1 is verdedigbaar, T > 1 is absoluut te vermijden. Meer nog dan bij parameter S echter geldt hier dat T < 1 aangewezen is, zodat het verloop van de interpolatiefout i.f.v. de

oppervlakte voor grote gebieden afgevlakt wordt. Immers, waar het voor kleine gebieden nog aannemelijk lijkt dat de gemiddelde hoogte fluctueert, zijn grote gebieden geneigd stabieler te zijn. Indien we de parallel trekken naar de centrale limietstelling uit de statistiek betekent dit dat T = 0,5 gekozen moet worden. B heeft dan niet meer de betekenis van de verwachte fluctuatie op de gemiddelde hoogteligging van een gebied, maar wel van verwachte fluctuatie in hoogteligging van een gebiedje van 1 m². Indien men T = 0,5 kiest dient men B dus groter te nemen dan hierboven aangegeven: 0,05 < B < 0,5 lijkt daarbij een verdedigbare keuze.
Merk op dat de term $B(S_{\text{ref}})^T$ in principe zou uitgebreid moeten worden met een afhankelijkheid van $t_{b,l}-t_{b,v}$, de lengte van het tijdsinterval waarover geïnterpoleerd wordt. Men kan immers verwachten dat over een langere periode grotere fluctuaties in hoogteligging kunnen optreden dan in kortere periodes. Ook hier zou dan moeten gelden dat deze afhankelijkheid minder dan lineair is. Deze afhankelijkheid is in de rekentool niet meegenomen, bij de keuze voor T = 0,5 houdt interpreteert ment B best als de gemiddelde fluctuatie in hoogteligging van 1 m² gebied gedurende een periode van 0,5 à 1 jaar. Dit is immers ruwweg de periode tussen de opnamedatums van twee opeenvolgende datasets.

- Parameter R (deelgrafiek 5):
  Deze parameter treedt op in de tweede factor van de formule voor $\Delta V_{b,\text{ int}}$ en bepaalt de manier waarop de interpolatiefout afhangt van de tijd. In deelgrafiek 5 zijn enkele onzekerheidsbanden weergegeven voor verschillende waarden van R. Voor R = 1 bestaan de grenzen van deze banden uit rechte lijnen, voor R < 1 vertoont de interpolatiefout een piek naar het midden toe, voor R > 1 worden de grenzen afgevlakt naar het midden toe. Bij zeer grote waarden voor R vertoont de onzekerheidsband overal quasi dezelfde breedte.
  Het lijkt aannemelijk van te kiezen voor enige afvlakking van de onzekerheidsbanden naar het midden toe, dus R > 1, zonder daarbij een al te grote R te nemen. Indien men de onzekerheidsbanden beschouwd als het gevolg van bovenop een algemene trend gesuperponeerde fluctuaties, zullen toevallige volumestijgingen afgewisseld worden met volumedalingen (anders gezegd: indien de fluctuaties willekeurig zijn, is het zeer onwaarschijnlijk dat vele toevallige volumestijgingen mekaar opvolgen zonder daarbij onderbroken te worden door volumedalingen). Hierbij dient wel opgemerkt te worden dat de mogelijkheid bestaat dat deze fluctuaties niet geheel toevallig zijn, maar al dan niet deels gedreven door een of andere onderliggende (bijvoorbeeld seizoenale) trend.
  Verder kan het nuttig zijn om te weten dat de krommen die de onzekerheidsbanden afbakenen bij twee parametersets (R, A, B, S, T) en (R', A', B', S', T') aan mekaar raken in de punten $t = t_{b,v}$ en $t = t_{b,l}$ indien geldt:

$$\begin{aligned} S &= S' \\ T &= T' \\ R \cdot A &= R' \cdot A' \\ R \cdot B &= R' \cdot B' \quad . \end{aligned}$$

  Een te rechtvaardigen keuze is dan ook R = 2. Merk op dat de eerder bepaalde begrenzingen 0,5 < A < 1 bepaald werden bij R = 1. Bij de keuze voor R = 2 en rekening houdend met de gelijkheden hierboven wijzigen deze grenzen dan ook in 0,25 < A < 0,5. Voor parameter B daarentegen behoudt men best de eerder aanbevolen begrenzingen. Voor B waren deze begrenzingen immers gebaseerd op een fysische interpretatie van de parameter B, voor A waren de begrenzingen bepaald door de vorm van de onzekerheidsbanden.

- Het verschil $V_{b,l}-V_{b,v}$ (deelgrafiek 6):
  In de laatste deelgrafiek worden louter ter info enkele onzekerheidsbanden getoond voor een vaste parameterset maar voor wijzigend volume $V_{b,l}$.

Figure 45 – Invloed op de interpolatiefout van de verschillende interpolatieparameters.

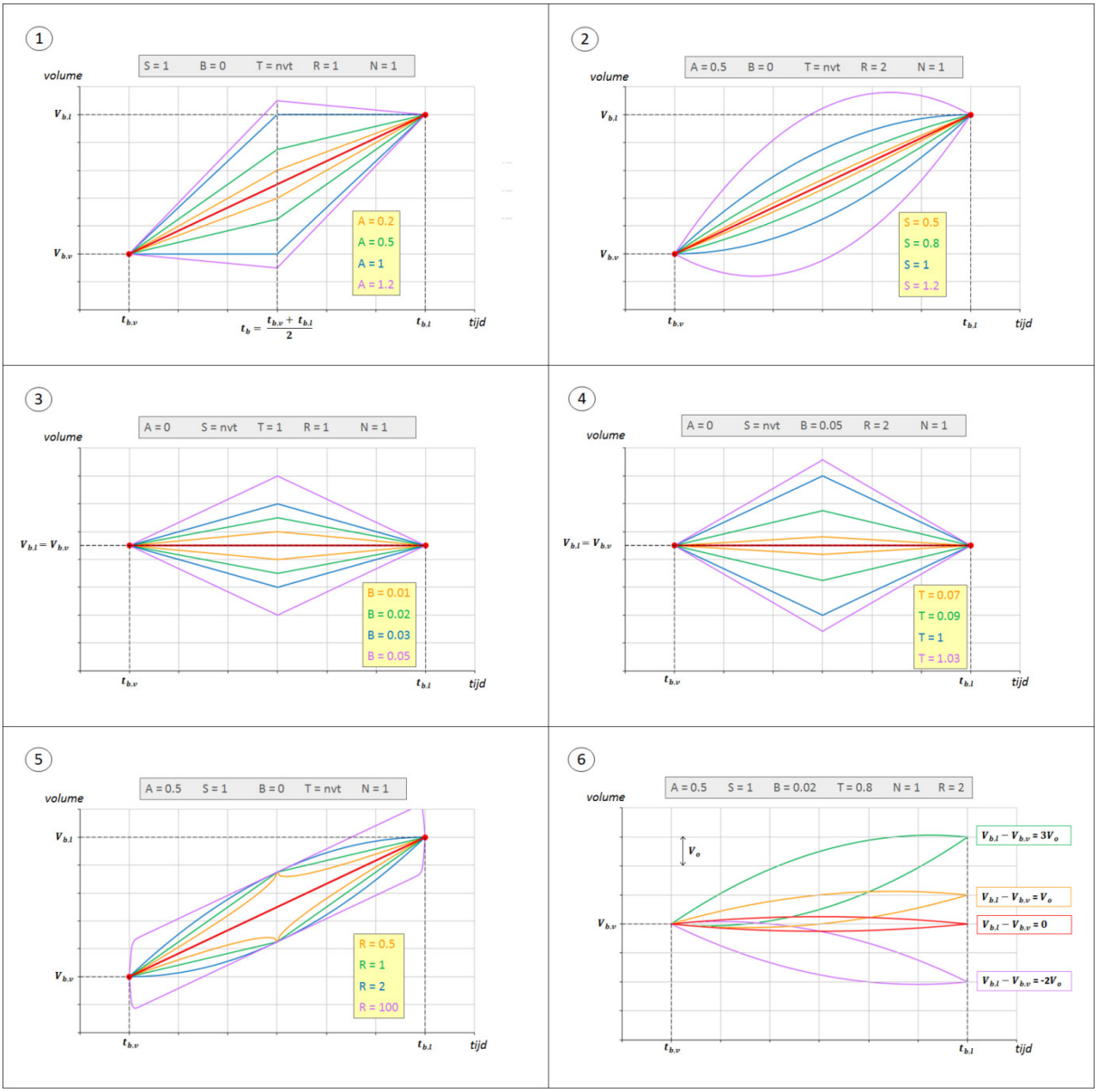

Tot slot vatten we de aanbevolen waarden voor de verschillende parameters nog even samen:

$$R = 2$$
$$0{,}25 < A < 0{,}5$$
$$S = 1$$
$$0{,}25 < B < 0{,}5$$
$$T = 1.$$

Het staat de gebruiker echter vrij van andere waarden in te vullen indien dit nodig geacht wordt. Merk ook op dat de hier voorgestelde formulering voor de interpolatiefout $\Delta V_{b,\,\mathrm{int}}$ slechts een model is, gebaseerd op enkele –weliswaar voor de hand liggende– veronderstellingen. Uiteraard zouden nog andere modellen uitgedacht kunnen worden.

A.3.3 Stap 2: indeling cellen Belgische kust

De basisdata in de Excel rekentool bestaan uit tijdreeksen van sedimentvolumes voor verschillende deelgebieden langs de Belgische kust. Deze deelgebieden ontstaan door de kust te verdelen in 4 (min of meer kustparallelle) zones en 277 (min of meer) kustdwarse secties. Aldus ontstaat een raster van 4 x 277 cellen. De tijdreeks van sedimentvolumes voor elk van deze cellen worden berekend door toepassen van enkele ArcGIS- en MATLAB-routines op de beschikbare strandopmetingen en vooroeverlodingen. In principe kan men in deze routines de grenzen van de zones en secties vrij kiezen, maar de oorspronkelijke bedoeling is om de 4 zones te laten samenvallen met de indeling vooroever – nat strand – droog strand – duinen en de indeling in secties te laten overeenstemmen met de gekende indeling in kustsecties. In de rekentool kunnen in elk geval de gegevens van maximaal 4 zones en maximaal 277 secties verwerkt worden. Merk op dat de Belgische kust loopt vanaf kustsectie 2 tot halverwege kustsectie 255. Verschillende strandopmetingen en echolodingen overschrijden echter de Franse en/of Nederlandse grens, en kunnen lopen van kustsectie 1 tot kustsectie 277, wat meteen de reden is waarom de Excel rekentool de mogelijkheid biedt om tot 277 secties mee te nemen.
In stap 2 kunnen de verschillende zones en/of secties samengevoegd worden om zo een groffer raster te vormen. Bedoeling is om zo grotere cellen te bekomen die samenvallen met bijvoorbeeld morfologische eenheden of gebieden met eenduidige morfologische trend.
Figuur 46 toont een schermafdruk van stap 2 in de Excel rekentool. Enkel in de rode kaders dienen gegevens ingevoerd te worden, voor de goede werking van de rekentool wordt in de overige cellen best niets gewijzigd. In de rode kader in kolom AK dient men onder elkaar en opeenvolgend telkens de eerste sectie in te vullen van de verschillende opeenvolgende cellen van de gewenste indeling. In de kolom ernaast zal dan ter info telkens de laatste sectie van de opeenvolgende cellen verschijnen. Aangezien de cellen op mekaar aansluiten is het groene getal telkens één minder dan het rode getal in de rij eronder (afgezien van de laatste cel). Let er ook op dat de laatste sectie van de laatste cel apart ingevuld dient te worden (AP12). In de rode kader in kolom AK kunnen tot 277 afzonderlijke getallen ingevuld worden, wat inhoudt dat indien gewenst de gebruiker kan kiezen voor de fijnst mogelijke indeling, nl. de indeling volgens de afzonderlijke kustsecties. Merk op dat de gebruiker de eerste cel niet hoeft te starten met kustsectie 1: in het voorbeeld van Figuur 46 wordt gestart met kustsectie 28. Dit betekent wel dat met kustsecties 1 t.e.m. 27 geen rekening wordt gehouden. Ook wat betreft de laatste kustsectie van de laatste cel is de keuze volledig vrij. Men dient er wel op te letten dat de getallen ingevuld in de rode kader van kolom AK een strikt stijgende rij vormen, niet-ingevulde Excel-cellen worden best leeg gelaten.
Op een volledig analoge manier kan men in de rode kader van kolom AV verschillende zones samenvoegen. Ook hier moet men niet starten met zone 1 of eindigen met zone 4.
Merk ook op dat bij de indeling in cellen elke cel een koppel indices (i,j) meekrijgt, deze indices zullen in de volgende stappen nog terugkeren. De aanduiding van de indices i en j kunnen teruggevonden worden in de respectievelijke kolommen AJ en AU. Zo is in het voorbeeld van Figuur 46 cel (4,2) het gebied dat de doorsnede is van enerzijds de secties 80 t.e.m. 84 en anderzijds de zones 3 t.e.m. 4.
Nadat de indeling in cellen is uitgevoerd door de rode kaders van de nodige input te voorzien zal de Excel rekentool voor elke cel de sedimentvolumes berekenen voor de in stap 1 ingegeven start- en einddatum, dit door de sedimentvolumes van de afzonderlijke kustsecties en zones op de gepaste manier op te tellen. Ook de onzekerheid op deze sedimentvolumes wordt voor elke cel berekend, en dit volgens de gebruikelijke regel voor foutpropagatie bij sommering:

$$A = B + C \Rightarrow \Delta A = \sqrt{(\Delta B)^2 + (\Delta C)^2} \ .$$

Figure 46 – Stap 2 in de Excel rekentool: indelen van de Belgische kust in verschillende cellen.

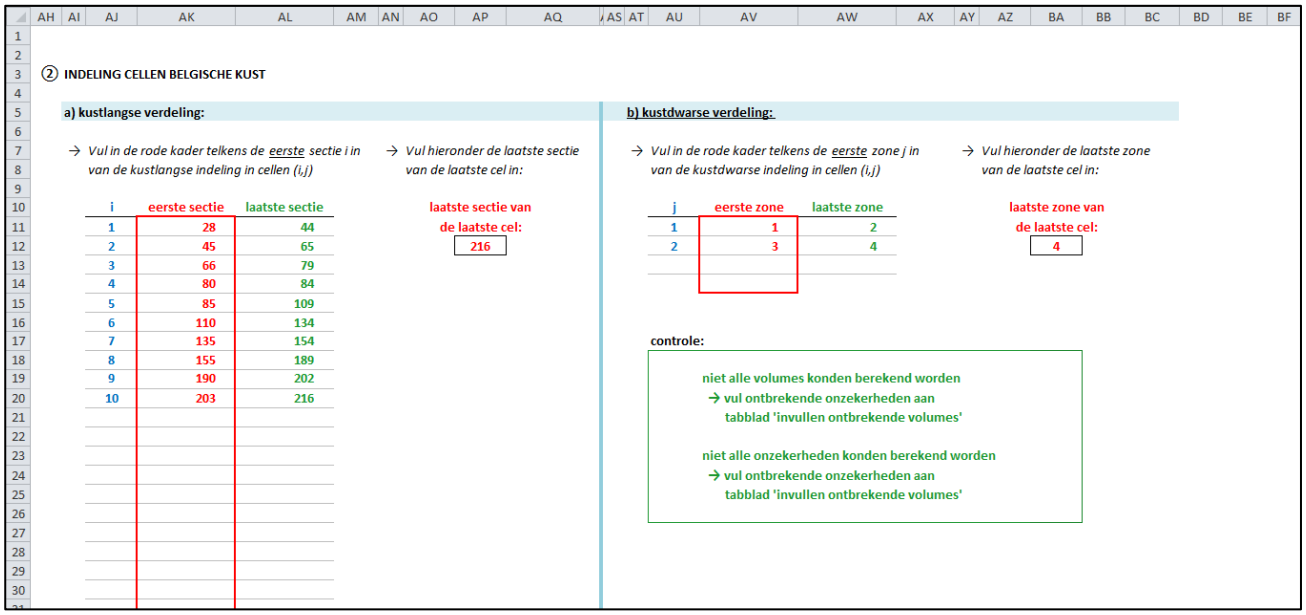

In de groene kader (AU18-BA26) wordt vervolgens aangegeven of de verschillende sedimentvolumes en/of hun onzekerheden berekend konden worden. Indien dit het geval is, kan overgegaan worden naar stap 3. Indien bepaalde sedimentvolumes of onzekerheden echter niet berekend konden worden (omdat de basisdatasets onvolledig zijn voor een bepaalde sectie en zone, al dan niet veroorzaakt door het instellen van een te lage tolerantie in stap 1), moeten deze volumes of onzekerheden manueel ingevuld worden in het daarvoor voorziene tabblad "INVULLEN ONTBREKENDE VOLUMES".
Figuur 47 toont een schermafdruk van dit tabblad. De opeenvolgende kolommen geven voor elke zone de volumes en hun onzekerheden voor zowel start- als einddatum, de rijen corresponderen met de opeenvolgende kustsecties. We overlopen hieronder in enkele puntjes de werking van dit tabblad.

- Rijen 1 t.e.m. 3 informeren of de betreffende kolom nog ontbrekende volumes of onzekerheden bevat (rode tekst indien wel, groene tekst indien niet). Rij 4 geeft dan waar relevant een opsomming van de sectienummers waar de volumes of onzekerheden in de betreffende kolom ontbreken.
- De Excel cellen die corresponderen met een bepaalde zone en bepaalde sectie waar het volume of de onzekerheid niet berekend kon worden hebben een oranje kleur, zodat ze visueel gemakkelijk te herkennen zijn. Bij het invullen van een getal in de cel verdwijnt de oranje kleur, het ingevulde getal krijgt een rode kleur. De lijst in rij 4 wordt instantaan bijgewerkt. Let erop dat volumes dienen ingevuld te worden in m^3 boven TAW.
- Ook indien in een bepaalde zone en sectie het volume berekend kon worden, kan de gebruiker ervoor kiezen in de corresponderende Excel cel een getal in te vullen. Het berekende volume wordt dan verworpen en in de volgende stappen zal de rekentool het hier door de gebruiker ingevulde getal nemen. Wanneer een volume wordt ingevuld niettegenstaande het door de rekentool berekend kon worden, krijgt het ingevulde getal een zwarte kleur.

Wanneer geen volumes of onzekerheden meer ontbreken kan de gebruiker terugkeren naar het tabblad "SEDIMENTBUDGET" en doorgaan naar stap 3.
Merk op dat ook in stap 2 (nog) geen macro's gebruikt worden: bij het veranderen van een waarde in een Excel cel worden de berekeningen dus instantaan uitgevoerd.

Figure 47 – - Het tabblad “INVULLEN ONTBREKENDE VOLUMES”.

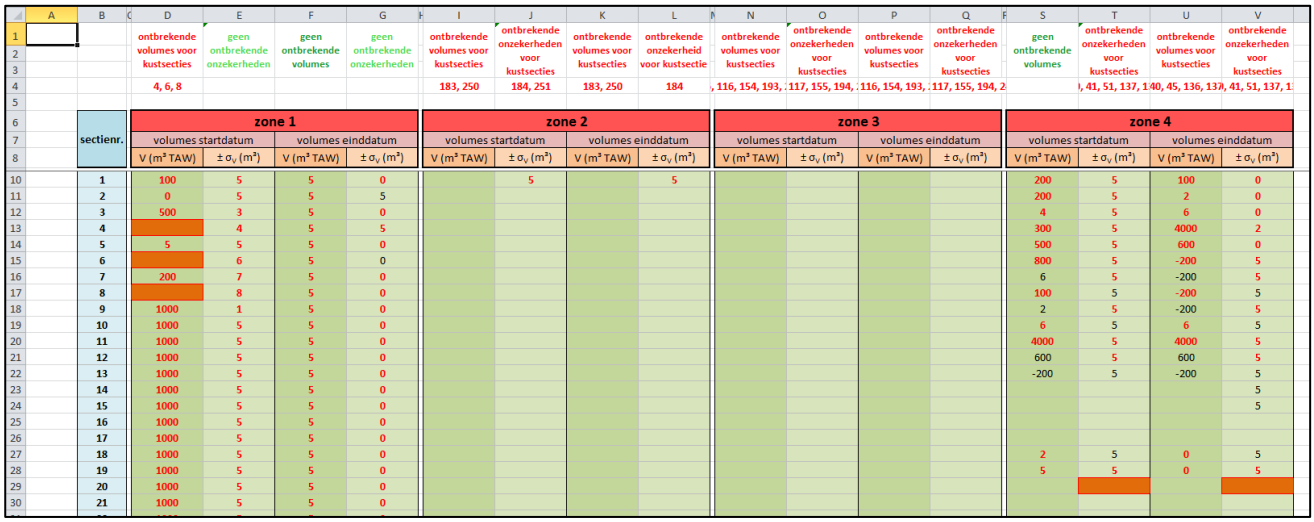

		zone 1				zone 2				zone 3				zone 4			
	sectienr.	volumes startdatum		volumes einddatum		volumes startdatum		volumes einddatum		volumes startdatum		volumes einddatum		volumes startdatum		volumes einddatum	
		V (m³ TAW)	± σ_v (m³)	V (m³ TAW)	± σ_v (m³)	V (m³ TAW)	± σ_v (m³)	V (m³ TAW)	± σ_v (m³)	V (m³ TAW)	± σ_v (m³)	V (m³ TAW)	± σ_v (m³)	V (m³ TAW)	± σ_v (m³)	V (m³ TAW)	± σ_v (m³)
10	1	100	5	5	0		5		5					200	5	100	0
11	2	0	5	5	5									200	5	2	0
12	3	500	3	5	0									4	5	6	0
13	4		4	5	5									300	5	4000	2
14	5	5	5	5	0									500	5	600	0
15	6		6	5	0									800	5	-200	5
16	7	200	7	5	0									6	5	-200	5
17	8		8	5	0									100	5	-200	5
18	9	1000	1	5	0									2	5	-200	5
19	10	1000	5	5	0									6	5	6	5
20	11	1000	5	5	0									4000	5	4000	5
21	12	1000	5	5	0									600	5	600	5
22	13	1000	5	5	0									-200	5	-200	5
23	14	1000	5	5	0												5
24	15	1000	5	5	0												5
25	16	1000	5	5	0												
26	17	1000	5	5	0												
27	18	1000	5	5	0									2	5	0	5
28	19	1000	5	5	0									5	5	0	5
29	20	1000	5	5	0												
30	21	1000	5	5	0												

A.3.4 Stap 3: invullen debieten / fluxen

Zoals reeds opgemerkt in hoofdstuk 0 bestaat het uitrekenen van het sediment budget erin om voor elke cel (i,j) alle grootheden uit de sedimentbalans te berekenen:

$$\frac{\Delta V_{ij}}{\Delta t} = \frac{P_{ij}}{\Delta t} + L_{ij} - L_{i,j+1} + T_{ij} - T_{i+1,j} \quad .$$

Indien we sedimentfluxen gebruiken i.p.v. sedimentdebieten wordt deze uitdrukking:

$$\frac{\Delta V_{ij}}{\Delta t} = \frac{P_{ij}}{\Delta t} + a_{ij} \cdot l_{ij} - a_{i,j+1} \cdot l_{i,j+1} + b_{ij} \cdot t_{ij} - b_{i+1,j} \cdot t_{i+1,j} \quad .$$

We verwijzen naar hoofdstuk 0 voor de betekenis van de gebruikte symbolen. Ervan uitgaande dat het hele systeem bestaat uit een raster met m rijen en n kolommen, komen we tot een totaal van m x n cellen en even veel sedimentbalansen. Indien we verder veronderstellen dat voor elke cel de verandering in sedimentvolume ΔV_{ij} en de door menselijke activiteit toegevoegde sedimenthoeveelheid P_{ij} gekend zijn, betekent dit dat het aantal a priori gekende sedimentdebieten (of -fluxen) gelijk moet zijn aan m·n + m + n opdat het stelsel van sedimentbalansen exact oplosbaar zou zijn.
In stap 3 kunnen deze a priori gekende sedimentdebieten of -fluxen (afhankelijk van de keuze gemaakt in stap 1) ingevuld worden. Figuur 48 toont een schermafdruk van deze stap.

Figure 48 – Stap 3: invullen van de a priori gekende sedimentdebieten of -fluxen.

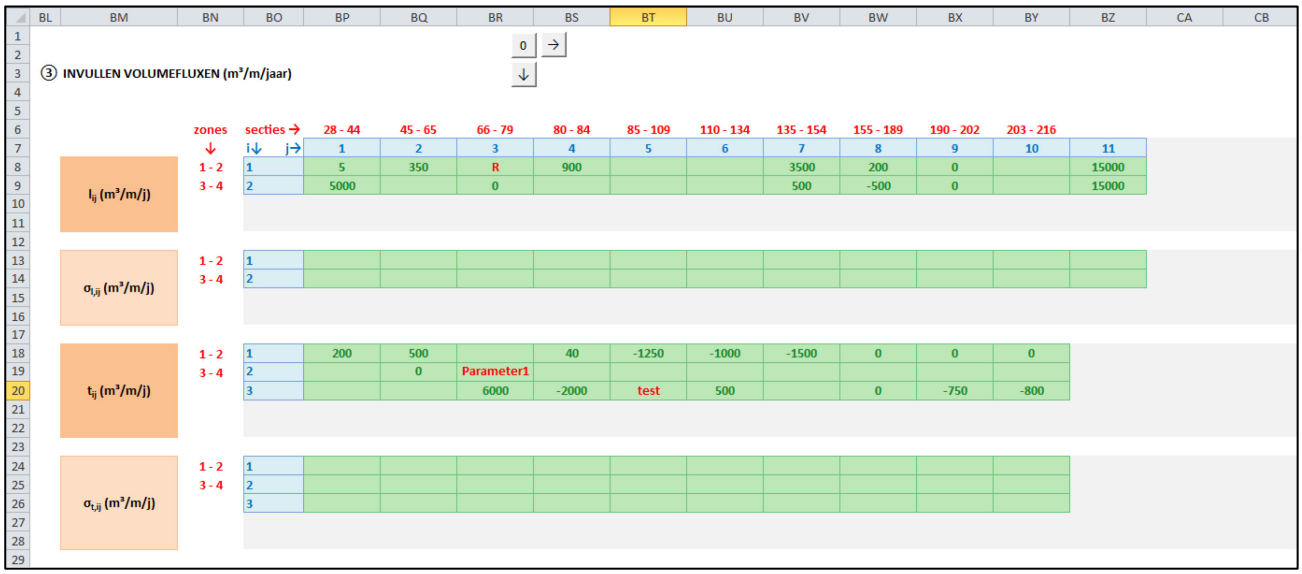

We overlopen hieronder enkele eigenschappen van dit deel van het tabblad.

- De gekende sedimentdebieten of -fluxen dienen ingevuld te worden in de groengekleurde Excel cellen. Er zijn 4 blokken van groene cellen, achtereenvolgens bestemd voor het invullen van de kustparallelle sedimentdebieten L_{ij}, de onzekerheden $\sigma_{L,ij}$ hierop, de kustdwarse sedimentdebieten T_{ij}, en de onzekerheden $\sigma_{T,ij}$ hierop (of analoog hiermee sedimentfluxen, met dezelfde symboliek maar aangeduid met kleine letter). Kolom BM geeft aan op welk sedimentdebiet of onzekerheid de groene blokken betrekking hebben. Merk op dat de groene blokken automatisch de juiste afmetingen hebben, afhankelijk van de gekozen indeling in cellen in stap 2 (deze blokken worden echter enkel correct gevormd indien in stap 2 alle ontbrekende volumes en/of onzekerheden worden aangevuld in het tabblad "INVULLEN ONTBREKENDE VOLUMES"). Merk verder op dat de blokken corresponderend met L_{ij} en $\sigma_{L,ij}$ een extra kolom hebben, terwijl de blokken corresponderend met T_{ij} en $\sigma_{T,ij}$ een extra rij bezitten, dit omwille van het optreden van de respectievelijke termen $L_{i,j+1}$ en $T_{i+1,j}$ in bovenstaande sedimentbalans.
- In de rekentool worden de onzekerheden aangeduid met σ, en niet met een Δ (zoals bij de bespreking in 0, 0 en 0).
- De blauwe getallen op een blauwe achtergrond geven de indices (i,j) weer en dienen als ondersteuning bij het invullen van de verschillende geïndexeerde grootheden L_{ij}, $\sigma_{L,ij}$, T_{ij} en $\sigma_{T,ij}$.
- De rode getallen op witte achtergrond geven voor elk koppel indices (i,j) de corresponderende secties en zones waaruit cel (i,j) is samengesteld. Deze worden uiteraard bepaald door de in stap 2 gekozen indeling.
- Ingevulde getallen verschijnen als groene cijfers. Merk op dat men ook parameters kan invullen, deze verschijnen in het rood. De rekentool is in staat om de oplossingen van het stelsel sedimentbalansen te geven in functie van hier opgegeven parameters. Er staat geen limiet op het aantal parameters dat ingegeven mag worden. Alles wat niet overeenkomt met een getal wordt door de rekentool als parameter beschouwd.
- Op de bovenste rijen kunnen nog de volgende icoontjes teruggevonden worden: ↓ , → , 0 en elders ook ← en ↑ . Deze knoppen helpen om snel te navigeren bij omvangrijke blokken en vermijden dat er zijwaarts gescrold moet worden. Merk op dat er ook omlaag gescrold kan worden, men vindt dan voor elke cel (i,j) de overeenkomstige volumeveranderingen $\Delta V_{ij}/\Delta t$ en

sedimentplaatsingen $P_{ij}/\Delta t$, zie Figuur 49. Met de knop 0 keert men terug naar het begin van stap 3.

Wanneer de a priori gekende sedimentdebieten (of -fluxen) en de overeenkomstige onzekerheden ingevuld zijn kan overgegaan worden naar stap 4.

Figure 49 – Stap 3: overzicht van de volumeveranderingen en plaatsingen.

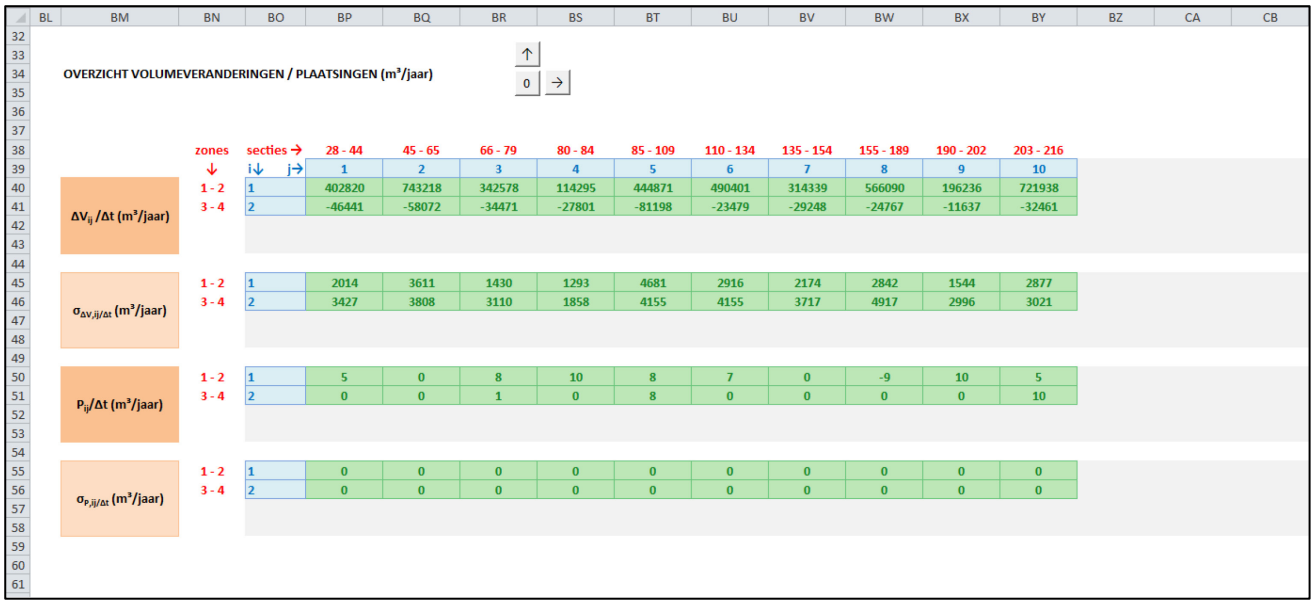

A.3.5 Stap 4: controleren oplosbaarheid

Het stelsel van vergelijkingen bestaande uit de m x n sedimentbalansen vereist zoal eerder vermeld het invullen van m·n + m + n sedimentdebieten (of -fluxen) opdat het stelsel een unieke oplossing zou hebben. Toch is dit niet de enige voorwaarde waaraan voldaan moet zijn. De m·n + m + n debieten (of fluxen) kunnen echter niet zomaar willekeurig ingevuld worden. Afhankelijk van de ingevulde debieten (of fluxen) kan het stelsel ook strijdig zijn of net een aantal vrijheidsgraden te veel hebben. De m·n + m + n debieten (of fluxen) kunnen echter niet zomaar willekeurig ingevuld worden. In stap 4 wordt gecontroleerd of de in stap 3 ingevulde debieten (of fluxen) leiden tot een unieke oplossing. Indien niet wordt ook aangegeven hoe de configuratie van ingevoerde debieten (of fluxen) gewijzigd moeten worden om een unieke oplossing mogelijk te maken. Hieronder volgt een woordje uitleg over hoe dit precies in zijn werk gaat.

A.3.5.1 Onafhankelijke deelgebieden en deelstelsels

Het is belangrijk in te zien dat de invoer van een welbepaalde configuratie van debieten (of fluxen) in stap 3 leidt tot het opsplitsen van het m x n raster van cellen (i,j) in een aantal onafhankelijke deelgebieden. Zo kan men in het voorbeeld van Figuur 48 zien dat l_{ij} voor j =3 is ingevuld voor alle waarden van i, zodat de sedimentfluxen over een volledige dwarssectie van het raster zijn vastgelegd. Hierdoor valt het raster uiteen in twee onafhankelijke deelgebieden: een deelgebied ten westen van deze dwarssectie (en die alle cellen bevat met j < 3) en een deelgebied ten oosten ervan (met alle cellen waarvoor j ≥ 3). Het volledige stelsel van sedimentbalansen valt eveneens uiteen in twee deelstelsels die onafhankelijk van mekaar zijn (vandaar de benaming “onafhankelijke deelgebieden”): deze deelstelsels bevatten geen gemeenschappelijke onbekenden en het is dus mogelijk elk van deze deelstelsels afzonderlijk op te lossen.

Let wel: opdat elk van deze deelstelsels uniek oplosbaar is, moet het corresponderende onafhankelijke deelgebied aan enkele voorwaarden voldoen.
Afhankelijk van de configuratie van ingegeven debieten of fluxen kan het raster in nog meer deelgebieden uiteenvallen. In het voorbeeld zijn de besproken deelgebieden rechthoekig, maar de deelgebieden kunnen uiteraard ook een grilligere vorm vertonen.
In stap 4 wordt op basis van de in stap 3 ingegeven configuratie van sedimentdebieten of -fluxen nagegaan in welke deelgebieden het raster van cellen uiteenvalt, en worden de oplosbaarheidsvoorwaarden nagegaan voor elk van deze deelgebieden. In de volgende subparagraaf worden deze oplosbaarheidsvoorwaarden opgelijst, de subparagraaf daarna geeft een woordje uitleg bij het gebruik van de rekentool bij het controleren van de oplosbaarheid.

A.3.5.2 Oplosbaarheidsvoorwaarden voor een deelstelsel

Veronderstel dat een deelgebied uit C cellen bestaat, dan zijn er ook C lineair onafhankelijke vergelijkingen, nl. de sedimentbalans voor elke cel. Verder beschikt elke cel over 4 randen, een aantal R_u daarvan vormen een deel van de uitwendige begrenzing van het deelgebied, terwijl een aantal R_i in het gebied liggen (en zo een grens vormen tussen twee tot het gebied behorende cellen). We stellen ook dat van de in stap 3 ingegeven sedimentdebieten of -fluxen een aantal F_u over een uitwendige rand gaan en een aantal F_i over een inwendige rand.
Een eerste voorwaarde opdat een stelsel uniek oplosbaar zou zijn, is dat het aantal onbekenden gelijk moet zijn aan het aantal (lineair onafhankelijke) vergelijkingen. Met de hierboven gedefinieerde symbolen kan dit vertaald worden als:

$$C = R_u + R_i - F_u - F_i \quad .$$

Als tweede voorwaarde mogen bovendien niet alle uitwendige randen tegelijk voorzien zijn van een in stap 3 ingegeven sedimentdebiet (of -flux). Anders zou men het netto sedimenttransport vanuit de omgeving naar het deelgebied toe vastleggen, en dit zou strijdig zijn met de gekende volumewijziging $\Delta V_{ij}/\Delta t$ en sedimentplaatsingen $P_{ij}/\Delta t$ in het deelgebied. Deze voorwaarde vertaald zich als:

$$R_u > F_u \quad .$$

Bovenstaande twee uitdrukkingen zijn nodige maar ook voldoende voorwaarden opdat het sediment budget oplosbaar is. Ze moeten uiteraard wel voldaan zijn voor elk deelgebied.

A.3.5.3 Controle van de oplosbaarheid in de Excel rekentool

Figuur 50 toont een schermafdruk van stap 4 in de Excel rekentool. Deze stap maakt gebruik van een macro, die men kan laten lopen door op de knop “controleer oplosbaarheid” (cellen ND3-NH3) te klikken. Het resultaat van het uitvoeren van deze macro is eveneens in de figuur te zien (het hier getoonde resultaat heeft de configuratie van sedimentfluxen uit Figuur 48 als input). We overlopen even:

- In puntje 1 ziet de gebruiker het m x n raster met de verschillende cellen, met in blauw de weergave van de celindices (i,j) en in rood de aanduiding van de kustsecties en zones die in elke cel vervat zijn. De verschillende kleuren geven de indeling in de verschillende onafhankelijke deelgebieden die het gevolg is van de in stap 3 ingegeven configuratie van sedimentdebieten of -fluxen. Voor verdere referentie is elk deelgebied ook genummerd, elke cel bevat dan ook een getal dat aangeeft tot welk deelgebied het behoort.
- Puntje 2 toont opnieuw het m x n raster, maar nu met een aanduiding van de in stap 3 ingevulde sedimentdebieten of -fluxen: elke celrand waarover een debiet of flux is ingegeven, is in vet rood weergegeven. Deze figuur is dus een visuele weergaven van de ingevoerde configuratie van debieten of fluxen en dient louter als hulpmiddel, zodat de gebruiker gemakkelijker kan inzien waar de configuratie moet gecorrigeerd worden.
- Puntje 3 is een oplijsting van de verschillende “foutmeldingen”. Eerst worden de verschillende deelgebieden weergegeven die volledig omsloten zijn door in stap 3 ingegeven debieten of fluxen en die aanleiding geven tot een strijdig stelsel. In dit voorbeeld zijn dat deelgebieden 2, 4, 6 en 7.

De nummering van de deelgebieden is die zoals aangeduid in de figuur van puntje 1. Vervolgens wordt voor elk deelgebied aangegeven of het corresponderende deelstelsel uniek oplosbaar is ("OK!"), dan wel of het over- of ondergedetermineerd is. Er wordt telkens ook weergegeven hoeveel sedimentdebieten (of -fluxen) er te veel of te kort zijn in het betreffende deelgebied om uniek oplosbaar te zijn. Merk op dat het al dan niet omsloten zijn door a priori opgegeven debieten of fluxen van een deelgebied niets zegt over het over- of ondergedetermineerd zijn van het corresponderende deelstelsel, wat dat betreft zijn zowat alle combinaties mogelijk: een deelgebied kan omsloten zijn terwijl het geassocieerde deelstelsel zowel uniek oplosbaar als over- of ondergedetermineerd (zoals uit dit voorbeeld mag blijken), en een niet-omsloten deelgebied kan corresponderen met zowel een uniek oplosbaar als een ondergedetermineerd stelsel. Enkel de combinatie niet-omsloten deelgebied/overgedetermineerd deelstelsel kan niet voorkomen. Merk ook op dat in dit voorbeeld voor het hele raster het totaal aantal a priori ingegeven fluxen gelijk is aan m·n + m + n, zoals vereist is voor unieke oplosbaarheid. Toch betekent dit dus niet dat het stelsel bestaande uit de sedimentbalansen van alle cellen oplosbaar is, het is dus een nodige, maar zeker geen voldoende voorwaarde.

Figure 50 – Stap 4: controleren van de oplosbaarheid.

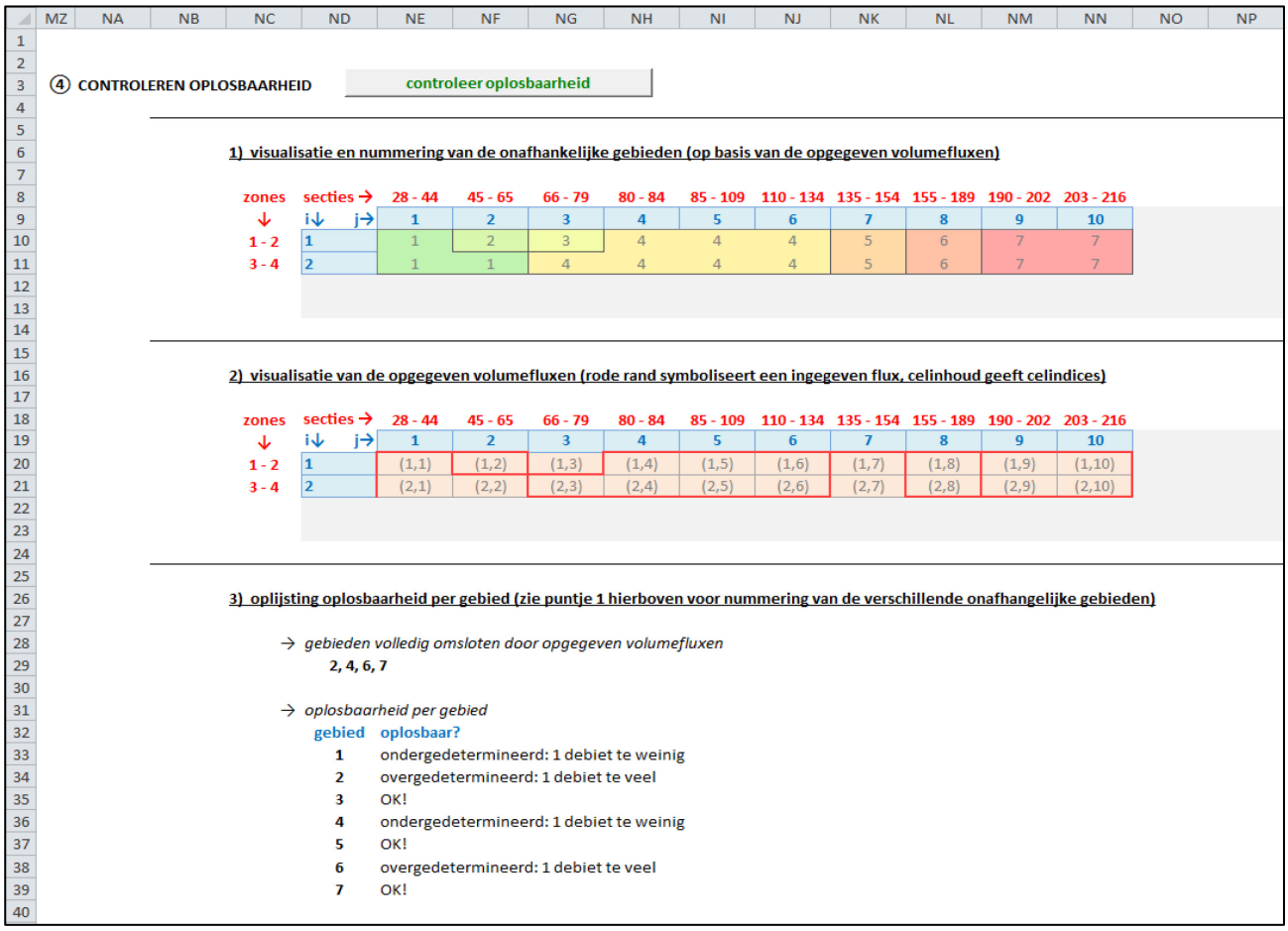

Zolang in stap 4 deelgebieden niet uniek oplosbaar blijven, moet naar stap 3 teruggekeerd worden en de configuratie van ingegeven sedimentdebieten of -fluxen aangepast worden. Pas wanneer geen enkel deelgebied een "foutmelding" oplevert mag naar stap 5 verdergegaan worden.
Let op: de controle wordt enkel uitgevoerd op de ingevoerde sedimentdebieten (of -fluxen) zelf, niet op hun onzekerheden! Er wordt vanuit gegaan dat voor de onzekerheden eenzelfde configuratie als bij de debieten (of -fluxen) zelf wordt ingevoerd. Hoewel vreemd zou het op zich niet verkeerd zijn voor de onzekerheden een andere configuratie in te vullen, de oplosbaarheid van het stelsel van de onzekerheden

wordt echter niet apart gecontroleerd. (Indien men de rekentool een niet-oplosbare configuratie zou laten oplossen, zou dit niet tot foutmeldingen leiden, de rekentool zal daarentegen een oplossing geven, die echter wel foutief is.)

A.3.6 Stap 5: oplossen van het stelsel van sedimentbalansen

In stap 5 lost de rekentool het stelsel van sedimentbalansen op, hiervoor wordt gebruik gemaakt van een macro. Indien de vorige stappen correct werden uitgevoerd, dient de gebruiker in stap 5 enkel nog deze macro te laten lopen door op de daarvoor voorziene knop “oplossen stelsel” te klikken (cellen YL3-YP3).
Voor de verdere bespreking maken we onderscheid tussen het regulier oplossen van het stelsel en een parameterstudie.

A.3.6.1 Regulier oplossen stelsel

Indien de vooraf ingegeven sedimentdebieten of -fluxen alle getallen zijn, leidt het laten lopen van de macro “oplossen stelsel” tot een unieke oplossing waarbij de onbekende debieten of fluxen ook getallen zijn. Het lopen van de macro kan enkele seconden duren, afhankelijk enerzijds van de grootte van het raster en anderzijds van de specifieke configuratie van de ingegeven debieten of fluxen.
Figuur 51 toont een schermafdruk van stap 6, nadat de macro “oplossen stelsel” gelopen heeft op een fictieve maar uniek oplosbare input (dus niet die van Figuur 48). Het m x n raster wordt opnieuw op de gekende wijze weergegeven (aanduiding celindices in blauw, aanduiding kustsecties en zones in rood). De door de rekentool berekende sedimentdebieten of -fluxen zijn onderlijnd, de in stap 3 door de gebruiker ingegeven debieten of fluxen zijn vet weergeven. Net als bij stap 3 zijn hier ook extra knoppen toegevoegd om het navigeren bij grotere rasters (links en rechts scrollen) te vergemakkelijken. Er zijn eveneens knoppen om omlaag en terug omhoog te scrollen, om zo net zoals bij stap 3 de volumewijzigingen en sedimentplaatsingen voor elke cel te kunnen raadplegen.

Figure 51 – Stap 6: oplossing van het stelsel van sedimentbalansen.

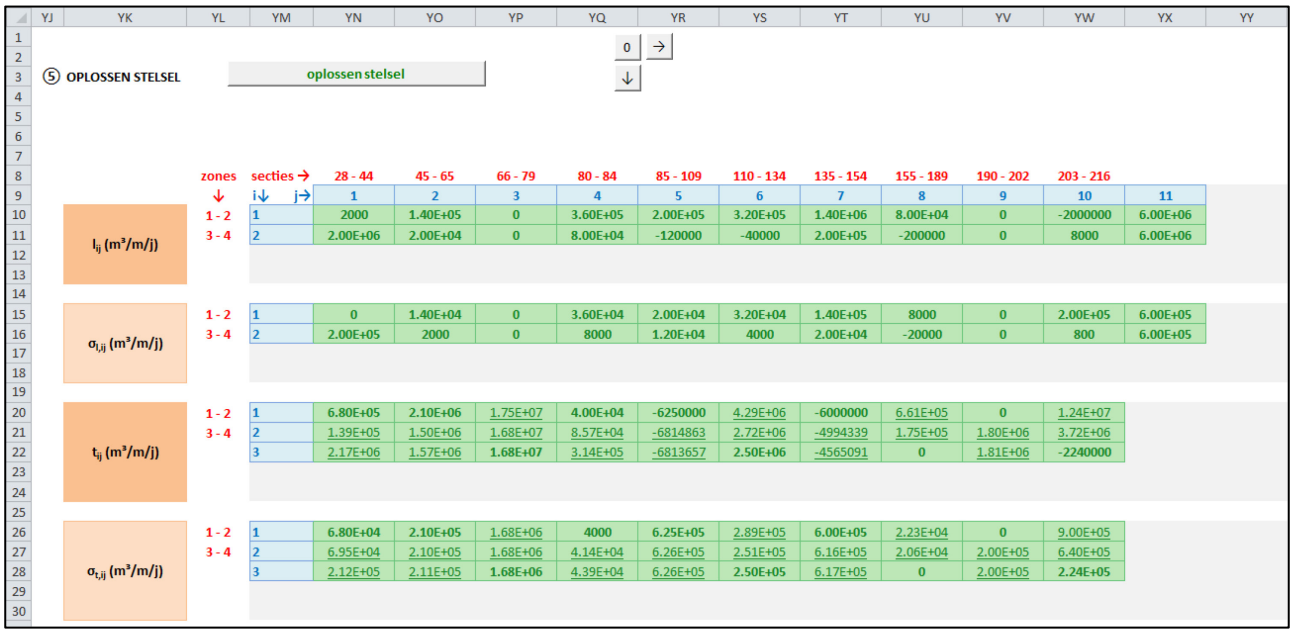

⑤ OPLOSSEN STELSEL

oplossen stelsel

zones	secties →	28 - 44	45 - 65	66 - 79	80 - 84	85 - 109	110 - 134	135 - 154	155 - 189	190 - 202	203 - 216	
↓	i↓ j→	1	2	3	4	5	6	7	8	9	10	11
1 - 2	1	2000	1.40E+05	0	3.60E+05	2.00E+05	3.20E+05	1.40E+06	8.00E+04	0	-2000000	6.00E+06
3 - 4	2	2.00E+06	2.00E+04	0	8.00E+04	-120000	-40000	2.00E+05	-200000	0	8000	6.00E+06

l_{ij} (m³/m/j)

1 - 2	1	0	1.40E+04	0	3.60E+04	2.00E+04	3.20E+04	1.40E+05	8000	0	2.00E+05	6.00E+05
3 - 4	2	2.00E+05	2000	0	8000	1.20E+04	4000	2.00E+04	-20000	0	800	6.00E+05

$\sigma_{l,ij}$ (m³/m/j)

1 - 2	1	6.80E+05	2.10E+06	1.75E+07	4.00E+04	-6250000	4.29E+06	-6000000	6.61E+05	0	1.24E+07
3 - 4	2	1.39E+05	1.50E+06	1.68E+07	8.57E+04	-6814863	2.72E+06	-4994339	1.75E+05	1.80E+06	3.72E+06
	3	2.17E+06	1.57E+06	**1.68E+07**	3.14E+05	-6813657	**2.50E+06**	-4565091	0	1.81E+06	-2240000

t_{ij} (m³/m/j)

1 - 2	1	6.80E+04	2.10E+05	1.68E+06	4000	6.25E+05	2.89E+05	6.00E+05	2.23E+04	0	9.00E+05
3 - 4	2	6.95E+04	2.10E+05	1.68E+06	4.14E+04	6.26E+05	2.51E+05	6.16E+05	2.06E+04	2.00E+05	6.40E+05
	3	2.12E+05	2.11E+05	**1.68E+06**	4.39E+04	6.26E+05	**2.50E+05**	6.17E+05	0	2.00E+05	**2.24E+05**

$\sigma_{t,ij}$ (m³/m/j)

A.3.6.2 Parameterstudie

Zoals reeds eerder vermeld laat de rekentool ook toe om parameterstudies uit te voeren, om zo de respons van het systeem op een of meerdere veranderende sedimentdebieten of -fluxen na te gaan. Dit doet men

eenvoudigweg door in stap 3 een parameter in te vullen in het raster waar de a priori gekende debieten of fluxen ingegeven moeten worden. De naam voor de parameter mag door de gebruiker zelf gekozen worden, alles wat geen getal is wordt door de rekentool als parameter beschouwd. Er kunnen ook meerdere parameters ingevoerd worden, in principe staat er zelfs geen limiet op (uiteraard wel niet meer dan m·n + m + n om geen overgedetermineerd stelsel te bekomen). Eenzelfde parameter kan ook meer dan eens ingevuld worden. Uitdrukkingen kunnen echter niet ingevuld worden (vult men bijvoorbeeld als debiet- of fluxwaarde "2*t+6" in, dan zal de rekentool deze hele uitdrukking als een parameter beschouwen, in plaats van de berekening met een parameter t te verwerken). Een ingevoerde parameter wordt in rode kleur weergegeven in het invulraster van stap 3 (zie Figuur 52). Tot slot: ook bij de onzekerheden kunnen parameters ingevuld worden, ook hier kunnen –teineinde geen overgedetermineerd stelsel te bekomen– maximaal m·n + m + n parameters ingevuld worden.

De controle van de oplosbaarheid van het stelsel sedimentbalansen (stap 4) bij een parameterstudie verloopt identiek als bij een regulier stelsel, en om het stelsel op te lossen dient men dezelfde macro te laten lopen (knop "oplossen stelsel" in stap 5). Het oplossen van een stelsel met parameters neemt wel meer tijd in beslag, de rekentijd is ongeveer een veelvoud gelijk aan het aantal verschillende parameters van de rekentijd nodig voor het oplossen van een regulier stelsel.

Bij een parameterstudie wordt de gebruiker nadat de macro gelopen heeft automatisch naar het tabblad "PARAMETERSTUDIE" geleid. Een typische oplossing van een parameterstudie ziet eruit zoals in Figuur 52. In kolom C vindt men de naam van de betreffende parameters, in de volgende kolommen wordt in de gebruikelijke vorm de afhankelijkheid van elk sedimentdebiet (of -flux) van de parameter in kwestie weergegeven. Als laatste in de rij van parameters is altijd de constante term. We geven nu aan hoe deze rasters geïnterpreteerd dienen te worden.

Veronderstel dat P_k een parameter is (verschillende parameters worden aangeduid met de index k), dat $A_{ijk}(L)$ de inhoud is van cel (i,j) bij het raster van het kustlangse sedimentdebiet bij parameter P_k, en dat $C_{ij}(L)$ de inhoud is van cel (I,j) bij het raster van het kustlangse debiet bij de constant term, dan geldt:

$$L_{ij} = C_{ij}(L) + \sum_k P_k \cdot A_{ijk}(L) \ .$$

Hierbij moet over alle parameters gesommeerd worden. Analoge formules gelden voor het kustdwarse debiet:

$$T_{ij} = C_{ij}(T) + \sum_k P_k \cdot A_{ijk}(T) \ .$$

Voor fluxen gelden identieke formules:

$$l_{ij} = C_{ij}(l) + \sum_k P_k \cdot A_{ijk}(l)$$

$$t_{ij} = C_{ij}(t) + \sum_k P_k \cdot A_{ijk}(t) \ .$$

De formules voor de onzekerheden zijn echter anders: waar de debieten (of fluxen) berekend worden met behulp van een stelsel van lineaire vergelijkingen (nl. de sedimentbalansens), is dit voor de onzekerheden niet het geval. De formules worden hier, voor respectievelijk de kustparallelle en kustdwarse debieten en fluxen:

$$\sigma_{L,ij} = \sqrt{\left(C_{ij}(\sigma_L)\right)^2 + \sum_k P_k \cdot \left[\left(A_{ijk}(\sigma_L)\right)^2 - \left(C_{ij}(\sigma_L)\right)^2\right]}$$

$$\sigma_{T,ij} = \sqrt{\left(C_{ij}(\sigma_T)\right)^2 + \sum_k P_k \cdot \left[\left(A_{ijk}(\sigma_T)\right)^2 - \left(C_{ij}(\sigma_T)\right)^2\right]}$$

$$\sigma_{l,ij} = \sqrt{\left(C_{ij}(\sigma_l)\right)^2 + \sum_k P_k \cdot \left[\left(A_{ijk}(\sigma_l)\right)^2 - \left(C_{ij}(\sigma_l)\right)^2\right]}$$

$$\sigma_{t,ij} = \sqrt{\left(C_{ij}(\sigma_t)\right)^2 + \sum_k P_k \cdot \left[\left(A_{ijk}(\sigma_t)\right)^2 - \left(C_{ij}(\sigma_t)\right)^2\right]}$$

Figure 52 – Stap 6: oplossing van het stelsel sedimentbalansen bij een parameterstudie.

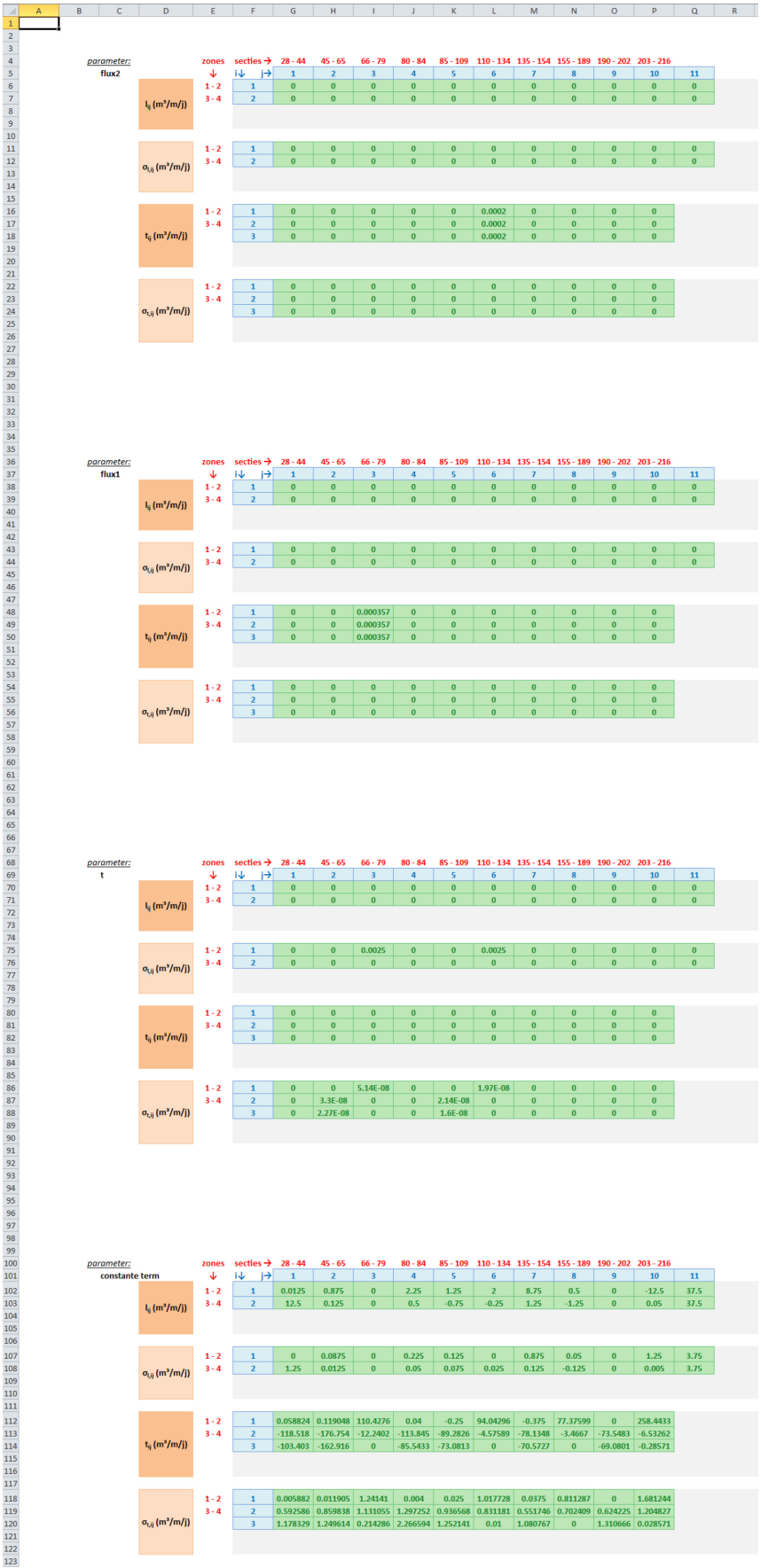

parameter: flux2

zones ↓	secties →	28 - 44	45 - 65	66 - 79	80 - 84	85 - 109	110 - 134	135 - 154	155 - 189	190 - 202	203 - 216
	↓ \ →	1	2	3	4	5	6	7	8	9	10	11
l_{ij} (m³/m/j)	1 - 2	1	0	0	0	0	0	0	0	0	0	0
	3 - 4	2	0	0	0	0	0	0	0	0	0	0
$\sigma_{l,ij}$ (m³/m/j)	1 - 2	1	0	0	0	0	0	0	0	0	0	0
	3 - 4	2	0	0	0	0	0	0	0	0	0	0
t_{ij} (m³/m/j)	1 - 2	1	0	0	0	0	0	0.0002	0	0	0	0
	3 - 4	2	0	0	0	0	0	0.0002	0	0	0	0
		3	0	0	0	0	0	0.0002	0	0	0	0
$\sigma_{t,ij}$ (m³/m/j)	1 - 2	1	0	0	0	0	0	0	0	0	0	0
	3 - 4	2	0	0	0	0	0	0	0	0	0	0
		3	0	0	0	0	0	0	0	0	0	0

parameter: flux1

zones ↓	secties →	28 - 44	45 - 65	66 - 79	80 - 84	85 - 109	110 - 134	135 - 154	155 - 189	190 - 202	203 - 216
	↓ \ →	1	2	3	4	5	6	7	8	9	10	11
l_{ij} (m³/m/j)	1 - 2	1	0	0	0	0	0	0	0	0	0	0
	3 - 4	2	0	0	0	0	0	0	0	0	0	0
$\sigma_{l,ij}$ (m³/m/j)	1 - 2	1	0	0	0	0	0	0	0	0	0	0
	3 - 4	2	0	0	0	0	0	0	0	0	0	0
t_{ij} (m³/m/j)	1 - 2	1	0	0	0.000357	0	0	0	0	0	0	0
	3 - 4	2	0	0	0.000357	0	0	0	0	0	0	0
		3	0	0	0.000357	0	0	0	0	0	0	0
$\sigma_{t,ij}$ (m³/m/j)	1 - 2	1	0	0	0	0	0	0	0	0	0	0
	3 - 4	2	0	0	0	0	0	0	0	0	0	0
		3	0	0	0	0	0	0	0	0	0	0

parameter: t

zones ↓	secties →	28 - 44	45 - 65	66 - 79	80 - 84	85 - 109	110 - 134	135 - 154	155 - 189	190 - 202	203 - 216
	↓ \ →	1	2	3	4	5	6	7	8	9	10	11
l_{ij} (m³/m/j)	1 - 2	1	0	0	0	0	0	0	0	0	0	0
	3 - 4	2	0	0	0	0	0	0	0	0	0	0
$\sigma_{l,ij}$ (m³/m/j)	1 - 2	1	0	0	0.0025	0	0	0.0025	0	0	0	0
	3 - 4	2	0	0	0	0	0	0	0	0	0	0
t_{ij} (m³/m/j)	1 - 2	1	0	0	0	0	0	0	0	0	0	0
	3 - 4	2	0	0	0	0	0	0	0	0	0	0
		3	0	0	0	0	0	0	0	0	0	0
$\sigma_{t,ij}$ (m³/m/j)	1 - 2	1	0	0	5.14E-08	0	0	1.97E-08	0	0	0	0
	3 - 4	2	0	3.3E-08	0	0	2.14E-08	0	0	0	0	0
		3	0	2.27E-08	0	0	1.6E-08	0	0	0	0	0

parameter: constante term

zones ↓	secties →	28 - 44	45 - 65	66 - 79	80 - 84	85 - 109	110 - 134	135 - 154	155 - 189	190 - 202	203 - 216
	↓ \ →	1	2	3	4	5	6	7	8	9	10	11
l_{ij} (m³/m/j)	1 - 2	1	0.0125	0.875	0	2.25	1.25	2	8.75	0.5	0	-12.5	37.5
	3 - 4	2	12.5	0.125	0	0.5	-0.75	-0.25	1.25	-1.25	0	0.05	37.5
$\sigma_{l,ij}$ (m³/m/j)	1 - 2	1	0	0.0875	0	0.225	0.125	0	0.875	0.05	0	1.25	3.75
	3 - 4	2	1.25	0.0125	0	0.05	0.075	0.025	0.125	-0.125	0	0.005	3.75
t_{ij} (m³/m/j)	1 - 2	1	0.058824	0.119048	110.4276	0.04	-0.25	94.04296	-0.375	77.37599	0	258.4433
	3 - 4	2	-118.518	-176.754	-12.2402	-113.845	-89.2826	-4.57589	-78.1348	-3.4667	-73.5483	-6.53262
		3	-103.403	-162.916	0	-85.5433	-73.0813	0	-70.5727	0	-69.0801	-0.28571
$\sigma_{t,ij}$ (m³/m/j)	1 - 2	1	0.005882	0.011905	1.24141	0.004	0.025	1.017728	0.0375	0.811287	0	1.681244
	3 - 4	2	0.592586	0.859838	1.131055	1.297252	0.936568	0.831181	0.551746	0.702409	0.624225	1.204827
		3	1.178329	1.249614	0.214286	2.266594	1.252141	0.01	1.080767	0	1.310666	0.028571

Annexe 2 Volume change plots by cell

This appendix presents graphs of volume changes in each coast cell (for above and below low water separately), as described in section 2.6 of the main report. Please refer to that section for an explanation of the data presented in these graphs.

Cell 1 - De Panne to Nieuwpoort Harbour

Above low water

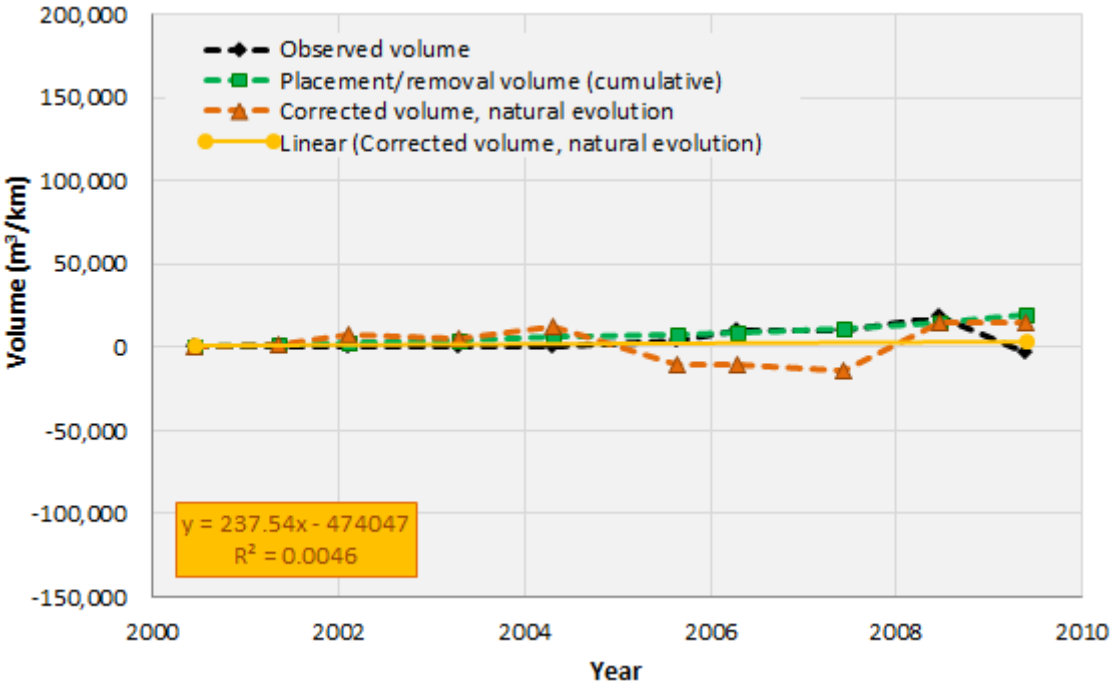

Below low water

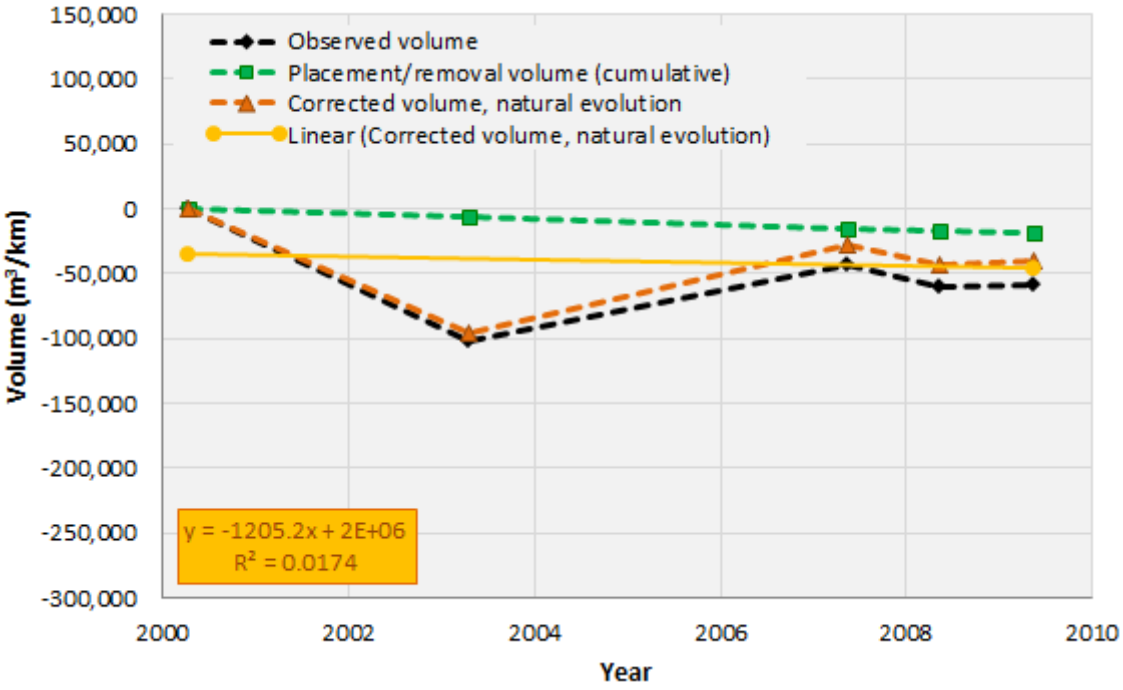

Cell 2 - Nieuwpoort Harbour to Middelkerke

Above low water

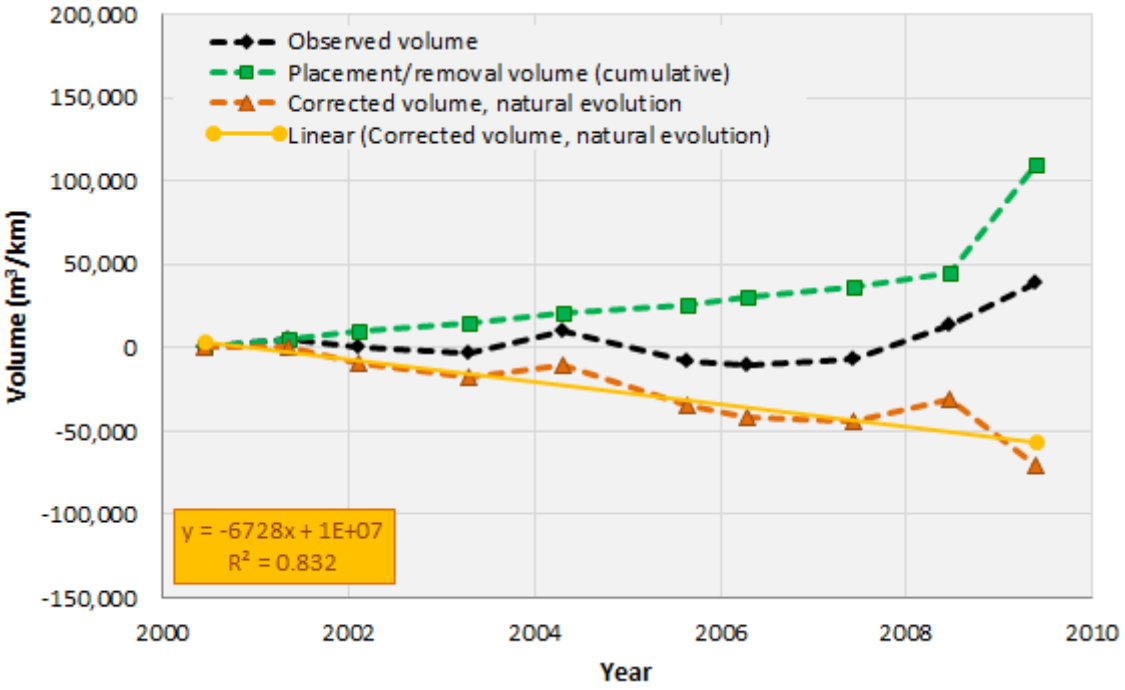

Below low water

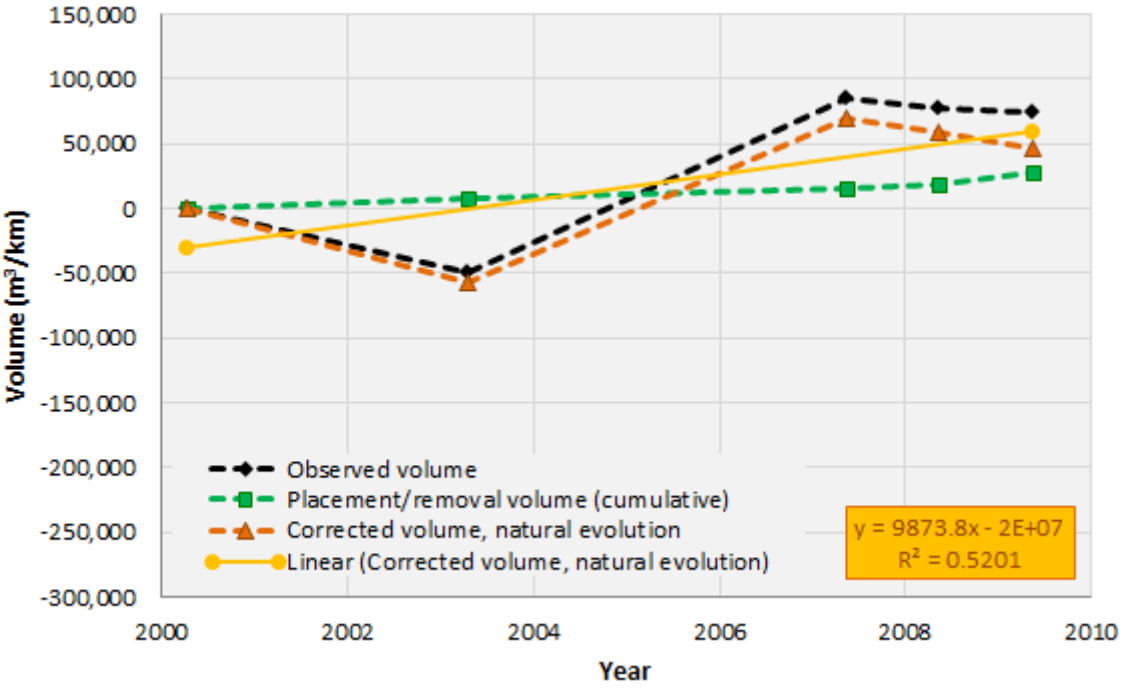

Cell 3 - Middelkerke to Oostende

Above low water

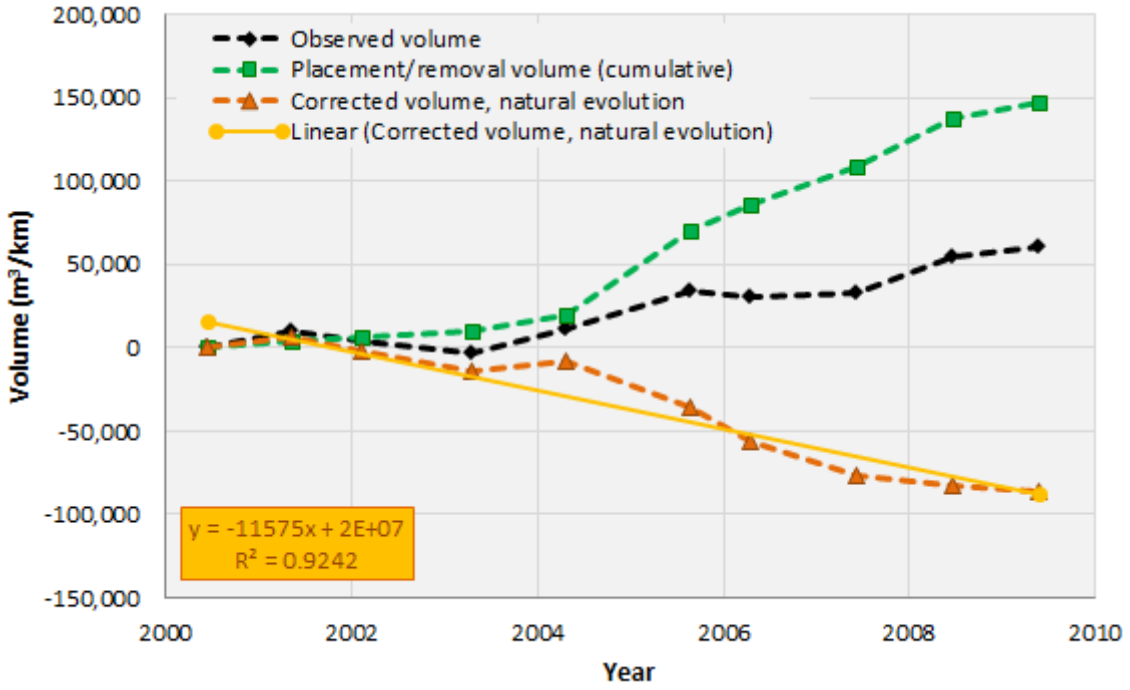

Below low water

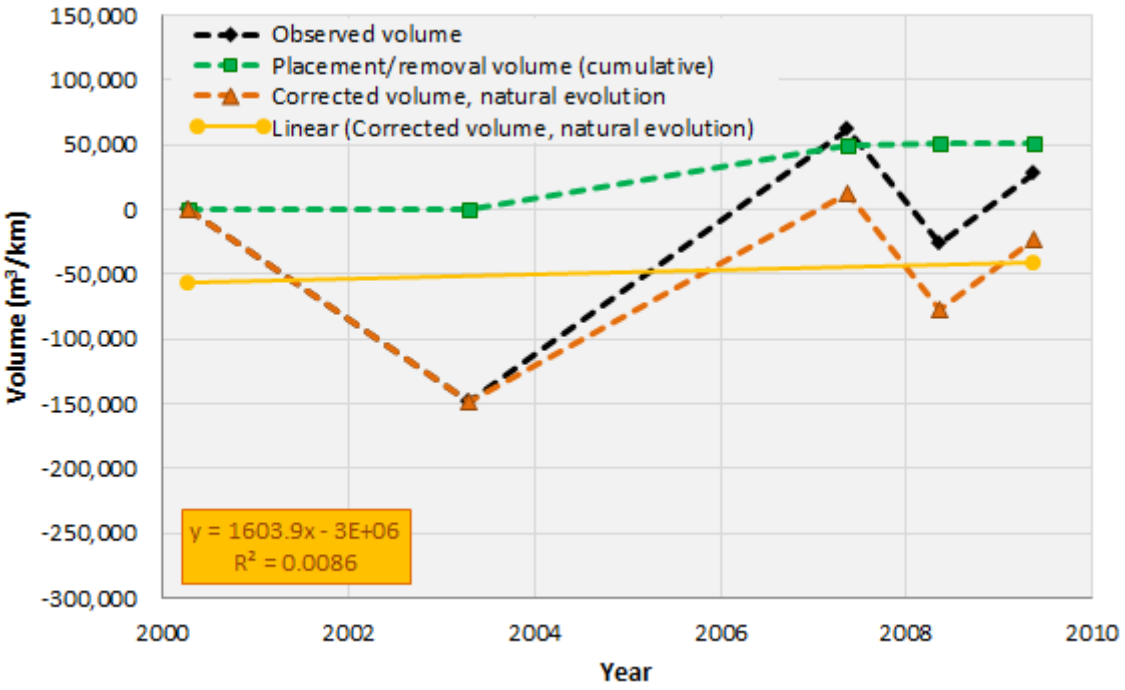

Cell 4 - Oostende Harbour through Bredene-aan-Zee

Above low water

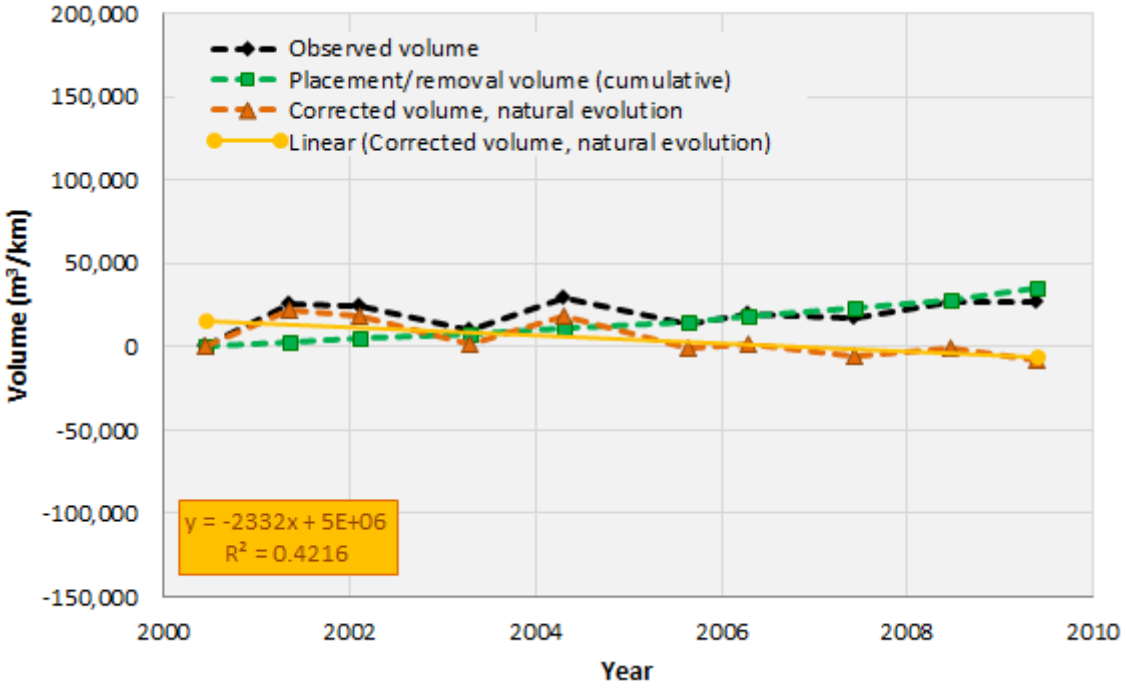

Below low water

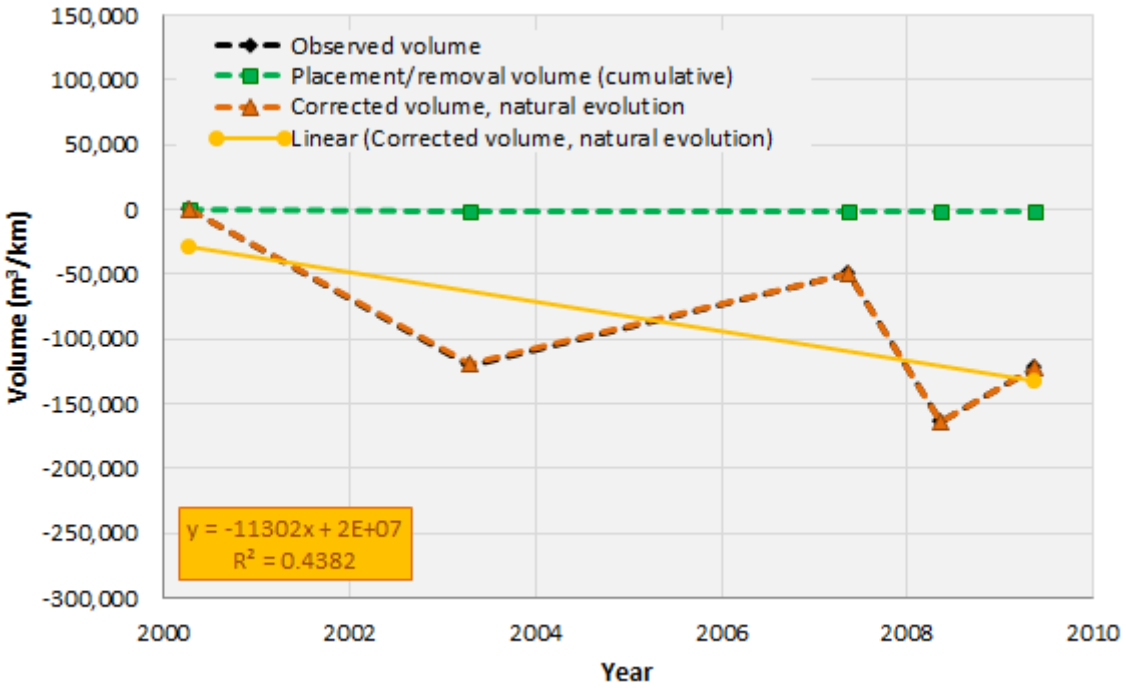

Cell 5 - De Haan to Wenduine

Above low water

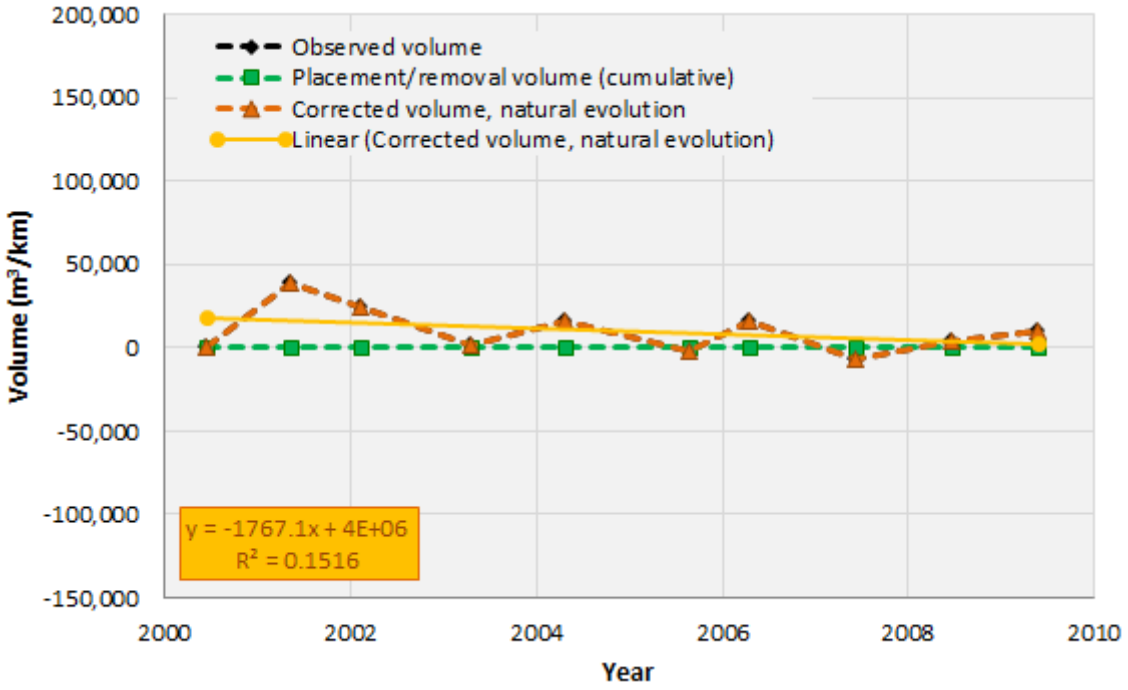

Below low water

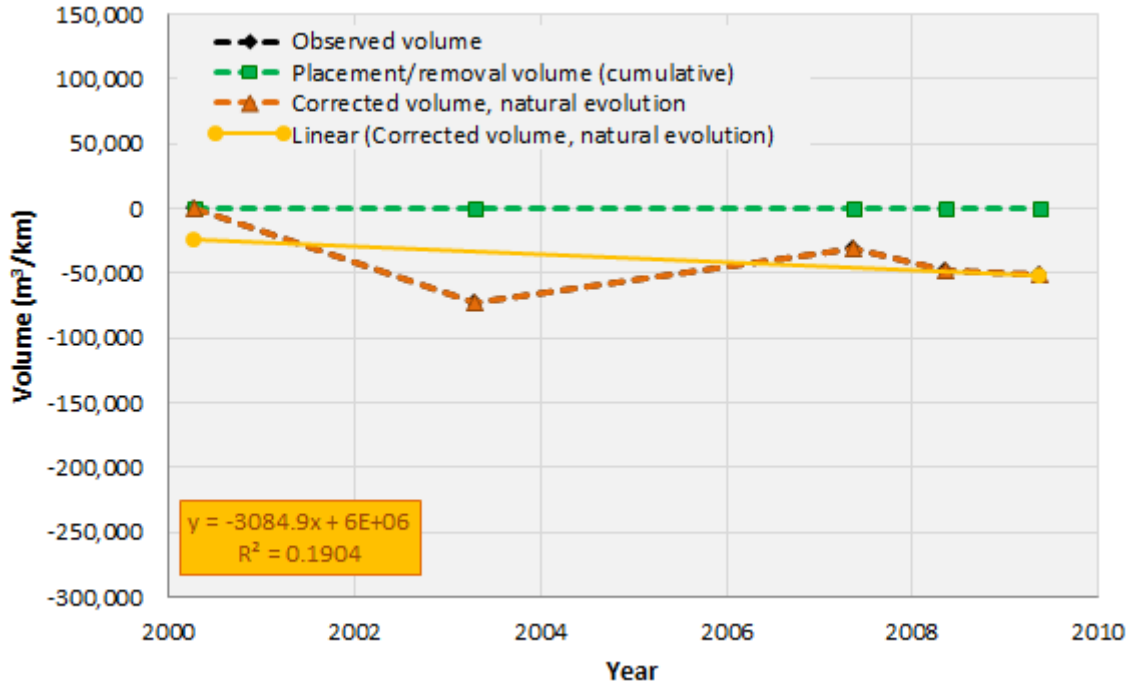

Cell 6 - Wenduine to Blankenberge Harbour

Above low water

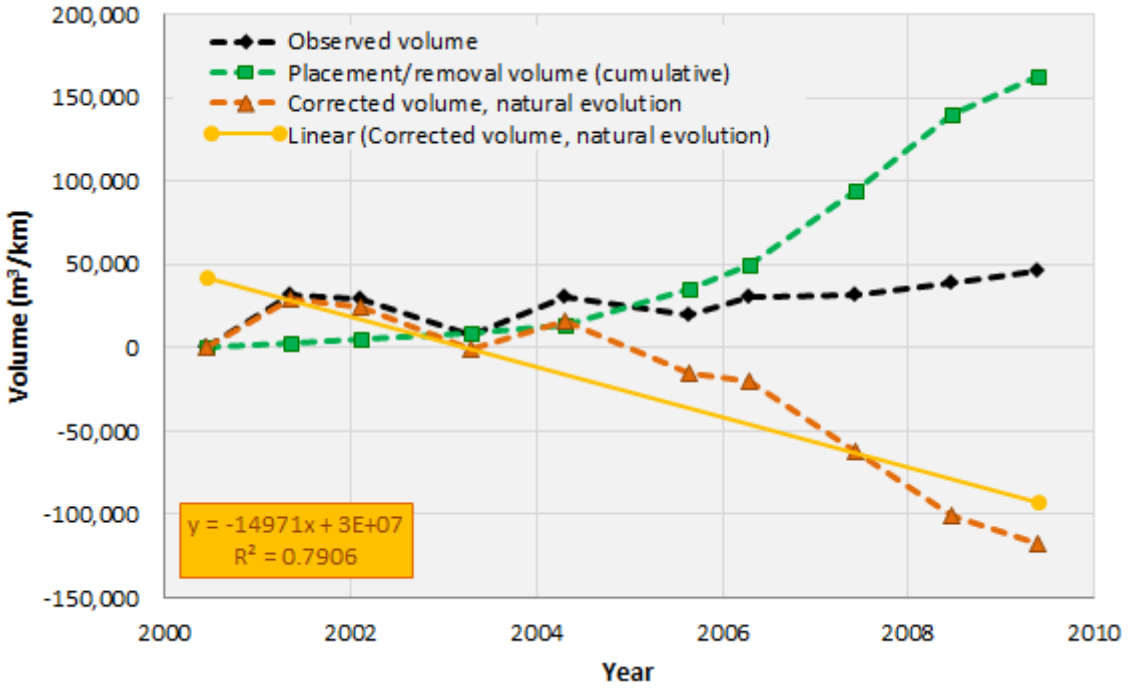

Below low water

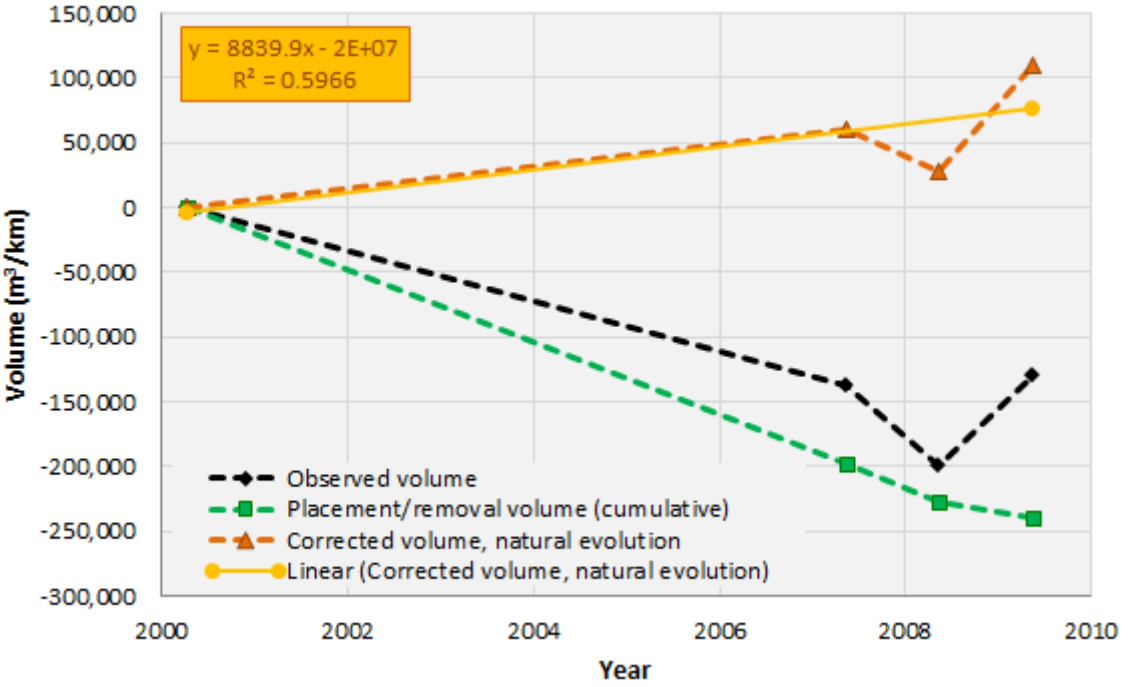

Cell 7 - Blankenberge Harbour to Zeebrugge Harbour

Above low water

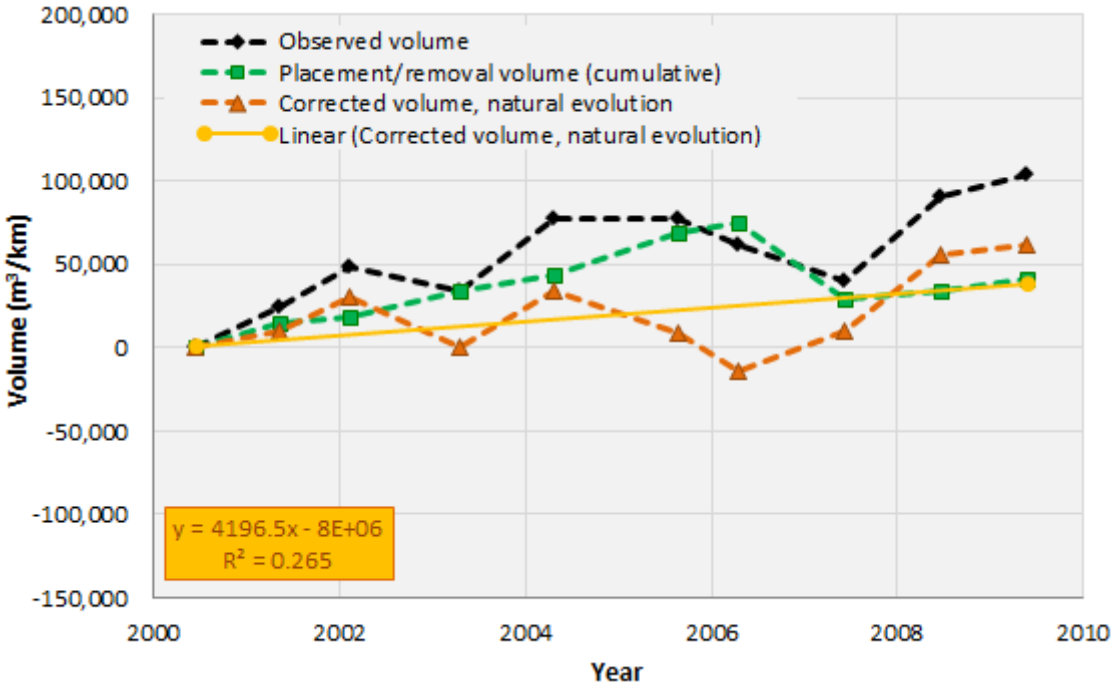

Below low water

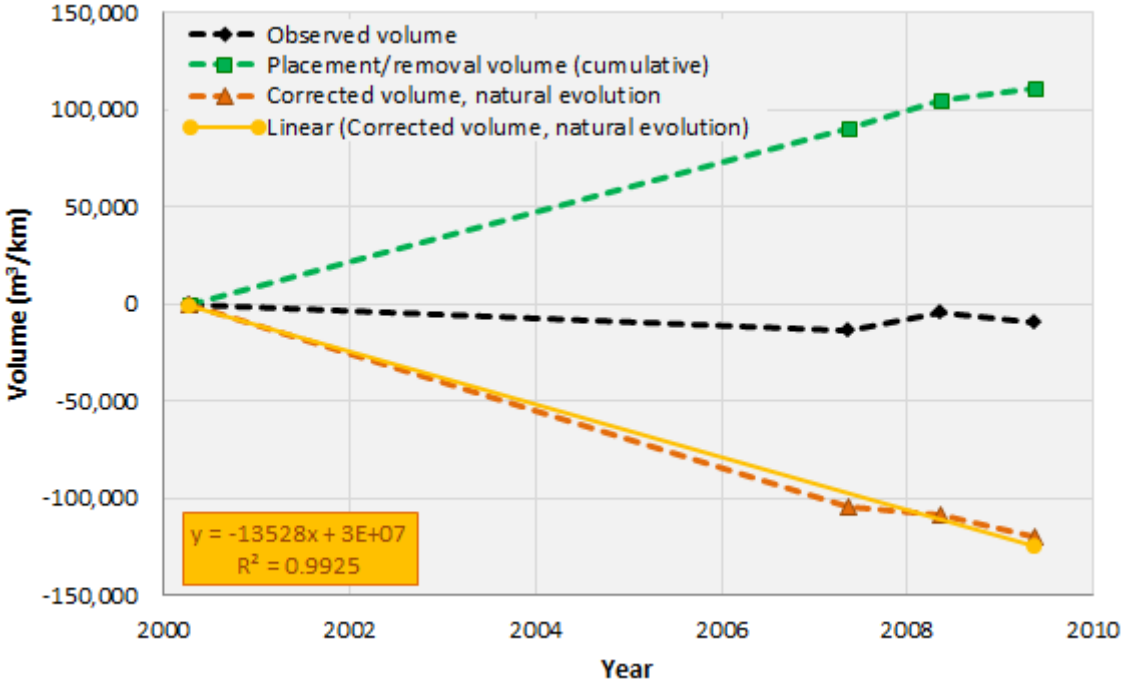

Cell 8 - Zeebrugge Harbour to Knokke Zoute

Above low water

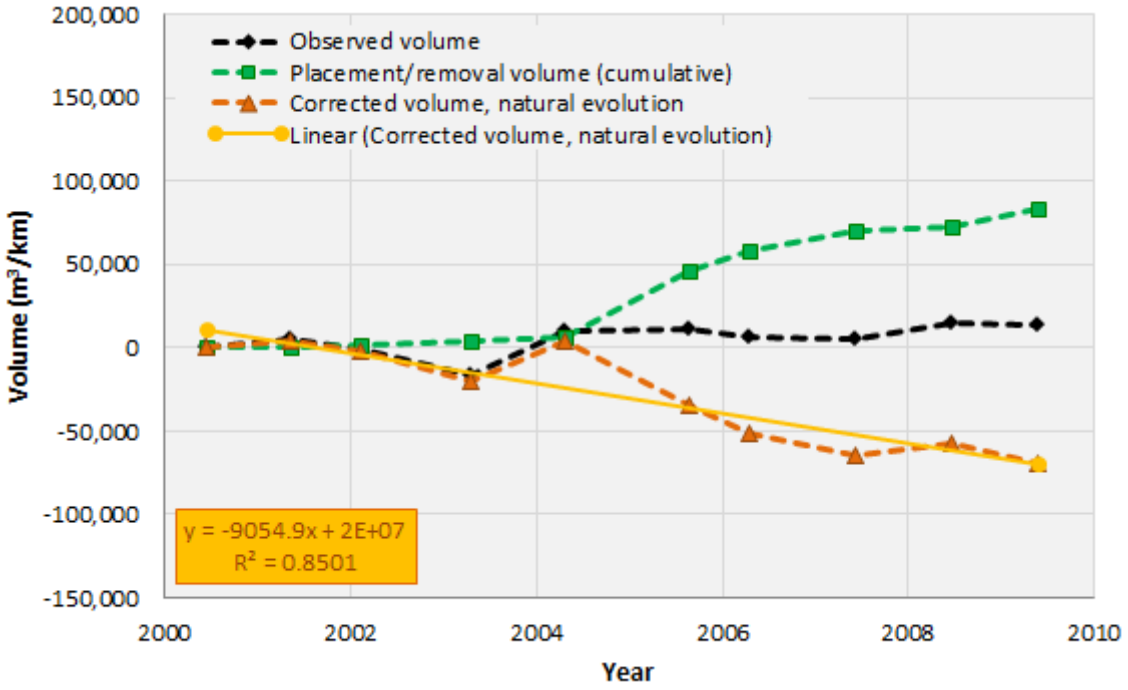

Below low water

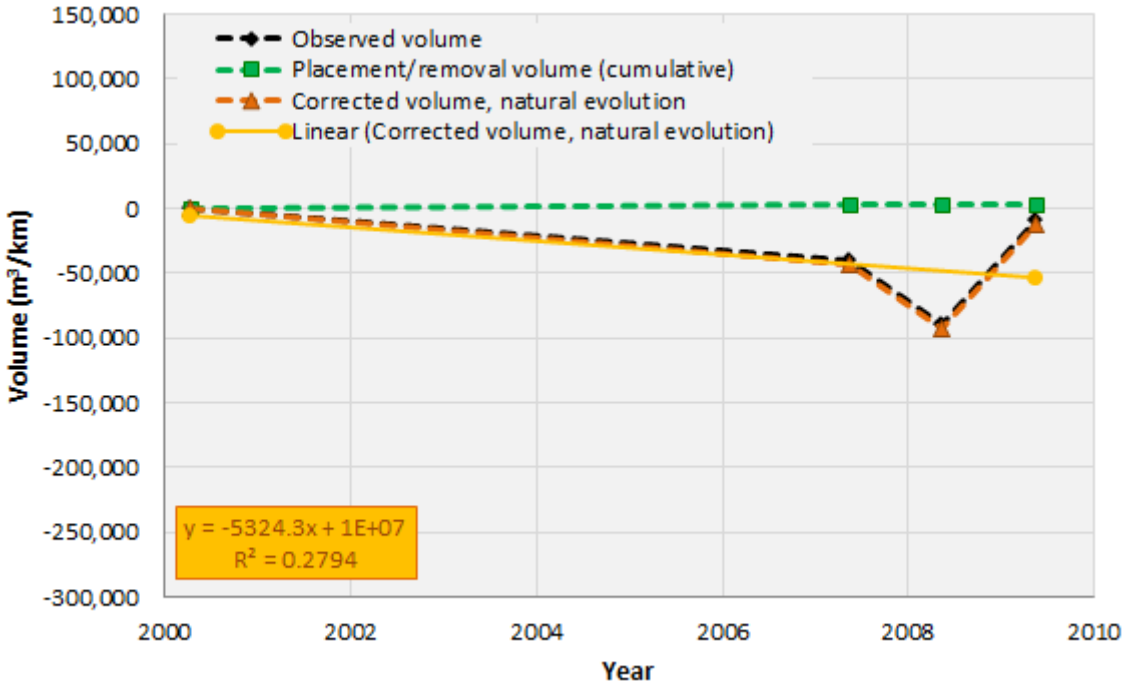

Cell 9 - Knokke Zoute to Het Zwin

Above low water

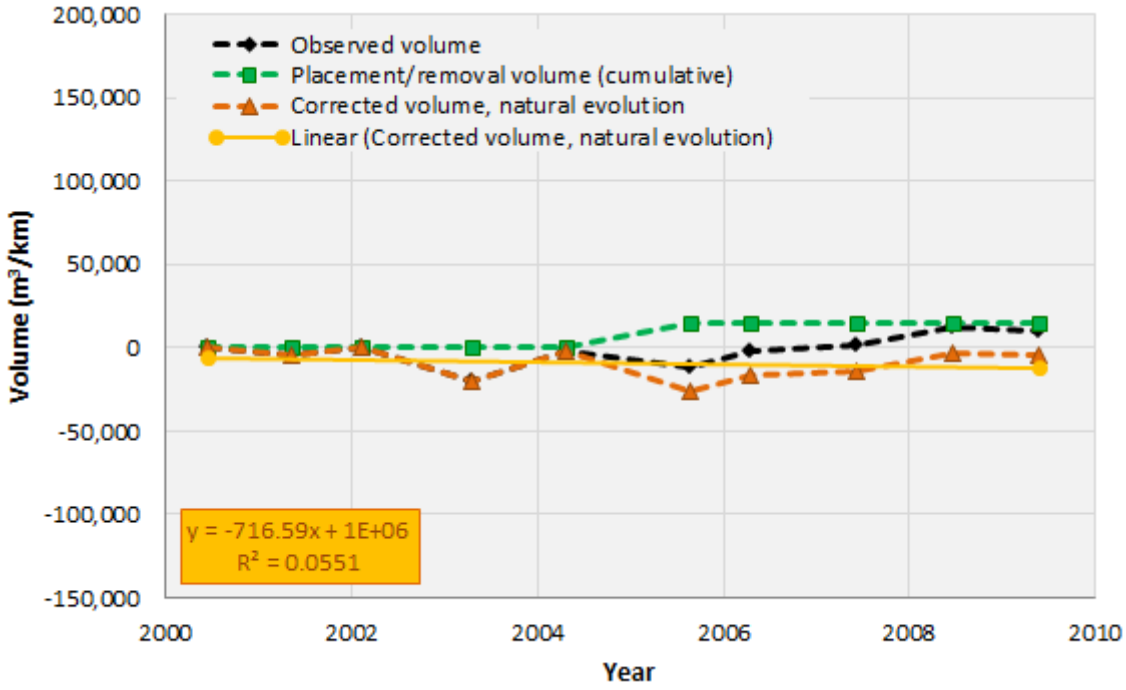

Below low water

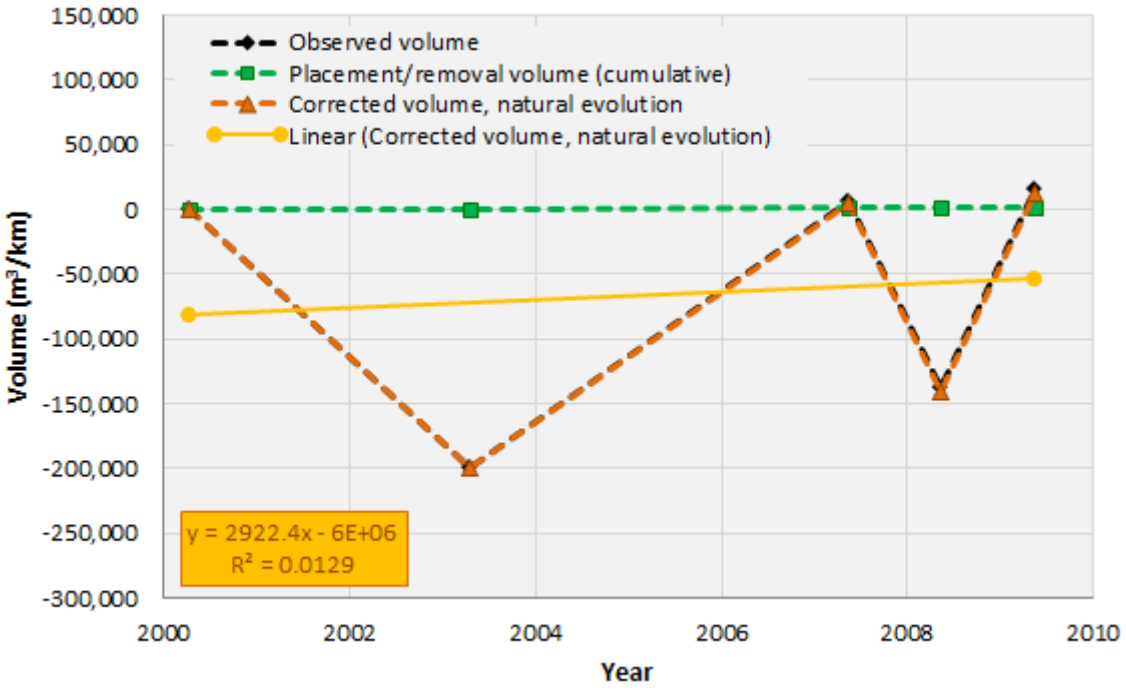

DEPARTMENT **MOBILITY & PUBLIC WORKS**
Flanders hydraulics Research

Berchemlei 115, 2140 Antwerp
T +32 (0)3 224 60 35
F +32 (0)3 224 60 36
waterbouwkundiglabo@vlaanderen.be
www.flandershydraulicsresearch.be